

**A UNIFORM APPROACH TO SURFACE COMPLEXATION
MODELING OF RADIONUCLIDE SORPTION**

Prepared for

**Nuclear Regulatory Commission
Contract NRC-02-93-005**

Prepared by

**Center for Nuclear Waste Regulatory Analyses
San Antonio, Texas**

January 1995



**A UNIFORM APPROACH TO SURFACE COMPLEXATION
MODELING OF RADIONUCLIDE SORPTION**

Prepared for

**Nuclear Regulatory Commission
Contract NRC-02-93-005**

Prepared by

David R. Turner

**Center for Nuclear Waste Regulatory Analyses
San Antonio, Texas**

January 1995

ABSTRACT

Sorption is typically a complex function of system chemistry, particularly pH, solid-mass to solution-volume ratio, and total carbon concentration. Commonly used empirical models cannot specifically take these dependencies into account. A mechanistic approach is needed to evaluate these effects quantitatively. Surface complexation models of differing complexity have been developed based on geochemical principles and successfully used to study and predict complex sorption behaviors for contaminants such as Zn^{2+} , Cd^{2+} , Pb^{2+} , Hg^{2+} , and CrO_4^{2-} . Three commonly used models include the Diffuse Layer, Constant Capacitance, and Triple Layer Models. Recent studies have indicated that radioelements such as the actinides exhibit similar chemistry-dependent sorption behavior. In many cases, however, radioelement sorption data have not been interpreted using surface complexation model approaches due to uncertainties in thermodynamic data or a lack of the appropriate mineral surface parameters. Those data that have been interpreted have generally been on a case-by-case basis, making comparison of model results difficult. To compare the performance of the different models, it is desirable to generate a set of uniform surface complexation model parameters for different minerals that share common reference values.

Using the numerical nonlinear parameter optimization code FITEQL, Version 2.0 to interpret available radioelement sorption data, the current study provides the necessary model-dependent parameters to describe pH-dependent sorption behavior of key actinides using the surface complexation model. This approach builds on earlier work that established the parameters to describe the acid-base behavior of a number of simple (hydr)oxides. In general, an approach has been adopted such that the simplest models that can describe the observed sorption behavior are used. These uniform methods are applied to actinide (and carbon) sorption, using data that are currently available in the literature for a number of simple (hydr)oxides and more complex aluminosilicates. Where data are available, these models have been used to investigate the effects of changing system chemistries. Although all three models proved capable of modeling the observed sorption behavior, the Diffuse Layer Model was able to do so using the fewest parameters, and may be preferred over the more complex models. Applied in this manner, the uniform surface complexation model approach has been used to develop a set of parameters based on common methodologies and reference points. This in turn will allow for the direct comparison and evaluation of model performance, and provides the parameters for those hydrogeochemical models that use surface complexation model approaches to account for sorption.

Compared to strictly empirical methods, approaches such as surface complexation models that are based on geochemical principles have the advantage of allowing extrapolation to physicochemical conditions outside of experimentally investigated ranges. In several cases, the surface complexation models developed here have been used to predict experimental results under differing conditions. In general, changes in experimental conditions involving pH, radioelement concentration, solid-mass to solution-volume ratio, and total carbon are predicted reasonably well using a relatively simple surface complexation modeling approach.

Ideally, mechanistic sorption models such as surface complexation models would be incorporated directly into reactive transport codes. While such hydrogeochemical transport codes may be used to examine particular aspects of reactive transport, the additional computational burden that results may be excessive for the purposes of performance assessment. It may be possible to use surface complexation models "off-line" to support K_d selection and to assess the effect of critical physicochemical parameters on radioelement sorption. While this approach is not an explicit incorporation of geochemistry in the transport calculations, it does provide a step towards a more theoretical basis for sorption modeling in performance assessment.

(This page intentionally left blank)

CONTENTS

Section	Page
FIGURES	vii
TABLES	ix
ACKNOWLEDGMENTS	xi
QUALITY OF DATA	xi
1 INTRODUCTION	1-1
1.1 REGULATORY BACKGROUND AND TECHNICAL OBJECTIVES	1-1
1.2 INTRODUCTION TO MODELING APPROACHES	1-2
2 INTRODUCTION TO SURFACE COMPLEXATION MODELS	2-1
2.1 SURFACE COMPLEXATION MODELS	2-1
2.2 GENERAL MODEL FEATURES	2-1
2.2.1 Diffuse Layer Model	2-2
2.2.2 Constant Capacitance Model	2-3
2.2.3 Triple Layer Model	2-3
2.3 SURFACE COMPLEXATION MODEL STRENGTHS AND WEAKNESSES	2-4
3 DEVELOPING A UNIFORM SET OF SCM PARAMETERS AND BINDING CONSTANTS	3-1
3.1 MINERAL ACID-BASE BEHAVIOR	3-1
3.2 RADIOELEMENT SORPTION DATA	3-1
3.3 BINDING CONSTANT ESTIMATION USING FITEQL, VERSION 2.0	3-4
3.3.1 Constructing a Chemical Equilibrium Model	3-5
3.3.2 Describing the Mineral Surface	3-5
3.3.3 Postulating a Surface Reaction	3-5
3.3.4 Estimating Model Suitability	3-6
3.4 CALCULATED BINDING CONSTANTS	3-6
4 MODELING RESULTS	4-1
4.1 MODELING RADIOELEMENT SORPTION ON SIMPLE (HYDR)OXIDES	4-1
4.2 MODELING RADIOELEMENT SORPTION ON ALUMINOSILICATES	4-1
4.3 SCM AND CHANGES IN SYSTEM CHEMISTRY	4-24
4.3.1 Effect of pH	4-24
4.3.2 Effect of Radionuclide Concentration	4-28
4.3.3 Effects of M/V Ratio	4-28
4.3.4 Effects of Carbon	4-28
4.4 IMPLEMENTATION OF SURFACE COMPLEXATION MODELS IN PERFORMANCE ASSESSMENT CALCULATIONS	4-31

CONTENTS (Cont'd)

Section	Page
5 DISCUSSION AND SUMMARY	5-1
6 REFERENCES	6-1
APPENDIX A — SUMMARY OF RADIONUCLIDE SORPTION DATA: EXPERIMENTAL CONDITIONS	
APPENDIX B — SCM BINDING CONSTANTS	

FIGURES

Figure		Page
4-1	Am(III) sorption on γ -Al ₂ O ₃ . SCM results are calculated using parameters derived from the experimental data shown in the figure	4-2
4-2	Am(III) sorption on α -Al ₂ O ₃ . SCM results are calculated using parameters derived from the experimental data shown in the figure	4-3
4-3	Am(III) sorption on amorphous-SiO ₂ . SCM results are calculated using parameters derived from the experimental data shown in the figure	4-4
4-4	Np(V) sorption on γ -Al ₂ O ₃ . SCM results are calculated using parameters derived from the experimental data shown in the figure	4-5
4-5	Np(V) sorption on goethite. SCM results are calculated using parameters derived from the experimental data shown in the figure	4-6
4-6	Np(V) sorption on synthetic magnetite. SCM results are calculated using parameters derived from the experimental data shown in the figure	4-7
4-7	Np(V) sorption on boehmite. SCM results are calculated using parameters derived from the experimental data shown in the figure	4-8
4-8	Np(V) sorption on lepidocrocite. SCM results are calculated using parameters derived from the experimental data shown in the figure	4-9
4-9	Np(V) sorption on α -Al ₂ O ₃ . SCM results are calculated using parameters derived from the experimental data shown in the figure	4-10
4-10	Np(V) sorption on ferrihydrite. SCM results are calculated using parameters derived from the experimental data shown in the figure	4-11
4-11	Np(V) sorption on amorphous SiO ₂ . SCM results are calculated using parameters derived from the experimental data shown in the figure	4-12
4-12	Pu(IV) sorption on goethite. SCM results are calculated using parameters derived from the experimental data shown in the figure	4-13
4-13	Pu(V) sorption on goethite. SCM results are calculated using parameters derived from the experimental data shown in the figure	4-14
4-14	Pu(V) sorption on γ -Al ₂ O ₃ . SCM results are calculated using parameters derived from the experimental data shown in the figure	4-15
4-15	Th(IV) sorption on γ -Al ₂ O ₃ . SCM results are calculated using parameters derived from the experimental data shown in the figure	4-16
4-16	Th(IV) sorption on amorphous SiO ₂ . SCM results are calculated using parameters derived from the experimental data shown in the figure	4-17
4-17	U(VI) sorption on magnetite. SCM results are calculated using parameters derived from the experimental data shown in the figure	4-18
4-18	U(VI) sorption on ferrihydrite. SCM results are calculated using parameters derived from the experimental data shown in the figure	4-19
4-19	U(VI) sorption on goethite. SCM results are calculated using parameters derived from the experimental data shown in the figure	4-20
4-20	U(VI) sorption on α -Al ₂ O ₃ . SCM results are calculated using parameters derived from the experimental data shown in the figure	4-21
4-21	U(VI) sorption on quartz. SCM results are calculated using parameters derived from the experimental data shown in the figure	4-22

FIGURES (cont'd)

Figure		Page
4-22	Carbon sorption on ferrihydrite. SCM results are calculated using parameters derived from the experimental data shown in the figure	4-23
4-23	SCM predictions of Np(V) sorption on biotite (a) DLM; (b) CCM; and (c) TLM results. $\text{Np(V)}_T = 6 \times 10^{-6}$ M, 0.1 M NaNO_3 , $M/V = 1$ g/L	4-25
4-24	SCM predictions of Np(V) sorption on kaolinite (a) DLM; (b) CCM; and (c) TLM results. $\text{Np(V)}_T = 1.25 \times 10^{-7}$ M, 0.1 M NaClO_4 , $M/V = 5$ g/L	4-26
4-25	SCM predictions of U(VI) sorption on kaolinite (a) DLM; (b) CCM; and (c) TLM results. $\text{U(VI)}_T = 1 \times 10^{-6}$ M, 0.1 M NaNO_3 , $M/V = 4$ g/L	4-27
4-26	SCM predictions of the effects of changing radionuclide concentration. The SCM curves at different concentrations are indistinguishable (see text)	4-29
4-27	SCM predictions of the effects of changing M/V ratio. (a) DLM results, Carbon sorption on ferrihydrite	4-30
4-28	DLM predictions of the effects of changing carbon concentration. (a) Model results, U(VI) sorption on goethite	4-32
4-29	DLM predicted K_d for U(VI) sorption on goethite. Values plotted as a function of: (a) pH. Experimental data from Hsi and Langmuir (1985)	4-33

TABLES

Table		Page
3-1	Best estimate values for SCM constants—simple (hydr)oxides (from Turner, 1993) . .	3-2
3-2	Potential sources of experimental sorption data for SCM parameter estimation	3-3

(This page intentionally left blank)

ACKNOWLEDGMENTS

This report was prepared to document work performed by the Center for Nuclear Waste Regulatory Analyses (CNWRA) for the Nuclear Regulatory Commission (NRC) under Contract No. NRC-02-93-005. The activities reported herein were performed on behalf of the NRC Office of Nuclear Regulatory Research (RES), Division of Regulatory Applications. The report is an independent product of the CNWRA and does not necessarily reflect the views or regulatory position of the NRC.

The author wishes to thank Stephen Sassman and Paula Muller, who provided invaluable assistance in conducting the computer modeling reported in this study. Able secretarial support was provided by Esther Cantu.

QUALITY OF DATA

DATA: Data used to develop the sorption models presented here were taken from published sources, which are referenced in this report. Experimental conditions are summarized in Appendix B. CNWRA-generated laboratory and field data contained in this report meet quality assurance requirements described in the CNWRA Quality Assurance Manual. Data from other sources, however, are freely used. Referenced sources for data from non-CNWRA sources should be consulted for determining their level of quality assurance.

ANALYSES AND CODES: Scientific and engineering computer codes were used in many of the analyses contained in this report. The geochemical computer codes FITEQL and MINTEQA2 are presently controlled under the CNWRA Software Configuration Procedure TOP-018. The spreadsheet QUATTRO-Pro was also used in these analyses; this is commercial software and only the object code is available to the CNWRA.

1 INTRODUCTION

1.1 REGULATORY BACKGROUND AND TECHNICAL OBJECTIVES

A fundamental concern in evaluating the suitability of Yucca Mountain, Nevada, as a potential repository for high-level nuclear wastes (HLW) is the possibility of radionuclide migration to the accessible environment as dissolved constituents in groundwaters. An important mechanism for attenuating radionuclide migration is sorption of radionuclides on minerals encountered along the flow paths. Sorption is specifically referred to in 10 CFR 60.122(b) as a favorable geochemical condition that will tend to inhibit radionuclide migration and "...favorably affect the ability of the geologic repository to isolate the waste" Conversely, geochemical processes that "...would reduce sorption of radionuclides..." are listed [10 CFR 60.122(c)(8)] as potentially adverse conditions that could reduce the effectiveness of the natural barrier system.

To support the Nuclear Regulatory Commission (NRC) HLW program, the Center for Nuclear Waste Regulatory Analyses (CNWRA) is conducting research activities under the Sorption Modeling for HLW Performance Assessment (PA) Research Project. The broad objectives are to develop sufficient understanding of radionuclide transport issues so that timely precicensing guidance can be provided to the U.S. Department of Energy (DOE) and a sound basis be available for evaluating the DOE license application (LA). Specifically, the results will be used in addressing NRC needs in evaluating the use of empirical sorption coefficients (e.g., K_d s) in modeling sorption.

As part of developing the NRC License Application Review Plan (LARP), NRC and CNWRA staffs have identified several Key Technical Uncertainties (KTUs) related to the retardation of radionuclide migration.

- Uncertainty in identifying geochemical conditions that would inhibit particulate and colloid formation (LARP Section 3.2.3.2—Favorable Conditions: Geochemical Conditions)
- Parametric representation of retardation processes involving radionuclide-bearing particulates, colloids, and complexes (LARP Section 3.2.3.2—Favorable Conditions: Geochemical Conditions)
- Equal or increased capacity of alteration mineral assemblages to inhibit radionuclide migration (LARP Section 3.2.3.3—Favorable Conditions: Mineral Assemblages)
- Uncertainty in identifying geochemical processes that reduce radionuclide retardation (LARP Section 3.2.3.5—Potentially Adverse Conditions: Geochemical Processes)
- Uncertainty in determining the magnitude of the effect of the geochemical processes that reduce radionuclide retardation (LARP Section 3.2.3.5—Potentially Adverse Conditions: Geochemical Processes)

NRC and CNWRA staffs are currently undertaking integration and revision of these KTUs to eliminate redundancies, and the final form of KTUs related to retardation may be different from that presented here.

From the NRC perspective, uncertainties about conditions and processes relevant to retardation make it difficult to provide a satisfactory evaluation of the approaches being taken by the DOE and adequate interpretation of DOE results. It is necessary, therefore, for the NRC to develop an independent understanding of conditions and processes relevant to retardation so that the DOE work may be evaluated. Alternatives to the DOE concepts and models must be independently developed by the NRC to assess the conservatism of the DOE models and bounding conditions. Because sorption is an important aspect of retardation, research into more mechanistic models of sorption processes will help to reduce this uncertainty and provide NRC and CNWRA staffs with a more sound theoretical basis for the timely evaluation of the DOE LA.

1.2 INTRODUCTION TO MODELING APPROACHES

Sorption is generally incorporated into PA models through the use of a single lumped sorption coefficient (K_d) determined by batch sorption experiments. These models do not explicitly consider changes in system chemistry or variations in the mineral-water interface, however, and it is difficult to extrapolate experimentally derived sorption coefficients beyond experimental conditions with any quantifiable certainty (Reardon, 1981; Kent et al., 1988; Davis and Kent, 1990; Pabalan and Turner, 1992). For example, traditional applications assign the sorption coefficient for each radionuclide as a physical property of the geologic medium of interest. The K_d value for each element is then assigned a probability density function (pdf), and sampled during multiple realizations (e.g., Wilson et al., 1994). These pdfs are typically based on expert elicitation, which in turn is based on experimental determinations of K_d . However, because many minerals exhibit complex sorption behavior (e.g., Kohler et al., 1992) that is dependent on system chemistry, K_d may vary over several orders of magnitude with fairly small changes in parameters such as pH. Given the difficulties in extrapolating sorption coefficients beyond the experimental conditions, a more mechanistic approach to sorption modeling that uses geochemical principles to simulate changes in the system and to model complex sorption behavior (Davis and Kent, 1990) may provide a more sound theoretical basis for the pdf selected for a given parameter.

Surface complexation models (SCM) represent one type of mechanistic approach that has been used to model contaminant sorption on (hydr)oxide surfaces over a wide range in chemical conditions (e.g., pH, ionic strength, total concentration of adsorbate) (Sanchez et al., 1985; Girvin et al., 1991; Payne et al., 1992; Turner, 1993). These models rely on the assumption that the formation of surface complexes with functional binding sites at the mineral-water interface is analogous to aqueous speciation reactions occurring in the bulk solution. These equilibrium models are distinctive in that they also include representations of the electrostatic interactions at the mineral-water interface. More commonly used SCM include Triple Layer (TLM), Diffuse Layer (DLM), and Constant Capacitance (CCM) models (Westall and Hohl, 1980; Hayes et al., 1990; Davis and Kent, 1990). The application of these models requires a set of model-specific parameters representing the system chemistry and the properties of the adsorbent; the number of parameters varies with the complexity of the model.

Only recently have experiments become available that cover radioelement sorption over a wide enough range in chemical conditions to allow quantitative application of SCM approaches. In many cases, however, these data have not been interpreted using mechanistic models due to uncertainties in thermodynamic data or a lack of the appropriate SCM mineral surface parameters. Those data that have been interpreted have generally been on a case-by-case basis, making consistent application of model results and comparison of different SCM approaches difficult. The objectives of this research are to investigate available radioelement sorption data using a uniform SCM approach as a mechanistic

alternative to empirical approaches. Earlier research (Turner, 1993) has focused on developing the necessary input parameters using a uniform and internally consistent approach based on the work of Hayes et al. (1991) and Dzombak and Morel (1990). Based on this description of the acid-base behavior of the mineral-water interface, these models are extended to existing radioelement sorption data to determine the suitability of this approach in modeling complex radioelement sorption behavior.

2 INTRODUCTION TO SURFACE COMPLEXATION MODELS

2.1 SURFACE COMPLEXATION MODELS

The surface charge of many minerals, primarily (hydr)oxides, is known to vary as a function of pH (Kent et al., 1988; Davis and Kent, 1990). SCMs deal with this pH dependence by assuming a surface comprised of hydroxyl groups ($>XOH^{\circ}$). The potential determining ion at the mineral-water interface is assumed to be hydrogen. By adding a hydrogen ion (protonation), a positively charged surface site, $>XOH_2^+$, is developed. Conversely, losing a proton (deprotonation) leads to the development of a negatively charged surface ($>XO^-$). At low pH, the $>XOH_2^+$ sites outnumber the $>XO^-$ sites, and the surface is positively charged. At higher pH, the $>XO^-$ sites are more numerous, and the net surface charge is negative. At some intermediate pH, referred to as the zero point of charge (pH_{ZPC}), the sites will balance and the surface will not exhibit any net charge. Therefore, depending on the pH, the electrostatic attraction from these sites can lead to the specific adsorption of cations and anions from solution. By assuming an analogy to aqueous speciation reactions, surface adsorption is then described using a combination of equilibrium protonation/deprotonation and complexation reactions (e.g., Davis and Leckie, 1978; Hayes et al., 1990). Mass balance and mass action relations, modified to include the electrostatic effects of a charged mineral surface, can be used in a manner analogous to that employed by geochemical speciation codes (Westall and Hohl, 1980; Allison et al., 1991) to determine the distribution of the elements between those dissolved in the bulk solution and those specifically sorbed onto the solid.

2.2 GENERAL MODEL FEATURES

To describe the acid-base behavior of a mineral surface, equilibrium protonation/deprotonation reactions are written for SCM in the form



where $>XOH^{\circ}$ represents a neutral surface site, and the equilibrium constants K_+ and K_- are referred to as intrinsic surface acidity constants. Equations (2-1) and (2-2) clearly show the pH dependence of surface charge development.

For the sorption of contaminants such as radionuclides, sorption reactions can be developed by analogy to aqueous speciation. For example, for the sorption of a cation C^{z+} , the formation of a surface complex can be written as



The corresponding equilibrium constant for this reaction, K_C , is commonly called a sorption or binding constant, and contains corrections for the effects of the electrostatic double layer at the mineral-water interface.

Electrical work done in moving ions across the zone of charge influence adjacent to the interface will affect the activity of aqueous species near the charged surface relative to the bulk solution. In the SCM approach, the change in activity of species such as H^+ and C^{z+} near the surface due to electrostatic forces is assumed to be governed by the Boltzmann relation such that:

$$\{C^{z+}\}_{\text{surface}} = \{C^{z+}\}_{\text{bulk}} [\exp(-\psi_J F/RT)]^z \quad (2-4)$$

where $\exp^{-\psi_J F/RT}$ is the Boltzmann factor, ψ_J is the electrostatic potential of the layer J, which depends on the model, z is the valence of the ion, F and R are the Faraday (J/volt equiv) and ideal gas (J/K•mole) constants, respectively, and T is absolute temperature (K). This correction is incorporated into the mass action expressions for surface reactions.

Mass balance for the total concentration of available surface sites (T_{XOH} in moles sites/L) is

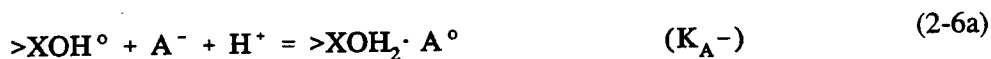
$$T_{XOH} = \frac{(N_S) \times (A_{SP}) \times (M/V) \times 10^{18} \text{ nm}^2/\text{m}^2}{6.023 \times 10^{23} \text{ sites/mole}} \quad (2-5)$$

where N_S is site density (sites/nm²), A_{SP} (m²/g) is specific surface area of the mineral, and M/V is the solid-mass to solution-volume ratio (g/L).

Although these general features are shared by different SCM approaches, the models differ in how the mineral-water interface is divided between the charged surface and the bulk solution, and in the charge/potential relationships used for the different layers. Specific aspects of the different models are discussed in detail elsewhere (e.g., Westall and Hohl, 1980; Davis and Kent, 1990), and only a brief summary is given here.

2.2.1 Diffuse Layer Model

The DLM assumes that protonation/deprotonation and adsorption only occur in one plane at the mineral-water interface, and that only those ions specifically adsorbed in this "o-plane" contribute to the total surface charge (i.e., $\sigma_s = \sigma_o$). Protonation and deprotonation of the surface sites are represented by the reactions given in Eqs. (2-1) and (2-2). For the adsorption of the contaminants M^+ and A^- , the general form of these reactions is



where the mass action equilibrium constants (binding constants) for these reactions are represented by K_{A^-} and K_{M^+} , respectively.

In the DLM, the Stern-Grahame extension of the Gouy-Chapman relationship for symmetrical electrolytes is used to describe the interdependence between ionic strength (I), charge ($\sigma_d = -\sigma_o - \sigma_s$ at the boundary with the o-plane), and electrostatic potential ($\psi_d = \psi_o$) such that:

$$-\sigma_o = \sigma_d = -(\sqrt{8\epsilon\epsilon_o RT}) \left[\sinh \frac{(z\psi_d F)}{2RT} \right] \quad (2-7)$$

where F, R, z, and T are as defined above, ϵ is the dielectric constant, ϵ_o is the permittivity in free space (8.85×10^{-12} coulombs²/J•m).

2.2.2 Constant Capacitance Model

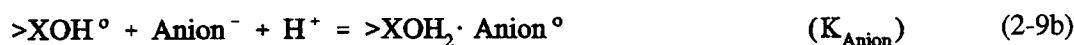
Like the DLM, the CCM also assumes a one-layer interface, and the reactions, mass balance, and mass action used to describe surface phenomena are the same as those presented for the DLM. In contrast to the DLM, the CCM assumes that the charged surface is separated from the bulk solution by a layer of constant capacitance. Based on this assumption, surface charge ($\sigma_d = -\sigma_o = -\sigma_s$) is related to surface potential ($\psi_o = \psi_d$) through the simple linear equation:

$$-\sigma_o = \sigma_d \approx C_1 \psi_o \quad (2-8)$$

where C_1 (Farads/m²) is a constant capacitance term. As described in Turner (1993), C_1 is fixed at 1.0 Farads/m² based on the work of Hayes et al. (1990; 1991). This relationship results in a linear potential gradient from the charged substrate to the bulk solution. The constant capacitance approach is limited to a specific ionic strength, however, and in a strict sense, changes in ionic strength require recalculation of C_1 . Generally, the constant capacitance term is not provided as a characteristic property of a given system, but applied instead as an empirical parameter fit to the data (Westall and Hohl, 1980; Hayes et al., 1990). This action has the advantage of providing a better fit to a given data set, but at the expense of the theoretical basis of the model.

2.2.3 Triple Layer Model

Unlike the DLMs and CCMs, the TLM divides the mineral-water interface into three layers. In its original construction (Davis et al., 1978), protonation/deprotonation of surface sites (K_+ and K_-) is restricted to the innermost o-plane, while specifically adsorbed ions are typically assigned to the β -plane (i.e., outer-sphere complexes). Subsequent modifications (Hayes and Leckie, 1987) provide for inner-sphere complexes to describe strongly bound metals. The outermost layer, the d-plane, is made up of a diffuse region of counterions extending into the bulk solution. Also, unlike the DLM and CCM, the TLM allows for adsorption of the background electrolyte. This allowance leads to the introduction of an additional set of reactions such that



where K_{Cation} and K_{Anion} represent the equilibrium constants for adsorption of the background cation (e.g., Na^+) and anion (e.g., NO_3^-), respectively.

Surface charges in the TLM are designated σ_o and σ_β for the o- and β -layers, respectively. At the boundary between the intermediate β -layer and the diffuse outer d-layer, the diffuse layer charge (σ_d) is defined such that $\sigma_o + \sigma_\beta + \sigma_d = 0$. Charge/potential relations for the different layers are

$$\sigma_o = (\psi_o + \psi_\beta)C_1 \quad (2-10a)$$

$$\sigma_o + \sigma_\beta = (\psi_\beta + \psi_d)C_2 = -\sigma_d \quad (2-10b)$$

$$\sigma_d = -(\sqrt{8\epsilon\epsilon_o IRT}) \left[\sinh \frac{(z\psi_d F)}{2RT} \right] \quad (2-10c)$$

where C_1 and C_2 are constant capacitances associated with the areas between the o- and β -planes and β - and d-planes, and, based on the work of Hayes et al. (1990, 1991), are fixed at 0.8 and 0.2 Farads/m², respectively, in the current models (Turner, 1993). ϵ , and ϵ_o are as defined previously.

2.3 SURFACE COMPLEXATION MODEL STRENGTHS AND WEAKNESSES

Relative to empirical sorption models, the strength of all SCMs is the ability to handle changes in chemistry in a quantitative fashion to predict complex, chemistry-dependent sorption behavior. An SCM approach incorporates a chemical equilibrium model of the system, and takes into account the aqueous speciation of the radionuclide in the system of interest. The major disadvantages are the complexity of the conceptual model and the number of parameters required to describe the mineral-water interface.

Although parameters such as site density, capacitance, and surface acidity constants all have physical or chemical significance, in practice, they are typically poorly characterized and are used on a case-by-case basis as adjustable parameters (e.g., Sanchez et al., 1985; Hsi and Langmuir, 1985; LaFlamme and Murray, 1987). This practice makes direct comparison of different models and model results difficult. Of the three approaches described previously, the DLM is the simplest model, and requires only four adjustable parameters: Protonation/deprotonation (K_+ , K_-); binding constants for sorbing radionuclides (such as $K_{UO_2^{2+}}$), and site density (N_s). Because the DLM uses the Gouy-Chapman expression for charge/potential relationships, this model is applicable at a variety of ionic strength conditions (Hayes et al., 1990). The CCM shares the same parameters as the DLM and adds a capacitance term (C_1) for charge/potential relationships. For the CCM the capacitance is determined at a single ionic strength; therefore, in a strict sense, the CCM binding constants are only valid at one ionic strength. New capacitances and surface equilibrium constants are necessary if conditions change. In practice, however, C_1 is not well constrained and is used as an adjustable parameter. As the most elaborate model, the TLM requires eight types of adjustable parameters; the four offered by the DLM plus sorbing background electrolytes (K_{Cation} and K_{Anion} such as K_{Na^+} , $K_{NO_3^-}$) and capacitances for the inner and outer layers (C_1 and C_2 , respectively). Like the DLM, the TLM uses the Gouy-Chapman relationship and is also applicable at different ionic strengths. The TLM is also able to handle ionic strength effects through its provisions for background electrolyte adsorption.

To minimize the number of adjustable parameters, recent work with SCMs has advocated adopting "standard" values for parameters such as acidity constants, site density, and capacitances that

are uniformly applied in all systems (Dzombak and Morel, 1990; Davis and Kent, 1990; Hayes et al., 1990, 1991; Bradbury and Baeyens, 1992, 1993; Mesuere, 1992; Turner, 1993). After the mineral surface is characterized in this fashion, the number of adjustable parameters is limited to the binding constant(s) of the assumed surface complex(es). While limiting the number of adjustable parameters, this approach preserves much of the strength of the SCM by maintaining the chemical equilibrium model of the radioelement system, aqueous speciation, and the electrostatic charge-potential relationships. Although this approach may not truly represent the exact physical, electrostatic, and chemical processes operating at the mineral-water interface, it does establish a geochemical basis for sorption models, and serves to establish a baseline that will allow future direct comparison of modeling results and the evaluation of model performance. In addition, such an approach may be desirable from the point of view of developing simple, flexible sorption models with internally consistent databases for the purposes of PA.

Although the SCM approach as described is not an explicit mechanistic model of processes at the mineral surface on an atomistic level, it incorporates aspects of thermodynamic principles to describe the mineral-water interface. As such, the different SCMs use a set of parameters that describe an idealized, but physically reasonable, model of the electrostatic and acid-base behavior of a given mineral. In spite of these limitations, SCMs represent a critical step towards more mechanistic models and are able to account for the effects of changes in the solution and surface chemistry in a quantitative way that greatly exceeds the capabilities of most purely empirical methods such as a linear K_d model.

3 DEVELOPING A UNIFORM SET OF SCM PARAMETERS AND BINDING CONSTANTS

Recent studies have begun to develop a number of data sets for radioelement sorption on a variety of different minerals. In many cases, however, these data have either not yet been interpreted in a quantitative way, or have been examined on a case-by-case basis, which makes it difficult to compare model results. Uniform SCM approaches have been developed for contaminant sorption on ferrihydrite (Dzombak and Morel, 1990) and applied with success. Similar approaches need to be investigated and extended to interpret the available data on sorption in different radioelement-solid systems.

3.1 MINERAL ACID-BASE BEHAVIOR

Earlier work (Turner, 1993) has focused on developing and applying a set of uniform parameters that define the physical conditions (e.g., site density, capacitance) to derive the acidity constants necessary to describe the acid-base behavior of the mineral-water interface ($\text{Log } K_+$ and $\text{Log } K_-$). This approach is based on the methods developed in Dzombak and Morel (1990) for sorption on ferrihydrite. Extending this approach to other minerals involved obtaining potentiometric titration data from readily available peer-reviewed literature for different (hydr)oxides. Using the nonlinear parameter optimization code FITEQL (Westall, 1982a,b), these data were interpreted following the techniques developed by Dzombak and Morel (1990) and Hayes et al. (1990; 1991). In this fashion, a consistent set of acidity constants that characterize the acid-base behavior of each mineral (Table 3-1) CNWRA were developed for each of the three surface complexation models described earlier. Other studies have assumed the existence of multiple site types (e.g., Benjamin and Leckie, 1980; Dzombak and Morel, 1990). This method requires a set of acidity constants and site densities-base parameters for each type of site invoked. Due to a lack of data on several of the minerals considered and a desire to maintain a simple conceptual model, a single site type is assumed here. The sources for the potentiometric titration data and the parameters used to characterize the mineral surface are also given in Table 3-1. The details of the methods used and the assumptions involved in developing the acidity constants are given in Turner (1993) and the references therein.

3.2 RADIOELEMENT SORPTION DATA

Because these acidity constants are based on a consistent set of reference parameters, model results can be compared in a more direct fashion. With the acidity constants as defined in Table 3-1, the next step in developing a uniform sorption model is to interpret available radioelement sorption data by defining surface complexes and determining the necessary binding constants for the different SCMs. To do this, it is also necessary to gather existing radioelement sorption data. These data should be from well characterized experiments covering a fairly wide pH range. A search of the open literature identified a number of recently published studies that can be interpreted using SCMs (Table 3-2). These studies examine the sorption of actinides to a variety of minerals, including simple (hydr)oxides such as goethite and amorphous SiO_2 and more complex rock-forming minerals such as kaolinite and biotite.

In most cases, actinide sorption is dependent on pH, exhibiting a strong sorption edge over a fairly narrow range in pH. Additional factors such as $p(\text{CO}_2)$, solid-mass to solutions-volume ratio (M/V), and I also contribute to the location of the sorption edge and the extent of the sorption maximum. Appendix A provides a brief summary of the experimental conditions. Some of these data have been modeled previously using an SCM approach and simultaneously adjusting several model parameters.

Table 3-1. Best estimate values for SCM constants—simple (hydr)oxides (from Turner, 1993)

Mineral	Mineral Properties ^a	References	Model	Log K ₊ (± 95%) ^b	Log K (± 95%) ^b	Log K _{Anion} (± 95%) ^b	Log K _{Cation} (± 95%) ^b
Goethite	pH _{ZPC} =8.0 A _{Sp} =50m ² /g	Yates and Healy (1975); Balistrieri and Murray (1981); Hsi and Langmuir (1985); Hayes et al. (1990); Mesuere (1992)	CCM(0.1M)	6.47±0.72	-9.03±0.22	n.a.	n.a.
			DLM	7.35±0.11	-9.17±0.08	n.a.	n.a.
			TLM(d)	6.00	-10.00	8.78±0.13	-7.64±0.07
Ferrihydrite _c	pH _{ZPC} =8.0 A _{Sp} =600m ² /g	Yates (1975); Davis (1977); Swallow (1978); Hsi and Langmuir (1985)	CCM(0.1M)	7.35±1.08	-8.45±2.23	n.a.	n.a.
			DLM	7.29±0.10	-8.93±0.07	n.a.	n.a.
			TLM(d)	6.00	-10.00	8.43±0.04	-7.66±0.12
Magnetite	pH _{ZPC} =6.7 A _{Sp} =5m ² /g	Regazzoni et al. (1983)	CCM(0.1M)(e)	6.26	-7.32	n.a.	n.a.
			DLM	6.72±0.02	-6.37±0.71	n.a.	n.a.
			TLM(d)	4.70	-8.70	7.95±0.11	-5.47±0.06
SiO ₂	pH _{ZPC} =2.8 A _{Sp} =175m ² /g	Abendroth (1970); Bolt (1957)	CCM(0.1M)	(f)	-7.04±0.09	n.a.	n.a.
			DLM	(f)	-7.20±0.05	n.a.	n.a.
			TLM(d)	0.90	-4.90	(f)	-6.22±0.05
α-Al ₂ O ₃	pH _{ZPC} =8.9 A _{Sp} =12m ² /g	Hayes et al. (1990)	CCM(0.1M)(e)	8.12	-9.56	n.a.	n.a.
			DLM	8.33±0.15	-9.73±0.12	n.a.	n.a.
			TLM(d)	6.90	-10.90	10.12±0.03	-7.73±0.07
γ-Al ₂ O ₃	pH _{ZPC} =8.4 A _{Sp} =120m ² /g	Huang and Stumm (1972); Sprycha (1989)	CCM(0.1M)	6.92±0.06	-9.00±0.15	n.a.	n.a.
			DLM	6.85±0.06	-9.05±0.09	n.a.	n.a.
			TLM(d)	6.40	-10.40	8.28±0.05	-7.95±0.11
δ-MnO ₂	pH _{ZPC} =1.9 A _{Sp} =270m ² /g	Murray (1974); Catts and Langmuir (1986)	CCM(0.1M)	(f)	-2.14±24.7	n.a.	n.a.
			DLM	(f)	-3.27±0.73	n.a.	n.a.
			TLM(d)	-0.10	-3.9	(f)	-0.75±0.84
TiO ₂ (anatase)	pH _{ZPC} =6.1 A _{Sp} = (c)	Sprycha (1984); Berube and de Bruyn (1968)	CCM(0.1M)(e)	6.64	-5.60	n.a.	n.a.
			DLM	5.37±0.30	-5.92±0.12	n.a.	n.a.
			TLM(d)	4.10	-8.10	7.13±0.17	-4.59±0.10
TiO ₂ (rutile)	pH _{ZPC} =5.9 A _{Sp} =30m ² /g	Berube and de Bruyn (1968); Yates (1975)	CCM(0.1M)(e)	3.91	-7.79	n.a.	n.a.
			DLM	4.23±0.09	-7.49±0.12	n.a.	n.a.
			TLM(d)	3.90	-7.90	5.24±0.08	-6.42±0.08

n.a. Parameters not applicable to CCM and DLM models.

- (a) N_S=2.31 sites/nm² (from Dzombak and Morel, 1990) assumed for all minerals.
- (b) 95-percent confidence interval based on FITEQL standard deviation and defined using the methods of Dzombak and Morel (1990).
- (c) Mineral properties and DLM parameters for ferrihydrite are from Dzombak and Morel (1990).
- (d) For TLM, Log K₊ and Log K₋ fixed using the relationships: [Log K₊ - Log K₋]/2 = pH_{ZPC} and -(Log K₊ + Log K₋) = -4.0. See Turner (1993) for discussion.
- (e) FITEQL did not converge at I=0.1 M. Extrapolated from Log₁₀(I) versus Log K₊ and Log K₋.
- (f) Not considered for δ-MnO₂ and am-SiO₂.

Table 3-2. Potential sources of experimental sorption data for SCM parameter estimation

I. URANIUM							
Goethite	HFO	Al ₂ O ₃	Zeolite	Clay/Mica	TiO ₂	Magnetite	SiO ₂
a,b,c	a,d	e	f,y	d,g,h	i,j	j	k
II. PLUTONIUM							
Goethite	Al ₂ O ₃						
l	m						
III. NEPTUNIUM							
Goethite	HFO	Clay/Mica	SiO ₂	Al ₂ O ₃	Zeolite		
n	o	c,h	p,h	m	h		
IV. AMERICIUM							
SiO ₂	Al ₂ O ₃	Clay/Mica					
p,q	m,p	r					
V. THORIUM							
Goethite	SiO ₂	Al ₂ O ₃	MnO ₂	Clay/Mica			
s,t	p,u	m	s	u			
VI. CARBON							
Goethite	HFO	Al ₂ O ₃					
v	w	x					

[a] Hsi and Langmuir (1985); [b] Tripathi (1984); [c] Kohler et al. (1992); [d] Payne et al. (1992); [e] Pabalan and Turner (1994); [f] Pabalan et al. (1993); [g] Della Mea et al. (1992); [h] Current experimental program at CNWRA; [i] Lieser and Thybusch (1988); [j] Venkataramani and Gupta (1991); [k] Waite et al. (1993); [l] Sanchez et al. (1985); [m] Righetto et al. (1988); [n] Nakayama and Sakamoto (1991); [o] Girvin et al. (1991); [p] Righetto et al. (1991); [q] Moulin et al. (1992); [r] Stammose and Dolo (1990); [s] Hunter et al. (1988); [t] LaFlamme and Murray (1987); [u] Riese (1982); [v] van Geen et al. (1994); [w] Zachara et al. (1987); [x] Schulthess and McCarthy (1990); [y] Vochten et al. (1990).

Many of the data have not yet, however, been interpreted in a quantitative sense. Therefore, the primary goal of this study was to use a uniform, simplified SCM approach to interpret currently available data. The current effort has focused on the actinides: U(VI), Pu(V), Pu(IV), Am(III), Np(V), and Th(IV). Carbon was also investigated due to the potential for ^{14}C transport in the subsurface (Meijer, 1993). Although carbon transport is likely to be in the gas phase, interactions between the gas, solid, and liquid phases may provide some degree of retardation through precipitation/dissolution and sorption (Codell and Murphy, 1992; Meijer, 1993). Carbon sorption is also of interest due to its strong effects in inducing desorption of actinides at higher pH. It should be noted that the listing of data sources given in Table 3-2 and Appendix A is not intended to be an exhaustive survey of the literature. As additional data become available, the methods outlined in this report can readily be extended to include new radionuclide-solid systems.

Radioelement sorption data are typically presented in graphical form only; figures were enlarged where necessary, and an electronic digitizing tablet linked to a personal computer was used to convert graphical data to numerical values in the appropriate coordinates. Results are typically reported as percent sorbed versus pH, which may lead to errors in calculating K_d values at sorption levels approaching 100 percent; small inaccuracies at sorption levels greater than 99.9 percent may lead to large variations in calculated K_d . In some cases, however, data are plotted as $\text{Log } K_d$ instead of percent sorbed. In these cases, the effects of digitizing error will be magnified relative to a linear percent sorbed scale. Some uncertainty is likely to be introduced due to the accuracy of the digitizing equipment itself and the precision with which the operator can use the equipment. Checks on reproducibility using endpoints on the graphs indicate that the digitization is generally reproducible to within about 0.1 mm. The absolute error will vary depending on the coordinate system and the size of the graph. The uncertainty due to digitization was not propagated through the calculations.

3.3 BINDING CONSTANT ESTIMATION USING FITEQL, VERSION 2.0

With the required acidity constants for the different SCMs determined from potentiometric titration data, SCMs can be used to interpret the gathered radioelement sorption data from the studies identified in Table 3-2. This interpretation requires the determination of a binding constant for a surface complexation reaction similar in form to Eq. (2-3). Modeling studies have frequently relied on trial and error methods to develop these binding constants (Tripathi, 1984; Sanchez et al., 1985; Hsi and Langmuir, 1985; LaFlamme and Murray, 1987). An alternative approach is to use nonlinear, least squares computer methods (Dzombak and Morel, 1990). This method has the advantage of providing some quantification of uncertainty and an objective measure of the performance of the model in describing the observed behavior.

As in the interpretation of the potentiometric titration data, the iterative nonlinear least squares optimization program FITEQL, Version 2.0 (Westall, 1982a,b) was used to determine binding constants for the three SCMs. The code requires data describing the physical properties of the solid surface, and reaction stoichiometries and mass action constants for the chemical equilibrium model with corresponding $\text{Log } K$ values. The radioelement sorption versus pH data are also entered in series. In calculating binding constants, FITEQL seeks to minimize the difference between experimental values and those calculated based on mass action constraints for those components where both the free and total concentrations are known. The program input is described briefly here. The reader is referred to Westall (1982a,b) and Dzombak and Morel (1990) for a more detailed description of program input and the numerical procedures employed in FITEQL, Version 2.0.

3.3.1 Constructing a Chemical Equilibrium Model

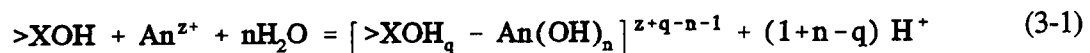
To use numerical optimization techniques, a chemical equilibrium model must be created for the system under consideration. This model includes a definition of the components in the system such as the appropriate oxidation state of the radionuclide of interest, background electrolytes, and any ligands added to the system (e.g., CO_3^{2-} , F^-). System components also include the model-dependent electrostatic terms for the SCM. Aqueous speciation reactions and equilibrium constants are then entered for the system of interest. These reactions/constants include the protonation/deprotonation reactions for the mineral surface (Section 3.1) and the stoichiometry for the postulated surface reaction (Section 3.3.3). It is important to note that the binding (equilibrium) constant for the postulated surface reaction will be determined in the context of the speciation reactions that make up the chemical equilibrium model. For this reason, the binding constant that is determined using FITEQL, Version 2.0 is dependent on the thermodynamic data used to describe the radioelement system. For the radioelements considered here (Am, Np, Pu, Th, U, C), the thermodynamic data come from the MINTEQA2 database, modified at the CNWRA to incorporate the radioelement data from Release Data0.com.r16 of the EQ3/6 database (Turner, 1993).

3.3.2 Describing the Mineral Surface

The physical and chemical properties of the mineral surface must be described for the optimization run. This description includes the surface area, site density, and acidity constants as described in Table 3-1 and in Turner (1993). Additional parameters include capacitance values for the CCM and TLM and background electrolyte binding constants for the TLM [Eq. (2-9)].

3.3.3 Postulating a Surface Reaction

A surface complex is postulated to account for sorption of the radionuclide of interest. This reaction is of the general form given in Eq. (2-3), and will vary depending on the oxidation state and hydrolysis of the radioelement at the surface. Since one objective of this exercise is to develop simple sorption models for PA, actinide (An) systems were generally modeled assuming only monodentate complexation reactions that produce only a single mononuclear actinide hydroxide species [e.g., $\text{UO}_2(\text{OH})_n^{2-n}$, $\text{Am}(\text{OH})_n^{3-n}$, $\text{NpO}_2(\text{OH})_n^{1-n}$, $\text{Pu}(\text{OH})_n^{4-n}$] of the general form:



where $q = 0, 1, \text{ or } 2$. Undoubtedly, the models could be further refined to better predict the data by invoking more than one surface complex, multidentate sorption, or consideration of polynuclear species such as was done by Kohler et al. (1992) and Payne and Waite (1991). Without independent analysis, however, the validity of the postulated complexes would be uncertain. Although Extended X-Ray Absorption Fine Structure (EXAFS) work indicates the formation of bidentate mononuclear uranyl-hydroxy surface complexes (Manceau and Charlet, 1991), this work only applies to fairly concentrated solutions (millimolar) at single pH values. Additional EXAFS work will be required to ascertain the extent to which SCMs represent the mineral-water interface (Sposito, 1992). To satisfy the need to develop simple models for the purposes of PA, the principal of parsimony has generally been adopted, and the simplest model capable of reproducing the observed data has been preferred. While this type of approach may not reflect the actual surface complex that is formed (Manceau and Charlet, 1991), it allows comparison of different modeling strategies.

3.3.4 Estimating Model Suitability

As a measure of how well the postulated surface complex reproduces the experimental data, output from FITEQL includes a "goodness-of-fit" parameter and standard deviations for the estimated binding constant (Westall, 1982a,b). The goodness-of-fit parameter generated by FITEQL can be used as a measure of how well the data are described by the assumed chemical and adsorption models. The smaller the value, the better the postulated surface complex is able to account for the observed sorption behavior (Westall, 1982a). These values are determined based on the experimental error specified in the optimization run and the size of the data set. For example, although binding constant estimates are not greatly affected, goodness-of-fit and parameter uncertainty generally deteriorate for smaller data sets because the chemical system is not as well constrained (Dzombak and Morel, 1990; Turner, 1993). In many cases, while counting error is reported for radioelement sorption data, the experimental error is not. In these cases, relative error (precision) has been assumed to be ± 10 percent (0.10), while absolute error (detection limits) has been assumed to be two orders of magnitude less than the minimum sorbed concentration. The sensitivity analyses of Dzombak and Morel (1990) indicated that the dissimilarities in binding constants due to differences in assumed experimental error are negligible, but the calculated uncertainty in the estimated values, as measured by the calculated standard deviation, increases with increasing error.

3.4 CALCULATED BINDING CONSTANTS

Using the acidity constants and the mineral properties as defined in Table 3-1 and Turner (1993), and the sorption data identified in Table 3-2, a series of monodentate, mononuclear sorption reactions of the general form given in Eq. (3-1) were developed for each of the radioelement-mineral systems under consideration. FITEQL, Version 2.0 input files were prepared for each of the reactions, and binding constants were determined. The binding constants are tabulated in Appendix B. These binding constants were then used with the speciation/sorption code MINTEQA2 (Allison et al., 1991) to predict radioelement sorption behavior as a function of system chemistry, principally by varying pH. Modeling results using these binding constants are presented and discussed in Section 4.

4 MODELING RESULTS

The ultimate goal of this study is to develop a simplified, uniform SCM approach and determine the binding constants necessary to model available radioelement sorption data. The first step towards this goal has been discussed earlier in Sections 2 and 3 in the development of the acidity constants necessary to describe the acid-base behavior of different minerals. It is now possible to take these parameters, and in a manner analogous to interpreting potentiometric titration data, use FITEQL to examine existing sorption data and develop a set of binding constants for a given radioelement-mineral system.

4.1 MODELING RADIOELEMENT SORPTION ON SIMPLE (HYDR)OXIDES

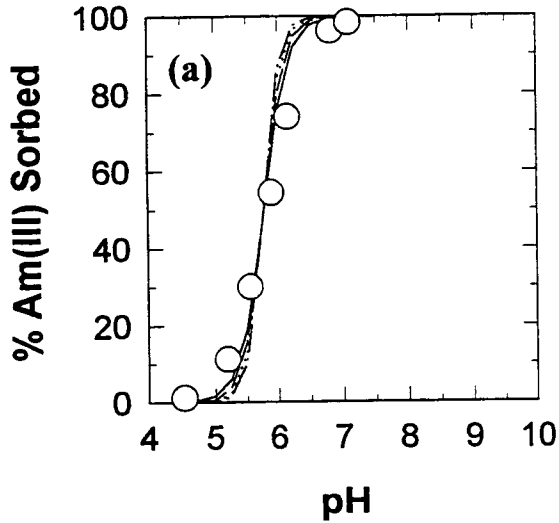
Because they were initially developed to address sorption on (hydr)oxides such as goethite and TiO_2 (Davis and Kent, 1990), application of SCM approaches to radioelement sorption on these simple minerals is relatively straightforward, and the results are typically very good. Figures 4-1 through 4-22 show some of the best-fit results of SCM interpretations of actinide and carbon sorption on simple (hydr)oxides using the data listed in Table 3-2 and the binding constants listed in Appendix B. The simplified uniform approach that has been adopted is suitable for reproducing the observed sorption behavior, and in most cases, a single monodentate, mononuclear surface complex is sufficient. For most of the systems studied, a single surface complex of the form $>\text{XO-An}^{(n-1)+}$ is inadequate to explain the observed behavior. Invoking a single hydrolyzed surface species of the form $>\text{XO-An(OH)}^{(n-2)+}$ is generally more successful. These types of simplification are a significant advantage given the complex speciation of the actinide- H_2O systems. The different models produce similar results; results from the DLM and CCM calculations are very similar, and are typically comparable to the best results from the more complicated TLM. In several cases, however, the single layer DLM and CCM best reproduce the observed behavior assuming a different surface complex than the multiple-layer TLM (e.g., Np-Amorphous SiO_2). It is difficult to objectively discriminate between models on this basis. In the absence of independent information on the complexes formed at the mineral-water interface, surface complexes are typically selected based on the goodness-of-fit to the observed data. However, on the basis of a simpler representation of the mineral-water interface and fewer model-specific parameters, the DLM is perhaps to be preferred for application in PA simulations.

4.2 MODELING RADIOELEMENT SORPTION ON ALUMINOSILICATES

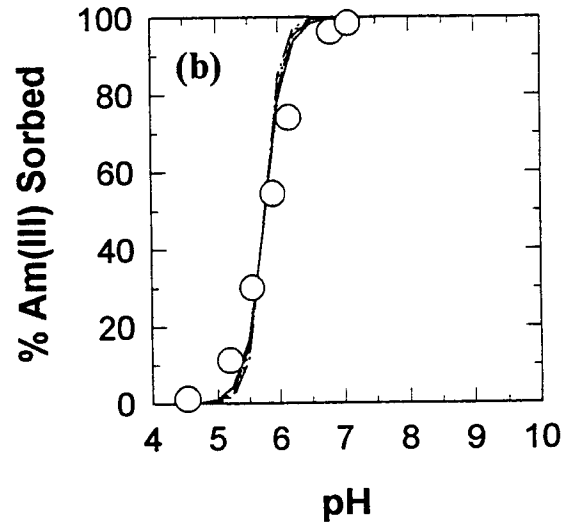
Radioelement sorption data are available for a number of common rock-forming aluminosilicate minerals such as clays and micas (Table 3-2). Because of their occurrence at YM, these minerals may contribute significantly to sorption processes in the subsurface. Since aluminosilicates are more complex, SCM approaches need to be modified to handle these minerals where the development of a surface charge and radioelement sorption may be due to more than one type of site.

One method of applying surface complexation models to more complex minerals has been used in several recent studies. Using a TLM, Rai et al. (1988) modeled chromate (CrO_4^{2-}) adsorption on kaolinite assuming a heterogeneous surface composed of stoichiometric proportions of silanol (SiOH^0) and aluminol (AlOH^0) sites. For example, stoichiometries for kaolinite ($\text{Al}_2\text{Si}_2\text{O}_5$) and biotite [$\text{K}(\text{Mg,Fe})_3\text{AlSi}_3\text{O}_{10}(\text{OH})_2$] yielded $\text{SiOH}^0:\text{AlOH}^0$ ratios of 1:1 and 3:1, respectively. The acidity constants from Table 3-1 for SiO_2 and $\alpha\text{-Al}_2\text{O}_3$ were used in these proportions, and binding constants were determined using FITEQL. Although there are probably complicating factors such as the effects of ion exchange in the clay structure, SCM approaches are able to reproduce actinide-aluminosilicate sorption behavior reasonably well.

Am(III)-Gamma Alumina
DLM



Am(III)-Gamma Alumina
CCM



Am(III)-Gamma Alumina
TLM

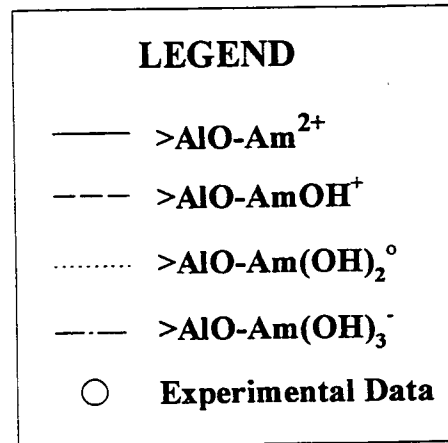
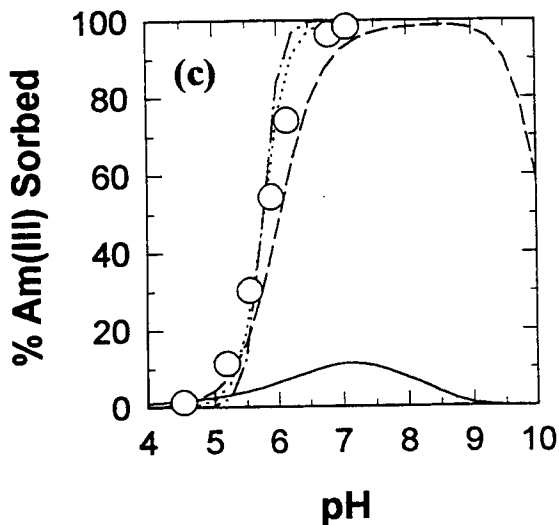


Figure 4-1. Am(III) sorption on $\gamma-Al_2O_3$. SCM results are calculated using parameters derived from the experimental data shown in the figure, and assuming a single adsorbed species (see text). (a) DLM; (b) CCM; and (c) TLM results. $Am(III)_T = 5 \times 10^{-10}$ M, 0.1 M $NaClO_4$, $M/V = 0.01$ g/L. Model parameters from Tables 3-1 and B-1. Data from Righetto et al. (1988).

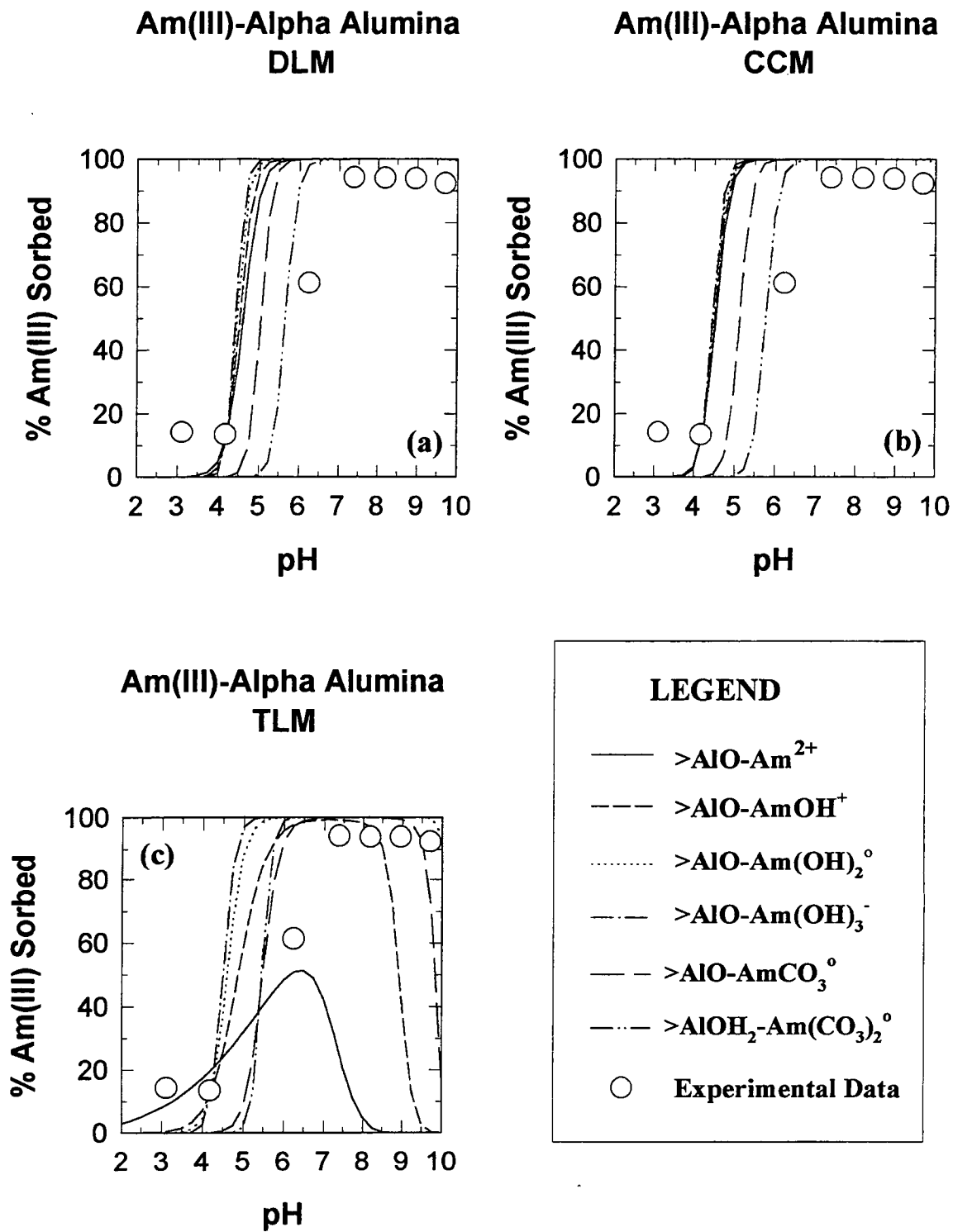
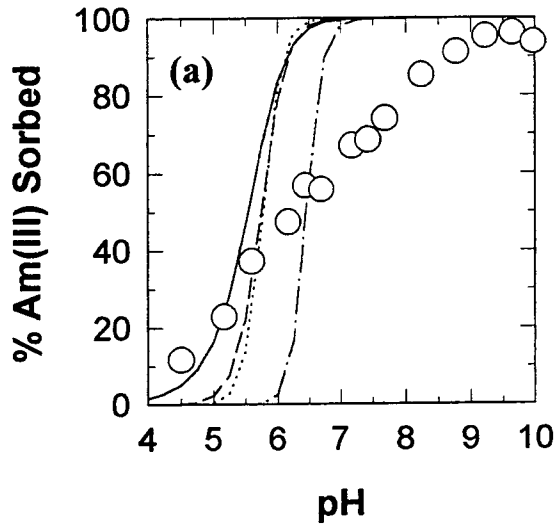
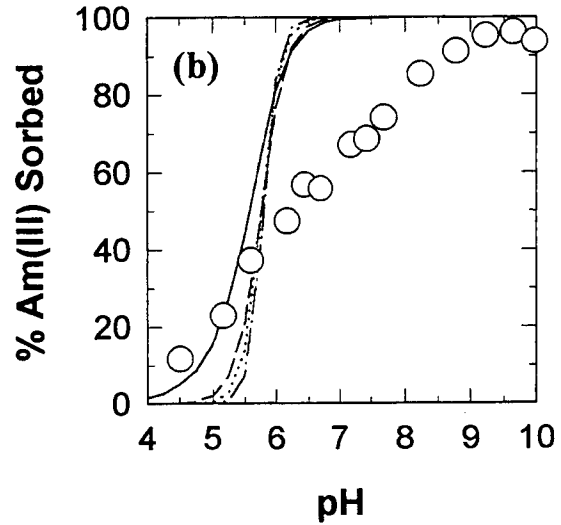


Figure 4-2. Am(III) sorption on $\alpha-Al_2O_3$. SCM results are calculated using parameters derived from the experimental data shown in the figure, and assuming a single adsorbed species (see text). (a) DLM; (b) CCM; and (c) TLM results. $Am(III)_T = 1 \times 10^{-8}$ M, 0.1 M $NaClO_4$, $M/V = 10$ g/L; $p(CO_2) = 10^{-3.5}$ atm. Model parameters from Tables 3-1 and B-2. Data from Moulin et al. (1992).

Am(III)-Amorphous SiO₂
DLM



Am(III)-Amorphous SiO₂
CCM



Am(III)-Amorphous SiO₂
TLM

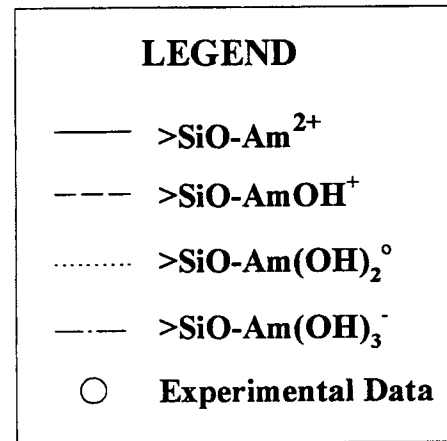
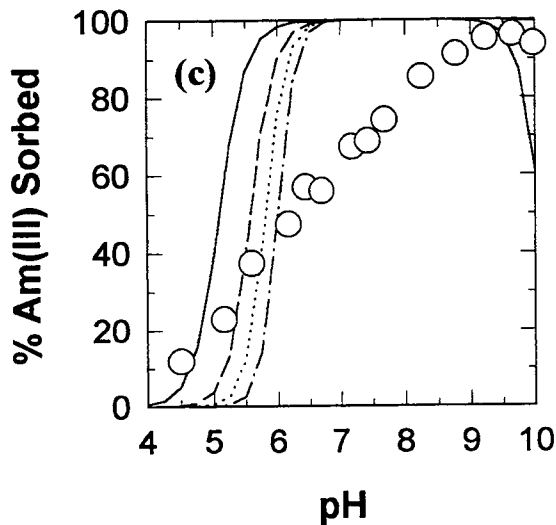
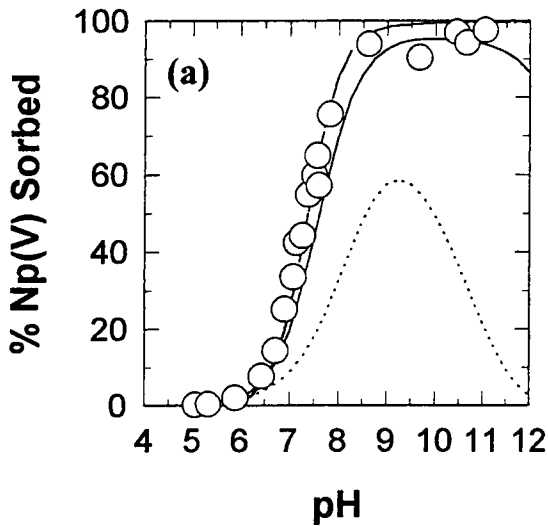
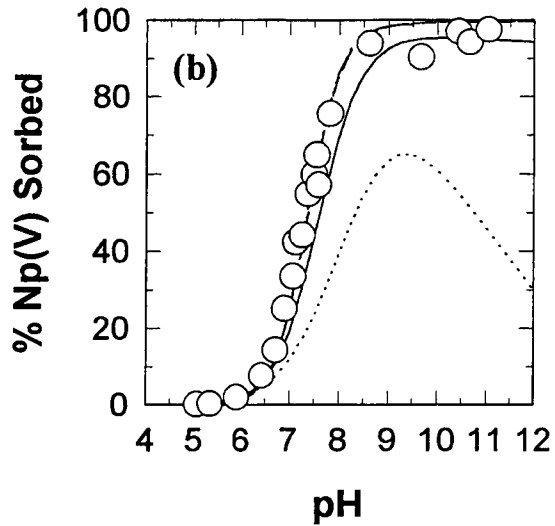


Figure 4-3. Am(III) sorption on amorphous-SiO₂. SCM results are calculated using parameters derived from the experimental data shown in the figure, and assuming a single adsorbed species (see text). (a) DLM; (b) CCM; and (c) TLM results. Am(III)_T = 5 × 10⁻¹⁰ M, 0.1 M NaClO₄, M/V = 1.2 g/L. Model parameters from Tables 3-1 and B-3. Data from Righetto et al. (1991).

Np(V)-Gamma Alumina
DLM



Np(V)-Gamma Alumina
CCM



Np(V)-Gamma Alumina
TLM

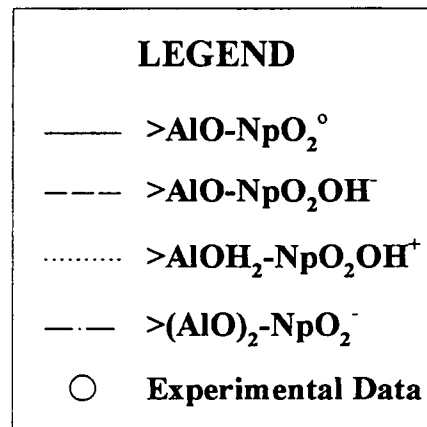
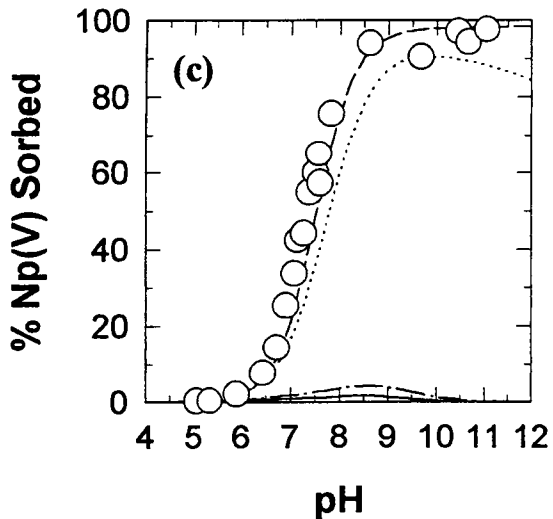


Figure 4-4. Np(V) sorption on $\gamma-Al_2O_3$. SCM results are calculated using parameters derived from the experimental data shown in the figure, and assuming a single adsorbed species (see text). (a) DLM; (b) CCM; and (c) TLM results. $Np(V)_T = 1 \times 10^{-14}$ M, 0.1 M $NaClO_4$, $M/V = 0.2$ g/L. Model parameters from Tables 3-1 and B-4. Data from Righetto et al. (1988).

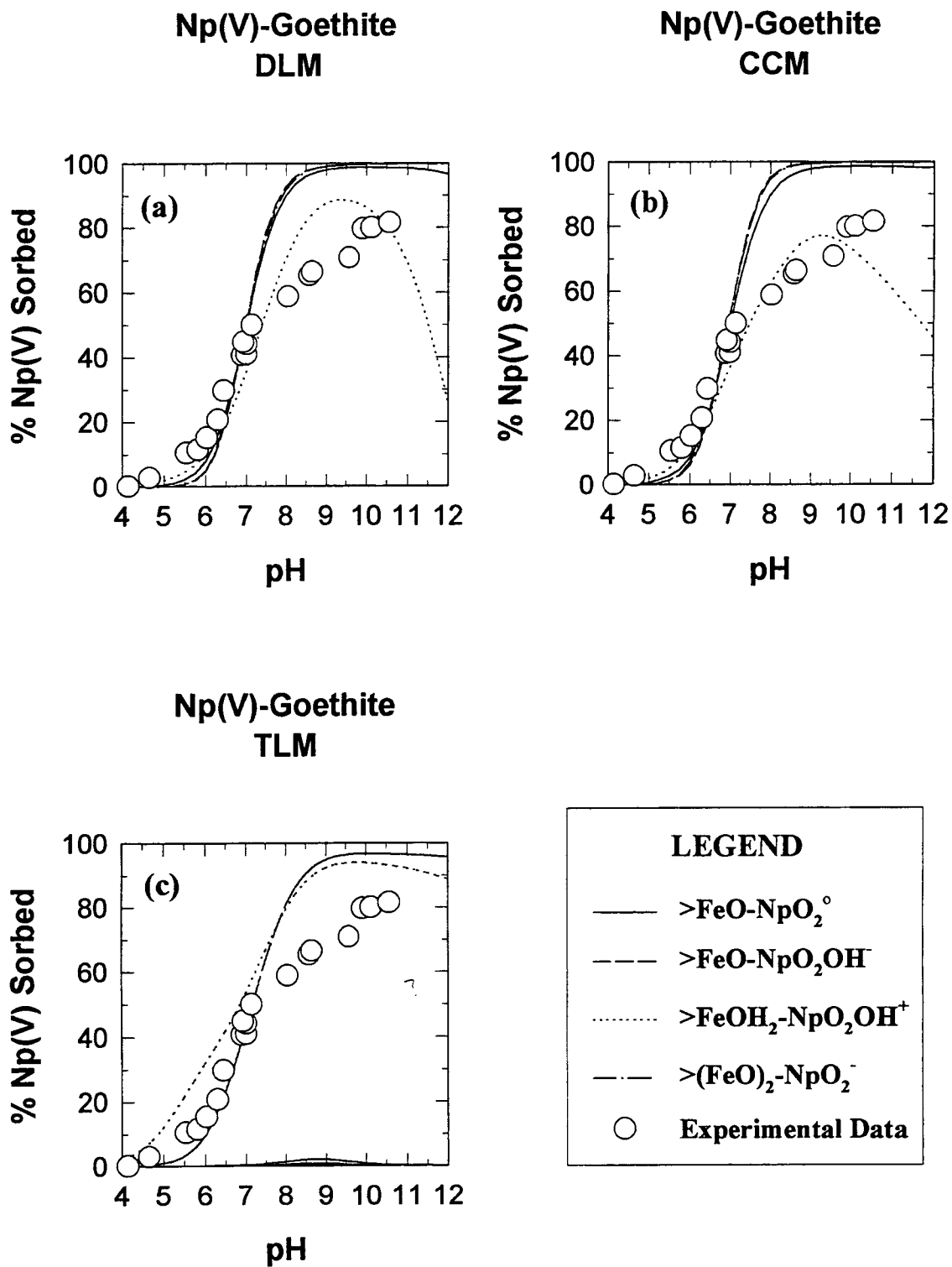


Figure 4-5. Np(V) sorption on goethite. SCM results are calculated using parameters derived from the experimental data shown in the figure, and assuming a single adsorbed species (see text). (a) DLM; (b) CCM; and (c) TLM results. $Np(V)_T = 6 \times 10^{-6}$ M, 0.1 M $NaNO_3$, M/V = 1 g/L. Model parameters from Tables 3-1 and B-5. Data from Nakayama and Sakamoto (1991).

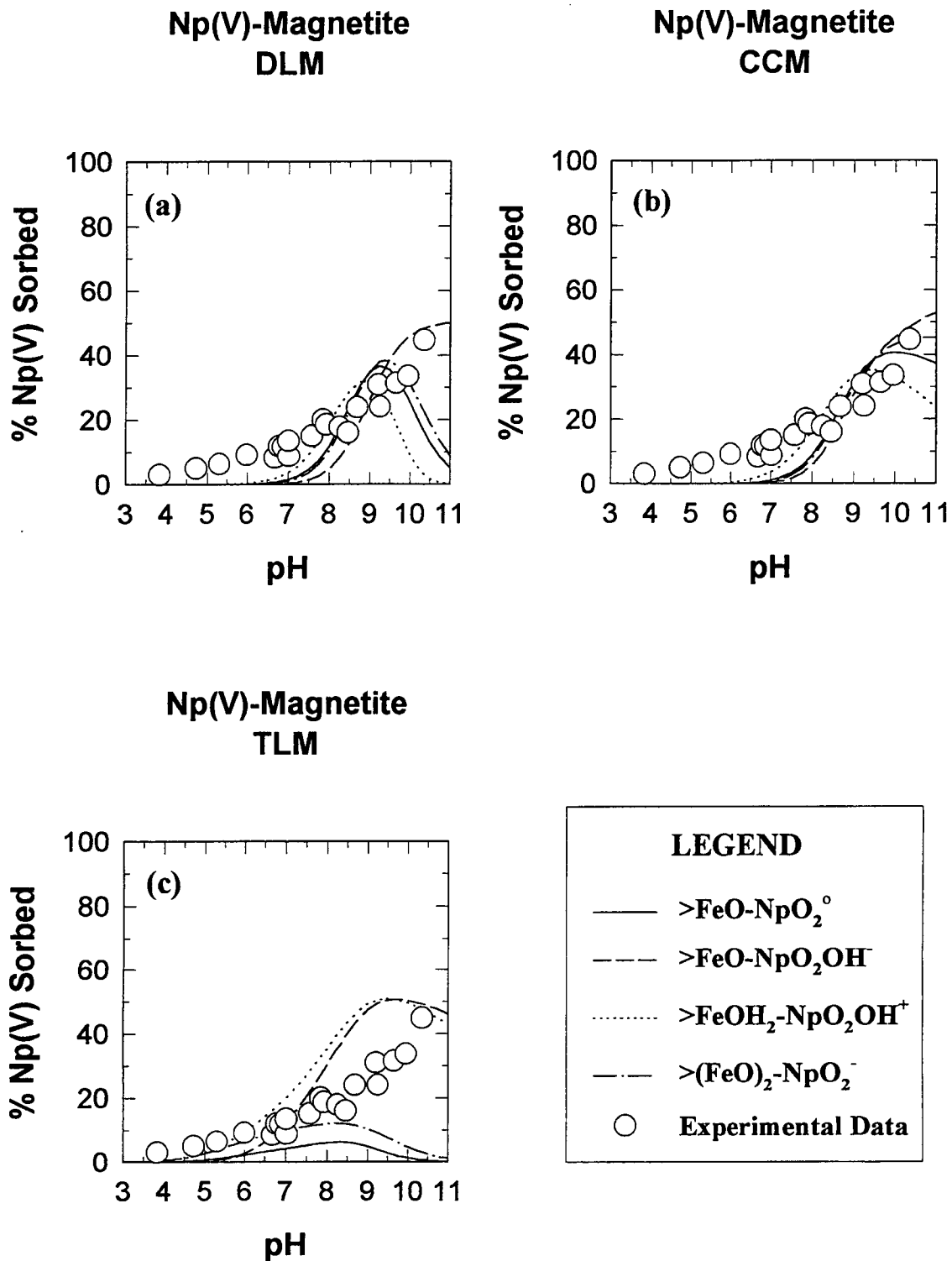


Figure 4-6. Np(V) sorption on synthetic magnetite. SCM results are calculated using parameters derived from the experimental data shown in the figure, and assuming a single adsorbed species (see text). (a) DLM; (b) CCM; and (c) TLM results. $Np(V)_T = 6 \times 10^{-6} M$, $0.1 M NaNO_3$, $M/V = 1 g/L$. Model parameters from Tables 3-1 and B-6. Data from Nakayama and Sakamoto (1991).

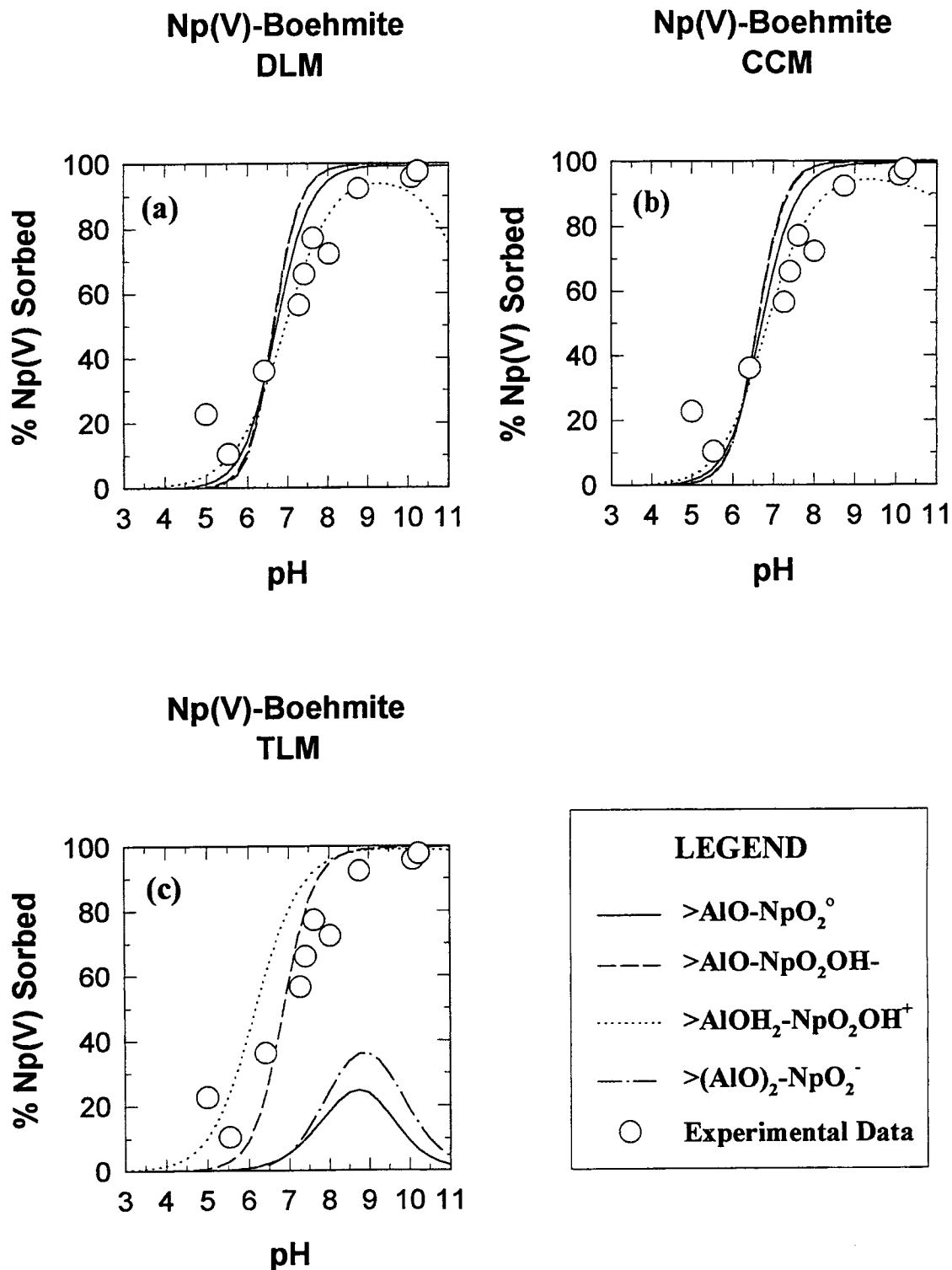
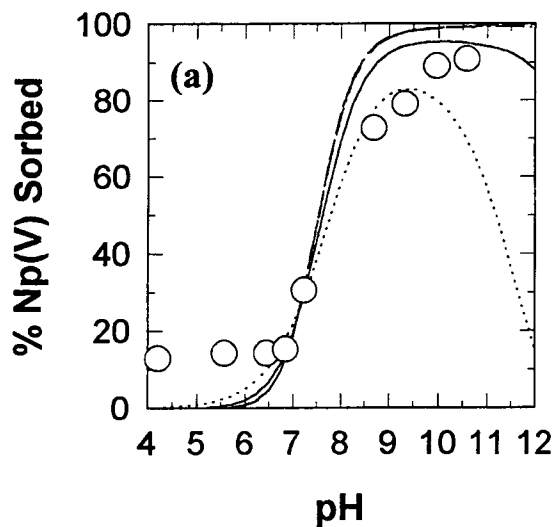
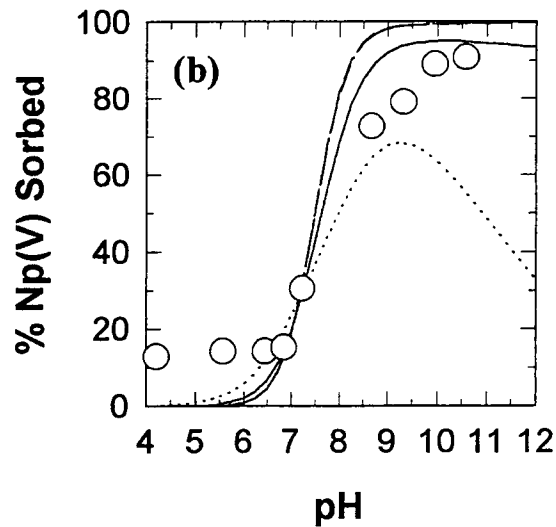


Figure 4-7. Np(V) sorption on boehmite. SCM results are calculated using parameters derived from the experimental data shown in the figure, and assuming a single adsorbed species (see text). (a) DLM; (b) CCM; and (c) TLM results. $Np(V)_T = 6 \times 10^{-6}$ M, 0.1 M $NaNO_3$, $M/V = 1$ g/L. Model parameters from Tables 3-1 and B-7. Data from Nakayama and Sakamoto (1991).

**Np(V)-Lepidocrocite
DLM**



**Np(V)-Lepidocrocite
CCM**



**Np(V)-Lepidocrocite
TLM**

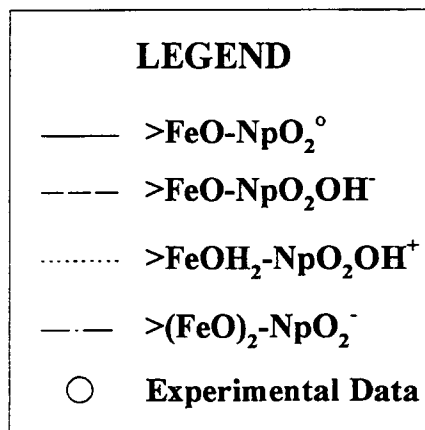
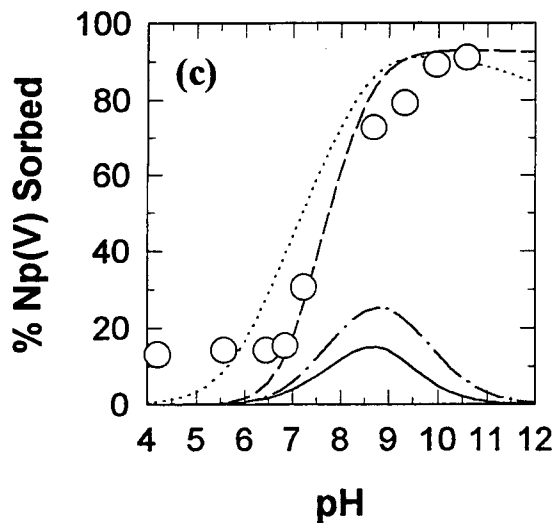
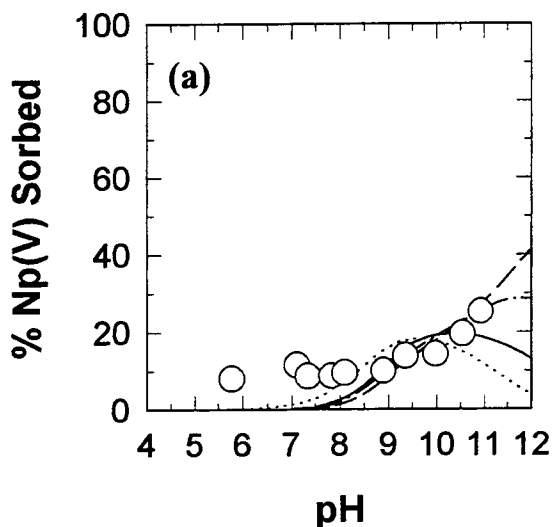
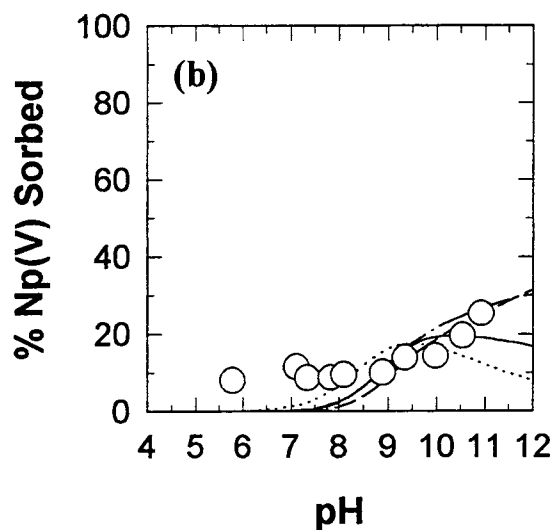


Figure 4-8. Np(V) sorption on lepidocrocite. SCM results are calculated using parameters derived from the experimental data shown in the figure, and assuming a single adsorbed species (see text). (a) DLM; (b) CCM; and (c) TLM results. $Np(V)_T = 6 \times 10^{-6}$ M, 0.1 M $NaNO_3$, M/V = 1 g/L. Model parameters from Tables 3-1 and B-8. Data from Nakayama and Sakamoto (1991).

**Np(V)-Alpha Alumina
DLM**



**Np(V)-Alpha Alumina
CCM**



**Np(V)-Alpha Alumina
TLM**

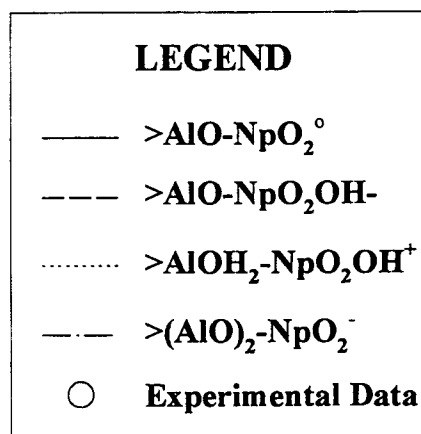
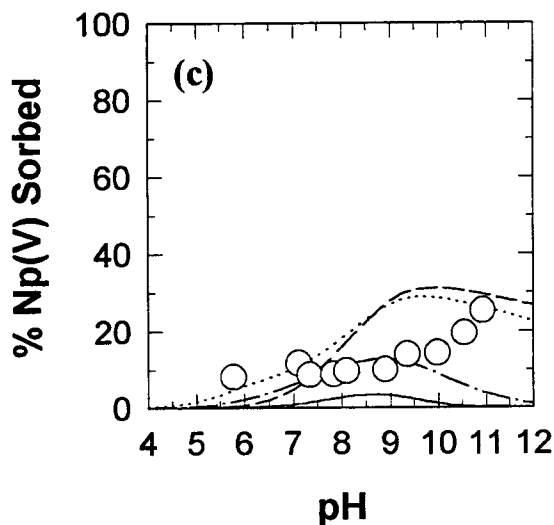


Figure 4-9. Np(V) sorption on $\alpha-Al_2O_3$. SCM results are calculated using parameters derived from the experimental data shown in the figure, and assuming a single adsorbed species (see text). (a) DLM; (b) CCM; and (c) TLM results. $Np(V)_T = 6 \times 10^{-6}$ M, 0.1 M $NaNO_3$, M/V = 1 g/L. Model parameters from Tables 3-1 and B-9. Data from Nakayama and Sakamoto (1991).

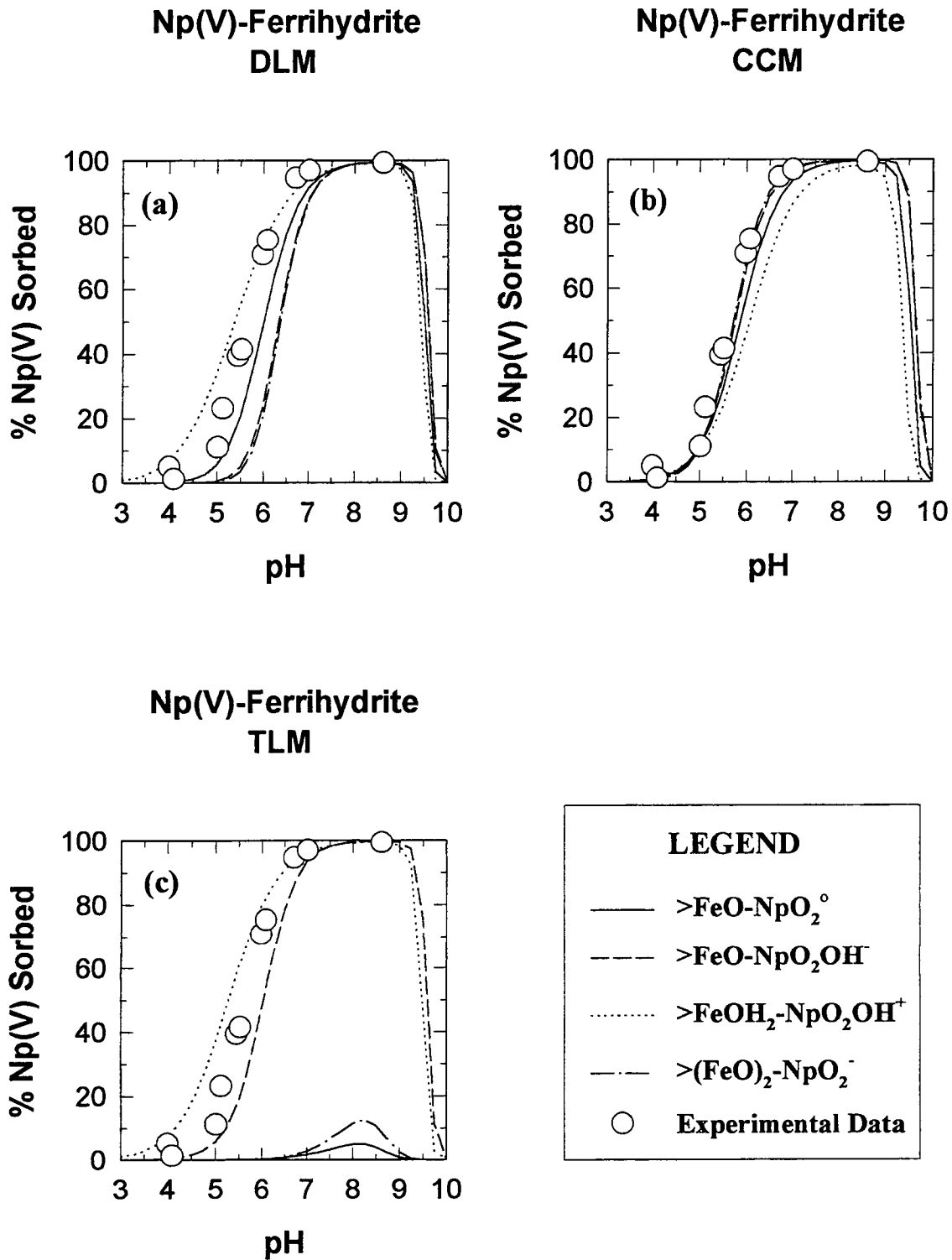
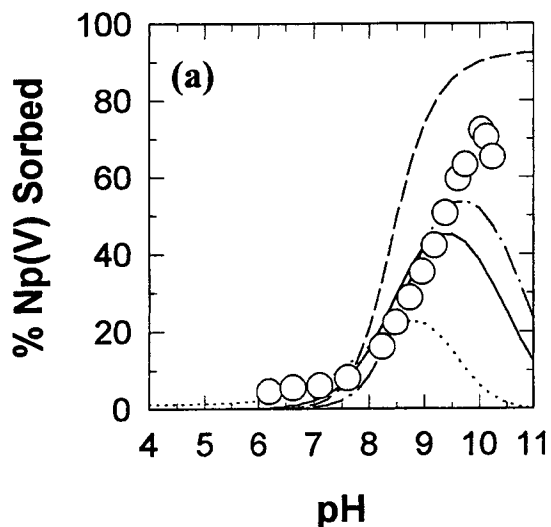
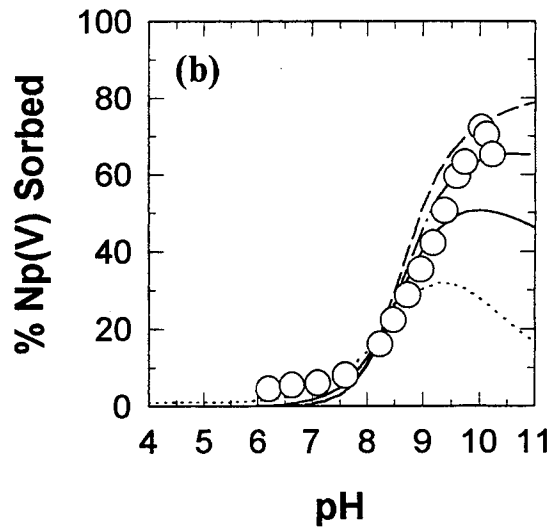


Figure 4-10. Np(V) sorption on ferrihydrite. SCM results are calculated using parameters derived from the experimental data shown in the figure, and assuming a single adsorbed species (see text). (a) DLM; (b) CCM; and (c) TLM results. $Np(V)_T = 4.7 \times 10^{-12}$ M, 0.1 M $NaNO_3$, $M/V = 0.89$ g/L. Model parameters from Tables 3-1 and B-10. Data from Girvin et al. (1991).

Np(V)-Amorphous SiO₂
DLM



Np(V)-Amorphous SiO₂
CCM



Np(V)-Amorphous SiO₂
TLM

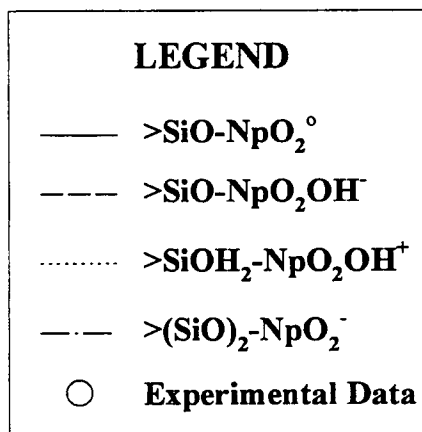
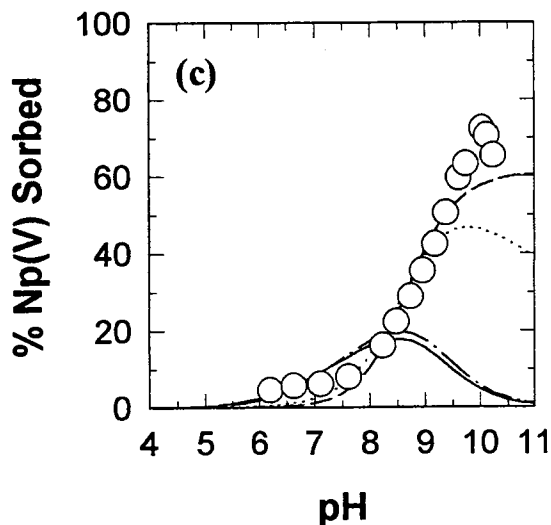


Figure 4-11. Np(V) sorption on amorphous SiO₂. SCM results are calculated using parameters derived from the experimental data shown in the figure, and assuming a single adsorbed species (see text). (a) DLM; (b) CCM; and (c) TLM results. $\text{Np(V)}_T = 1 \times 10^{-14}$ M, 0.1 M NaClO₄, M/V = 1.2 g/L. Model parameters from Tables 3-1 and B-11. Data from Righetto et al. (1991).

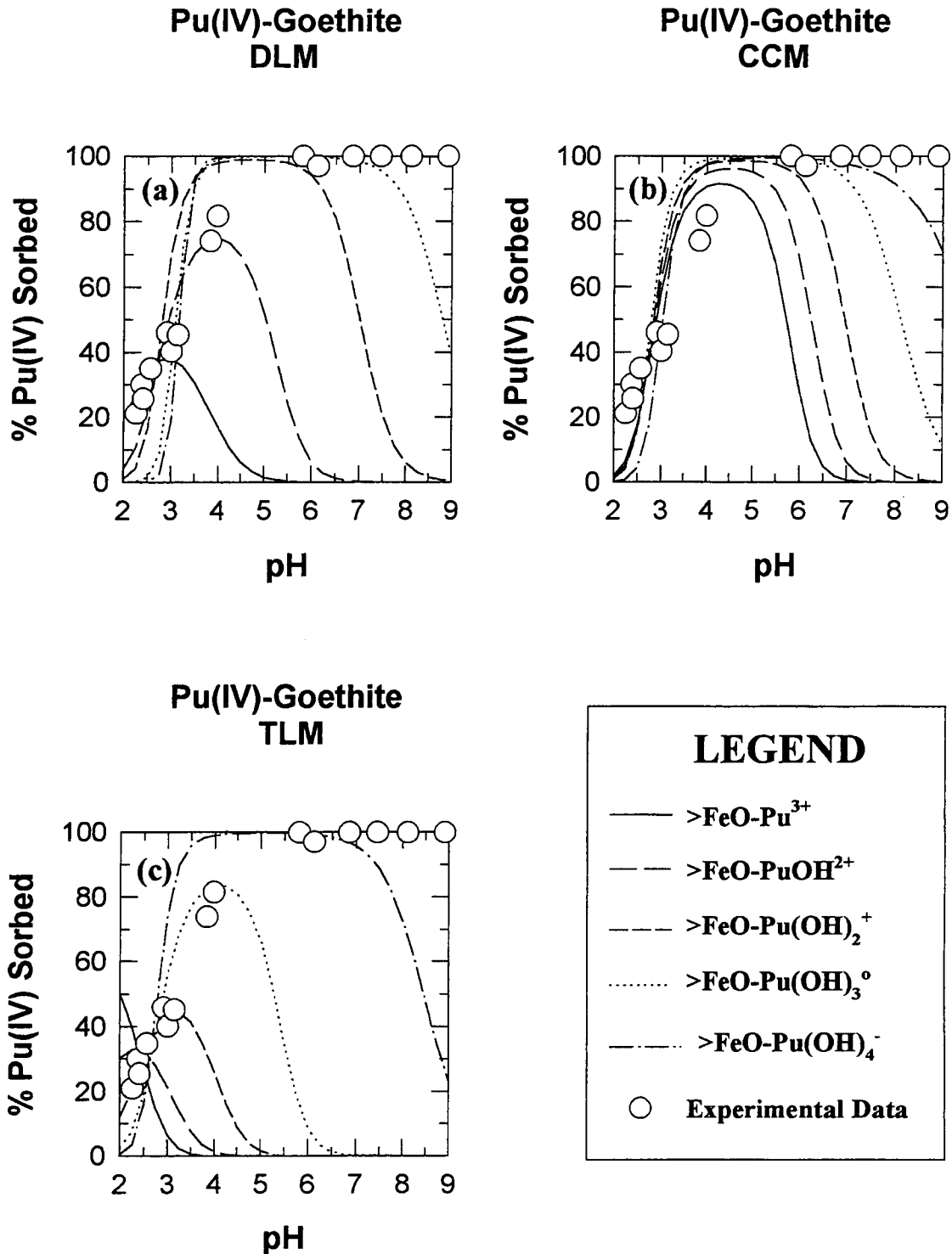


Figure 4-12. Pu(IV) sorption on goethite. SCM results are calculated using parameters derived from the experimental data shown in the figure, and assuming a single adsorbed species (see text). (a) DLM; (b) CCM; and (c) TLM results. $\text{Pu(IV)}_T = 1 \times 10^{-11}$ M, 0.1 M NaNO_3 , $M/V = 0.55$ g/L. Model parameters from Tables 3-1 and B-12. Data from Sanchez et al. (1985).

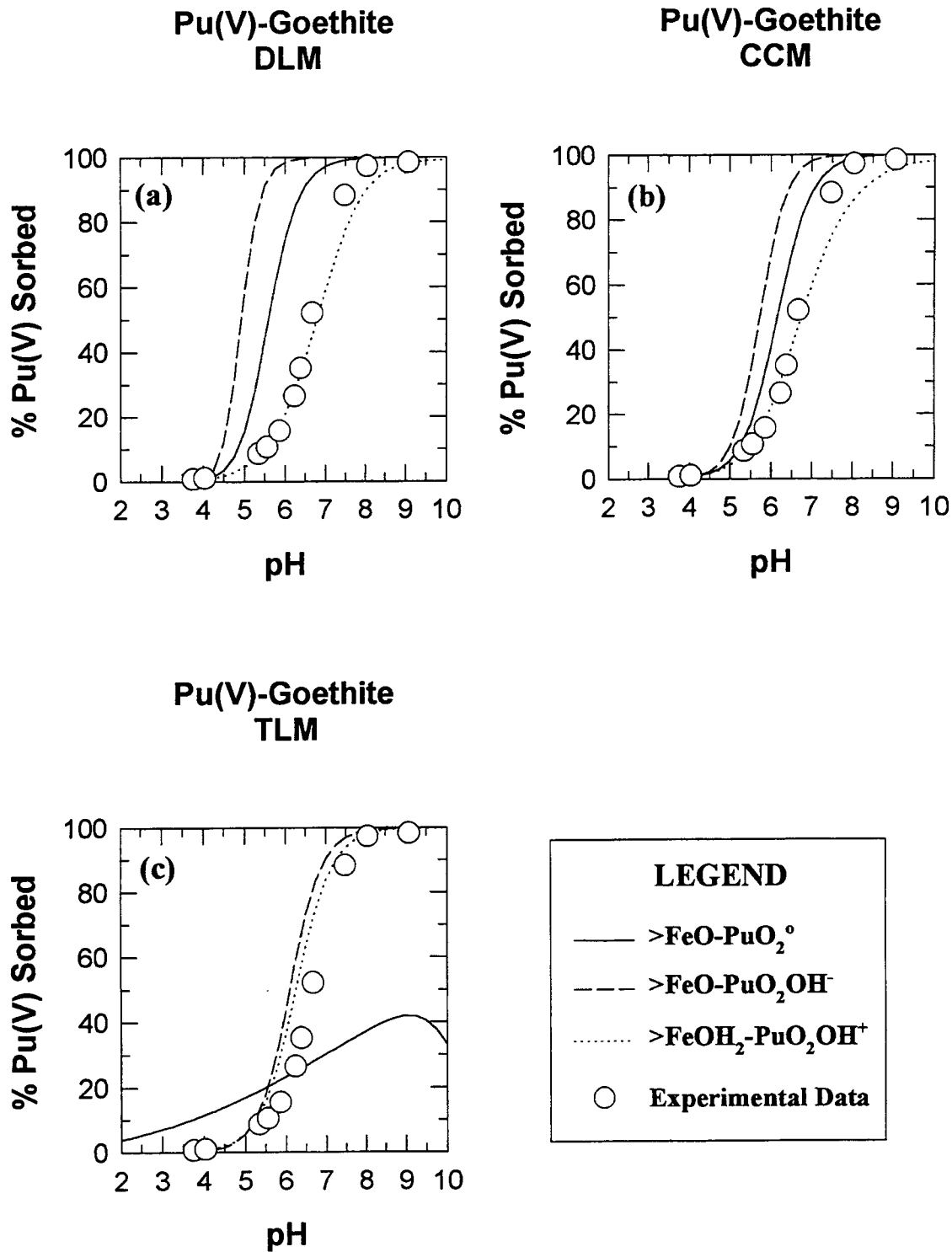


Figure 4-13. Pu(V) sorption on goethite. SCM results are calculated using parameters derived from the experimental data shown in the figure, and assuming a single adsorbed species (see text). (a) DLM; (b) CCM; and (c) TLM results. $Pu(V)_T = 1 \times 10^{-11}$ M, 0.1 M $NaNO_3$, $M/V = 0.55$ g/L. Model parameters from Tables 3-1 and B-13. Data from Sanchez et al. (1985).

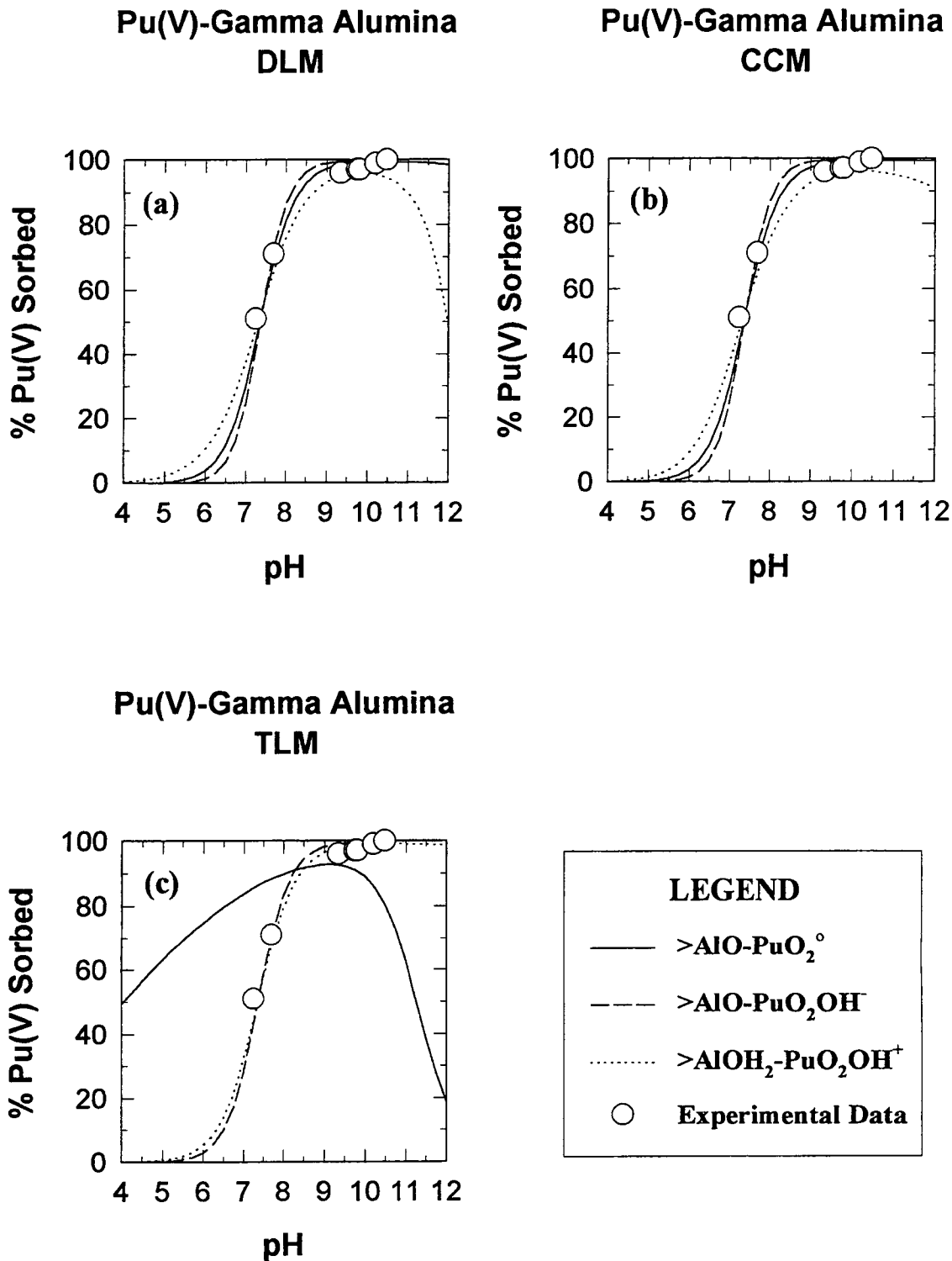
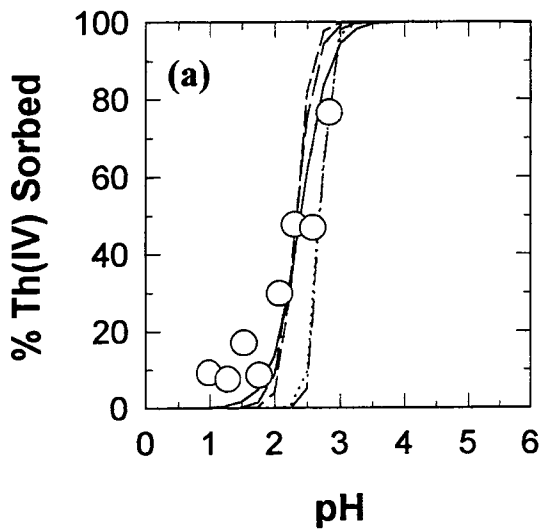
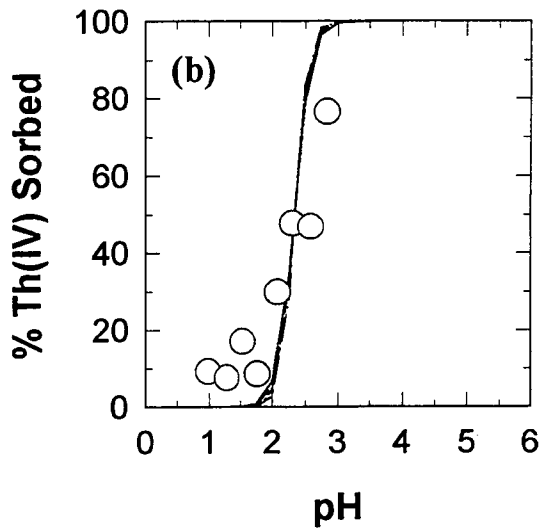


Figure 4-14. Pu(V) sorption on $\gamma-Al_2O_3$. SCM results are calculated using parameters derived from the experimental data shown in the figure, and assuming a single adsorbed species (see text). (a) DLM; (b) CCM; and (c) TLM results. $Pu(V)_T = 2 \times 10^{-10}$ M, 0.1 M $NaClO_4$, $M/V = 0.2$ g/L. Model parameters from Tables 3-1 and B-14. Data from Righetto et al. (1991).

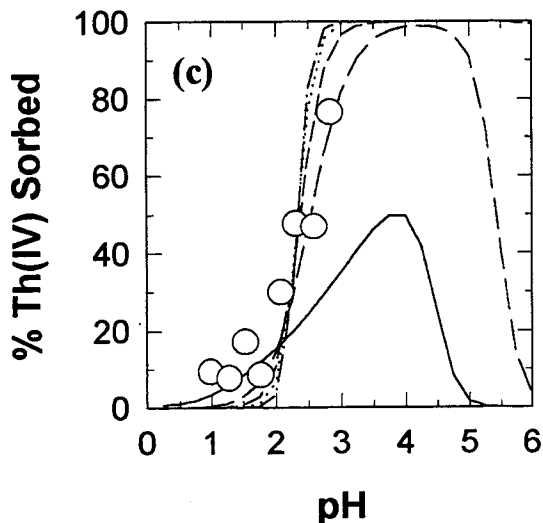
Th(IV)-Gamma Alumina
DLM



Th(IV)-Gamma Alumina
CCM



Th(IV)-Gamma Alumina
TLM



LEGEND

- $>AlO-Th^{3+}$
- - $>AlO-ThOH^{2+}$
- - - $>AlO-Th(OH)_2^+$
- $>AlO-Th(OH)_3^0$
- - - $>AlO-Th(OH)_4^-$
- Experimental Data

Figure 4-15. Th(IV) sorption on $\gamma-Al_2O_3$. SCM results are calculated using parameters derived from the experimental data shown in the figure, and assuming a single adsorbed species (see text). (a) DLM; (b) CCM; and (c) TLM results. $Th(IV)_T = 1 \times 10^{-11}$ M, 0.1 M $NaClO_4$, $M/V = 0.01$ g/L. Model parameters from Tables 3-1 and B-15. Data from Righetto et al. (1988).

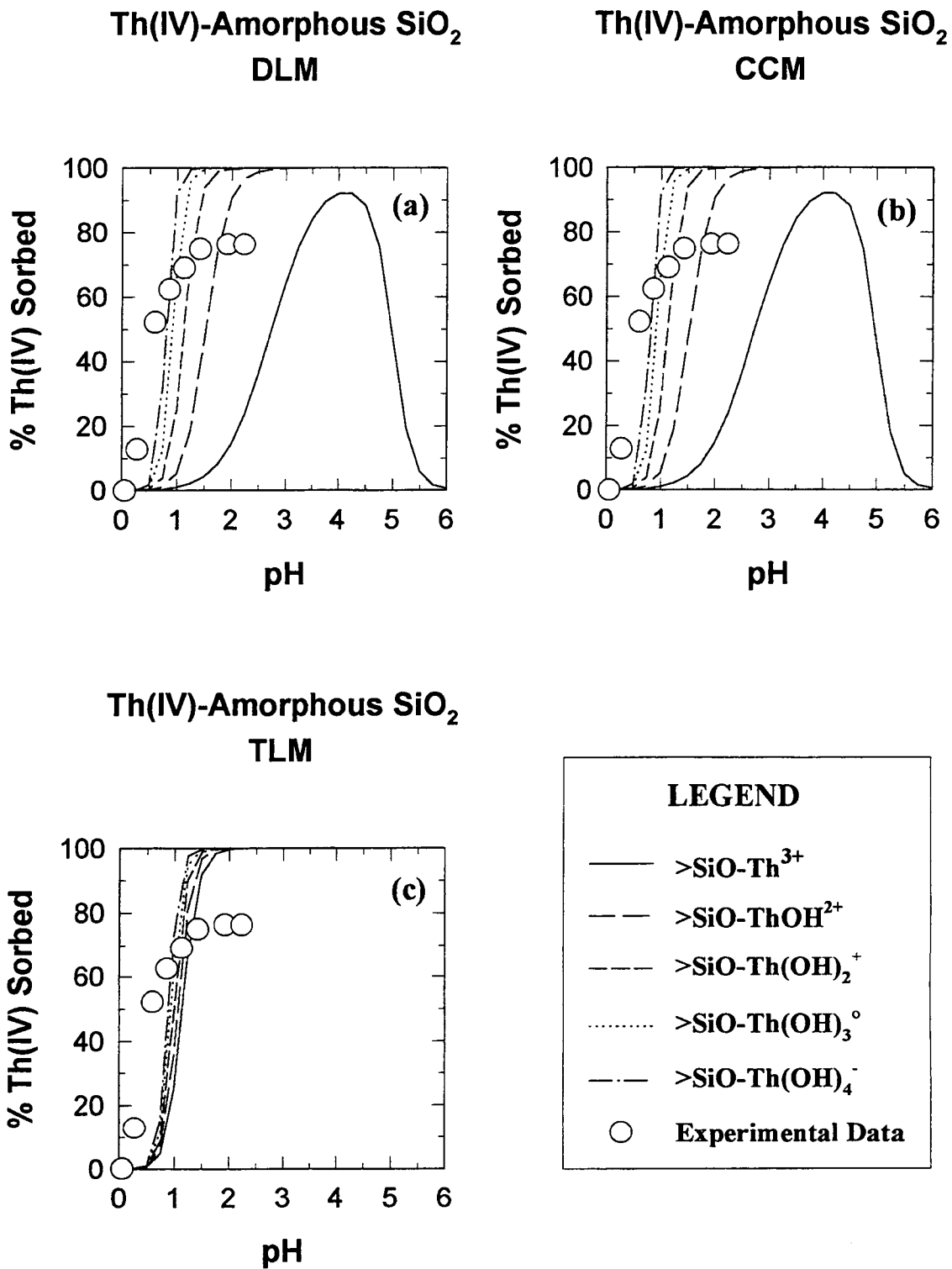


Figure 4-16. Th(IV) sorption on amorphous SiO₂. SCM results are calculated using parameters derived from the experimental data shown in the figure, and assuming a single adsorbed species (see text). (a) DLM; (b) CCM; and (c) TLM results. Th(IV)_T=1×10⁻¹¹ M, 0.1 M NaClO₄, M/V=0.06 g/L. Model parameters from Tables 3-1 and B-16. Data from Righetto et al. (1991).

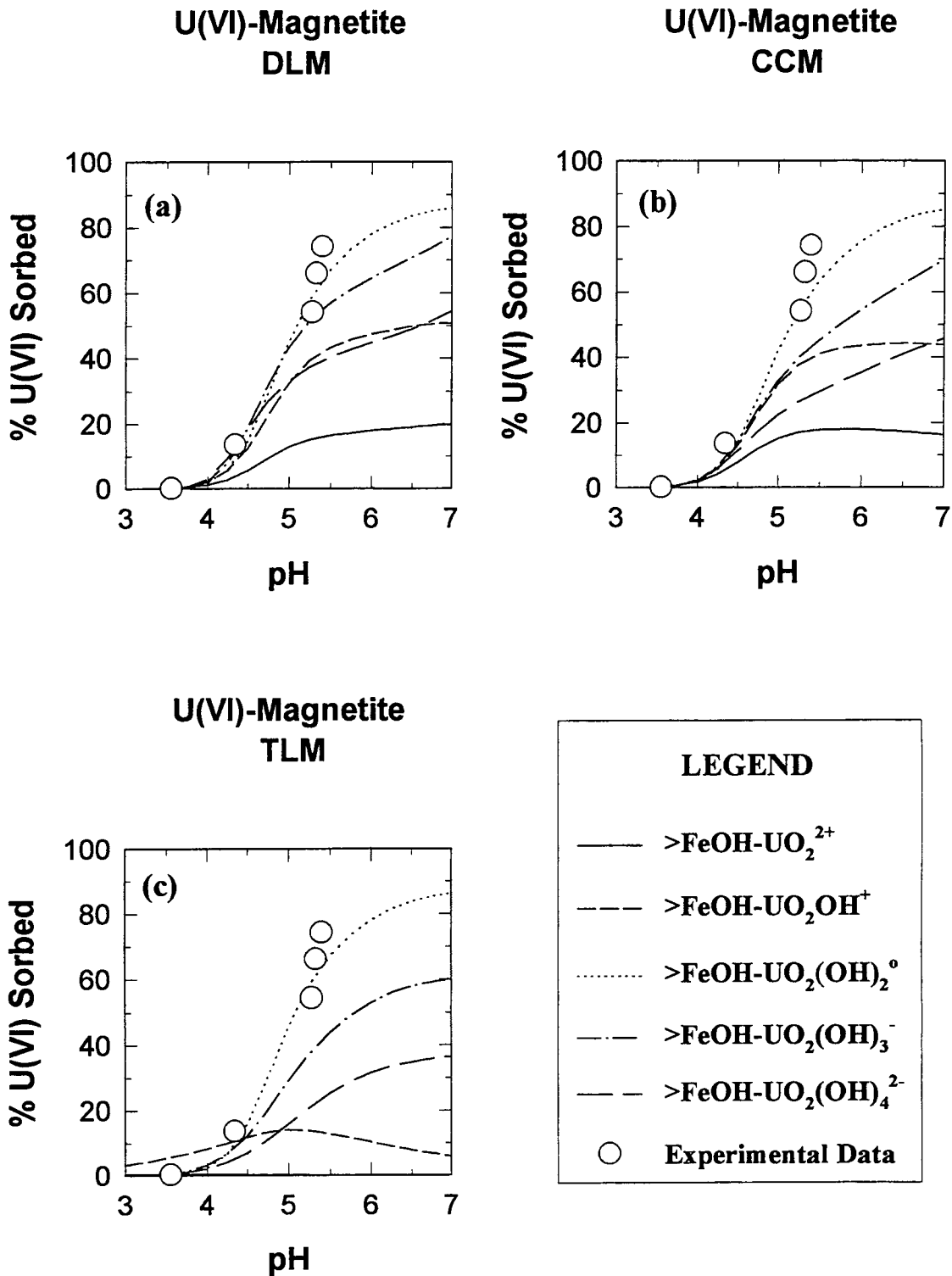


Figure 4-17. U(VI) sorption on magnetite. SCM results are calculated using parameters derived from the experimental data shown in the figure, and assuming a single adsorbed species (see text). (a) DLM; (b) CCM; and (c) TLM results. $U(VI)_T = 1 \times 10^{-4}$ M, 0.1 M NaCl, M/V = 8 g/L. Model parameters from Tables 3-1 and B-17. Data from Venkataramani and Gupta (1991).

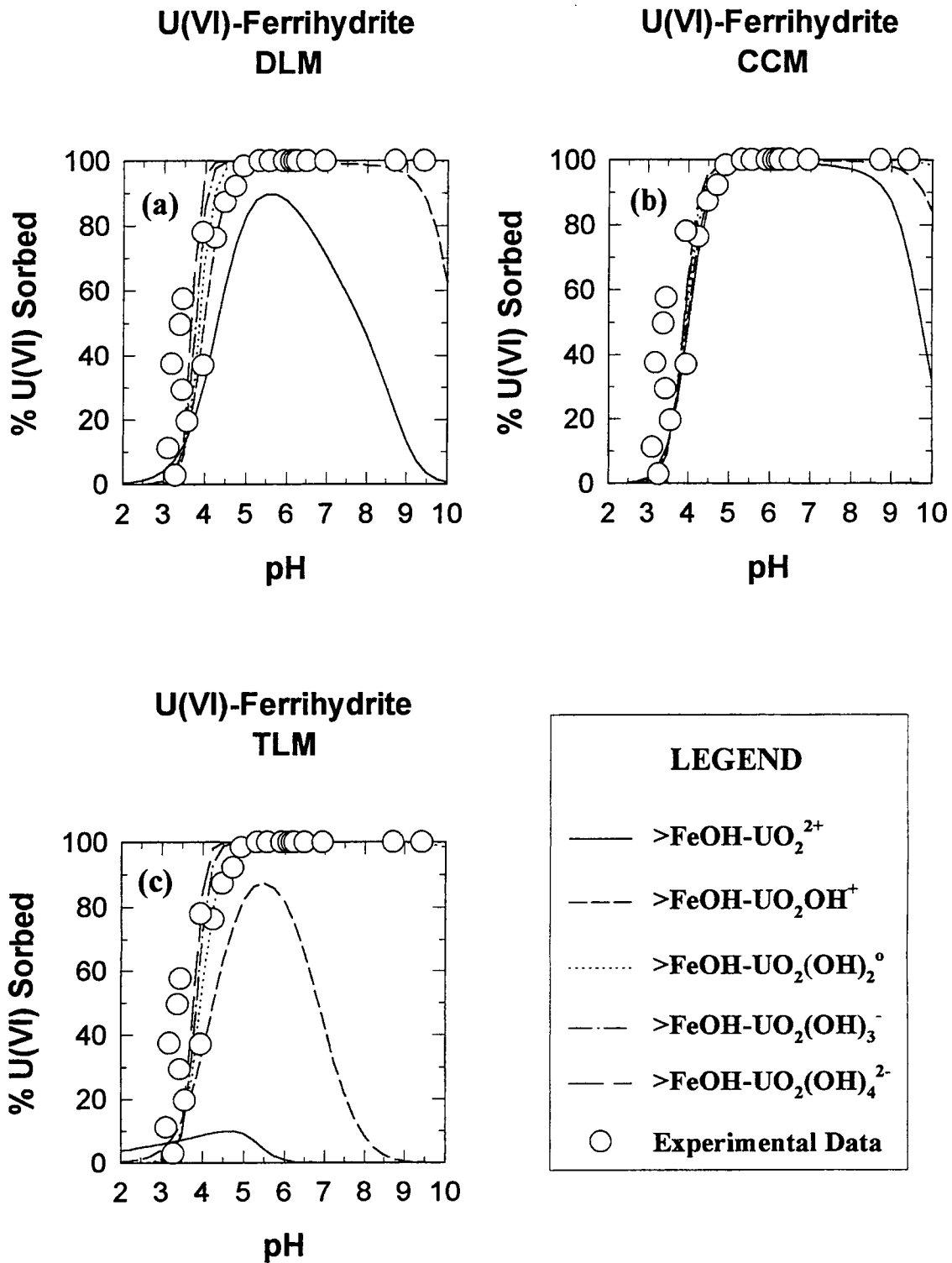


Figure 4-18. U(VI) sorption on ferrihydrite. SCM results are calculated using parameters derived from the experimental data shown in the figure, and assuming a single adsorbed species (see text). (a) DLM; (b) CCM; and (c) TLM results. $U(VI)_T = 1 \times 10^{-5} M$, $0.1 M NaNO_3$, $M/V = 1 g/L$. Model parameters from Tables 3-1 and B-18. Data from Hsi and Langmuir (1985).

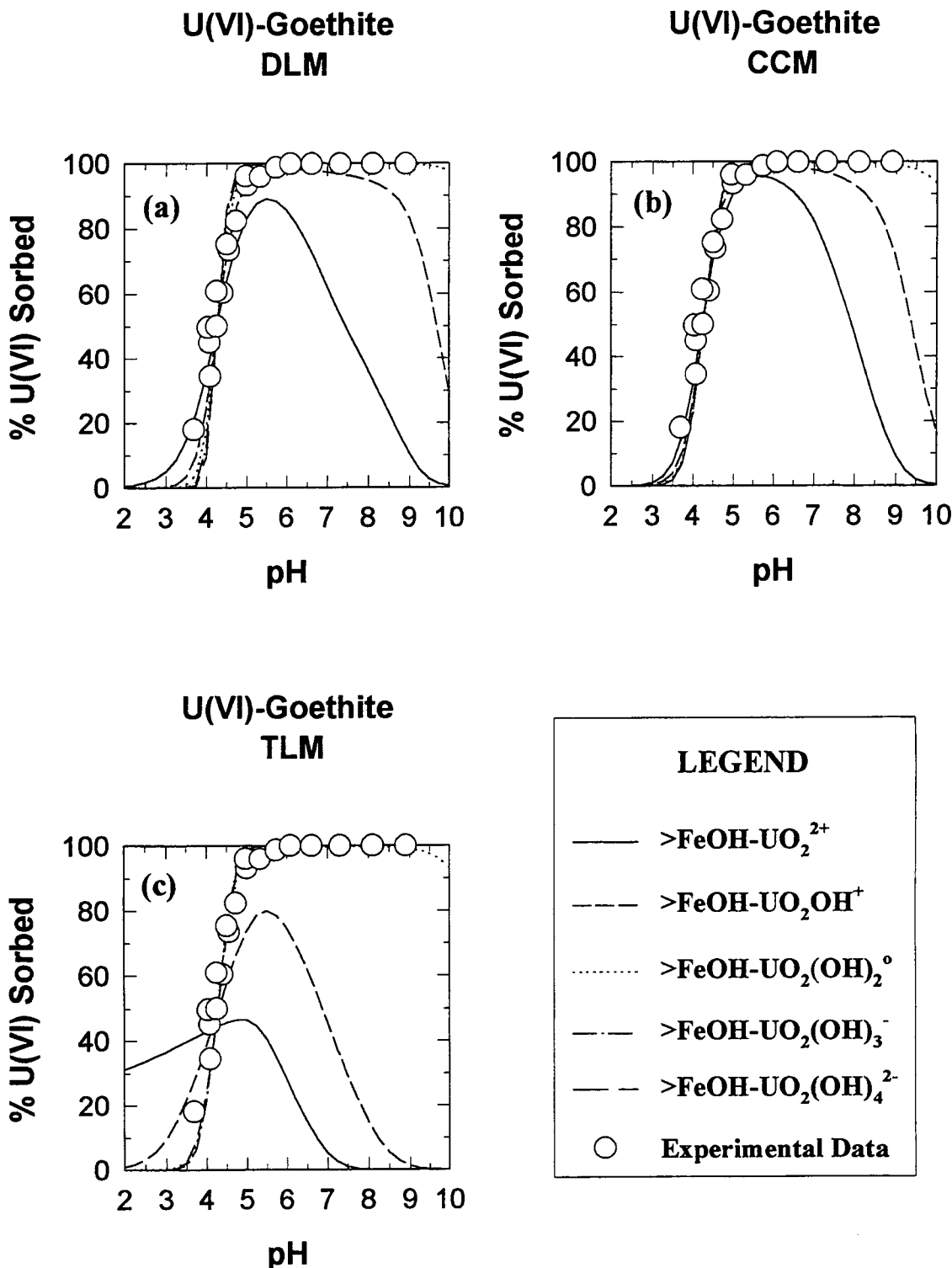


Figure 4-19. U(VI) sorption on goethite. SCM results are calculated using parameters derived from the experimental data shown in the figure, and assuming a single adsorbed species (see text). (a) DLM; (b) CCM; and (c) TLM results. $U(VI)_T = 1 \times 10^{-5} M$, $0.1 M NaNO_3$, $M/V = 1 g/L$. Model parameters from Tables 3-1 and B-19. Data from Hsi and Langmuir (1985).

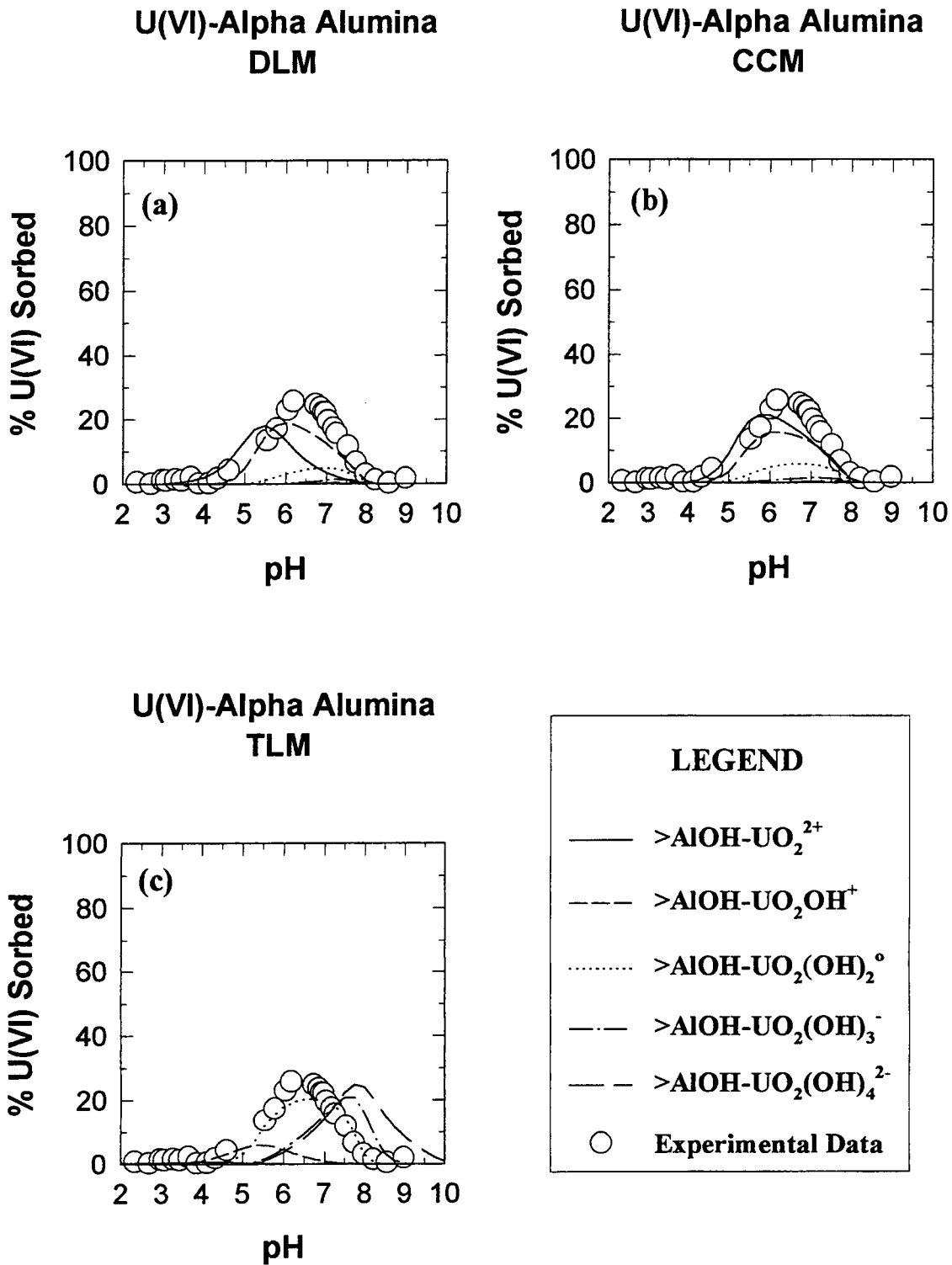


Figure 4-20. U(VI) sorption on $\alpha-Al_2O_3$. SCM results are calculated using parameters derived from the experimental data shown in the figure, and assuming a single adsorbed species (see text). (a) DLM; (b) CCM; and (c) TLM results. $U(VI)_T = 4.8 \times 10^{-7}$ M, 0.1 M $NaNO_3$, M/V = 2.5 g/L. Model parameters from Tables 3-1 and B-20. Data from Pabalan and Turner (1994).

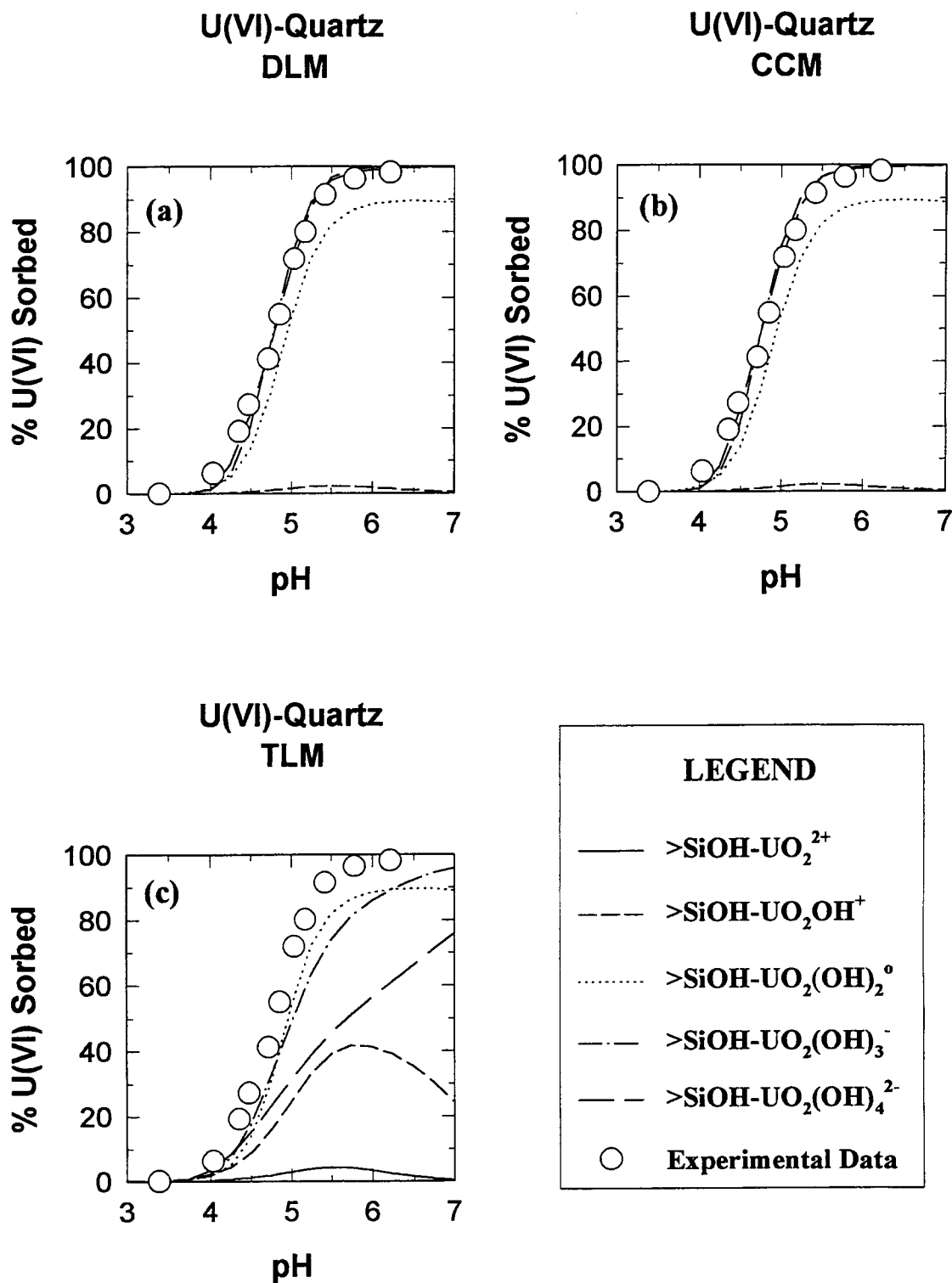


Figure 4-21. U(VI) sorption on quartz. SCM results are calculated using parameters derived from the experimental data shown in the figure, and assuming a single adsorbed species (see text). (a) DLM; (b) CCM; and (c) TLM results. $U(VI)_T = 1 \times 10^{-6}$ M, 0.1 M $KClO_4$, $M/V = 100$ g/L. Model parameters from Tables 3-1 and B-21. Data from Waite et al. (1993).

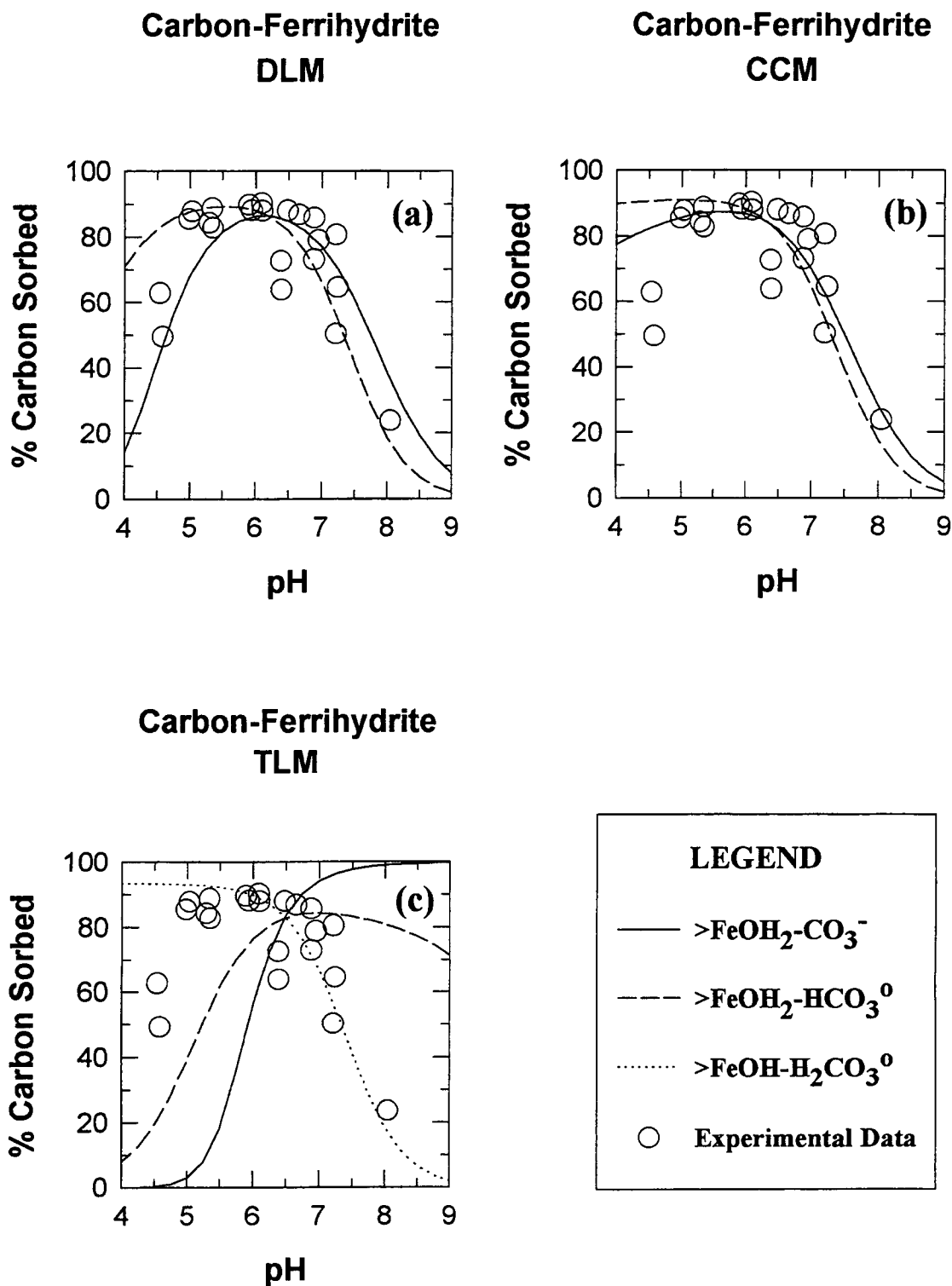


Figure 4-22. Carbon sorption on ferrihydrite. SCM results are calculated using parameters derived from the experimental data shown in the figure, and assuming a single adsorbed species (see text). (a) DLM; (b) CCM; and (c) TLM results. $C_T = 4.6 \times 10^{-6}$ M, 0.1 M $NaNO_3$, $M/V = 0.77$ g/L. Model parameters from Tables 3-1 and B-22. Data from Zachara et al. (1987).

4.3 SCM AND CHANGES IN SYSTEM CHEMISTRY

As demonstrated by the data investigated in this study, radioelement sorption is strongly influenced by system chemistry. For example, system pH clearly exerts a strong influence on sorption for most of the minerals investigated. Other factors include the concentrations of competing ligands such as CO_3^{2-} and HCO_3^- , radionuclide concentration, and M/V. One reason for investigating more complex mechanistic sorption models is to allow for an evaluation of the relative effects of these chemical parameters. Therefore, one measure of the suitability of uniform SCMs as mechanistic approaches to sorption modeling is the ability of these models to account for the effects of changes in system chemistry. It is important that these models be flexible and robust enough to predict changes in sorption behavior beyond experimental conditions to conditions likely to be encountered in the natural system. At the same time, it is desirable for PA that these models be as simple as possible to limit the computational burden placed on PA codes.

4.3.1 Effect of pH

Examining the experimental data that are presented in Figures 4-1 through 4-25, it is apparent that actinide and carbon sorption is very sensitive to changes in system pH. For simple (hydr)oxides (Figures 4-1 through 4-22), the models predict a very steep sorption edge as a function of pH. Given the high charge of the several actinide species (e.g., Th^{4+} and Am^{3+}), surface reactions of the form given in Eq. (3-1) tend to involve a large number of protons (H^+). This is particularly true for highly hydrolyzed surface species that involve more than one hydroxyl (e.g. $>\text{XOH-Th}(\text{OH})_4^0$). The large number of protons, combined with the model specific electrostatic corrections for highly charged species leads to the strong pH dependence shown in the model results. For most of the actinide-(hydr)oxide systems studied, this predicted behavior is consistent with the experimental evidence, and the match between the data and the model results is quite good. In some cases, however, such as Am(III)-amorphous SiO_2 (Righetto et al. 1988), the models predict a sorption edge that is much sharper than observed in the experimental data. This discrepancy suggests that the reactions selected are inappropriate to this data set; reactions that are less strongly a function of pH are perhaps more suitable. Contaminant speciation (especially for actinides) varies rapidly as a function of pH. For this reason, sorption edges that extend over wider pH ranges tend to require more than one surface complex (Davis and Leckie, 1978; Dzombak and Morel, 1990). Another possibility is the formation of multidentate surface complexes involving more than one surface site. Such surface complexes are possible given the relatively large ionic radius of the actinides (Hsi and Langmuir, 1985). Future efforts will focus on investigating these possibilities.

For the sorption data available for aluminosilicates, the sorption edge is typically steep, and for the pH range studied, there is no desorption edge (Figures 4-23 through 4-25). For example, for Np sorption on biotite and kaolinite, several of the models match the observed sorption edge, but predict a flattening or even a decrease in sorption at pH values beyond the experimental range. Although these predictions have yet to be evaluated and confirmed by a broader range in experimental conditions, this demonstrates the ability of SCM approaches to predict complex sorption behavior outside of the range in experimental conditions in a way that is beyond the capabilities of purely empirical approaches.

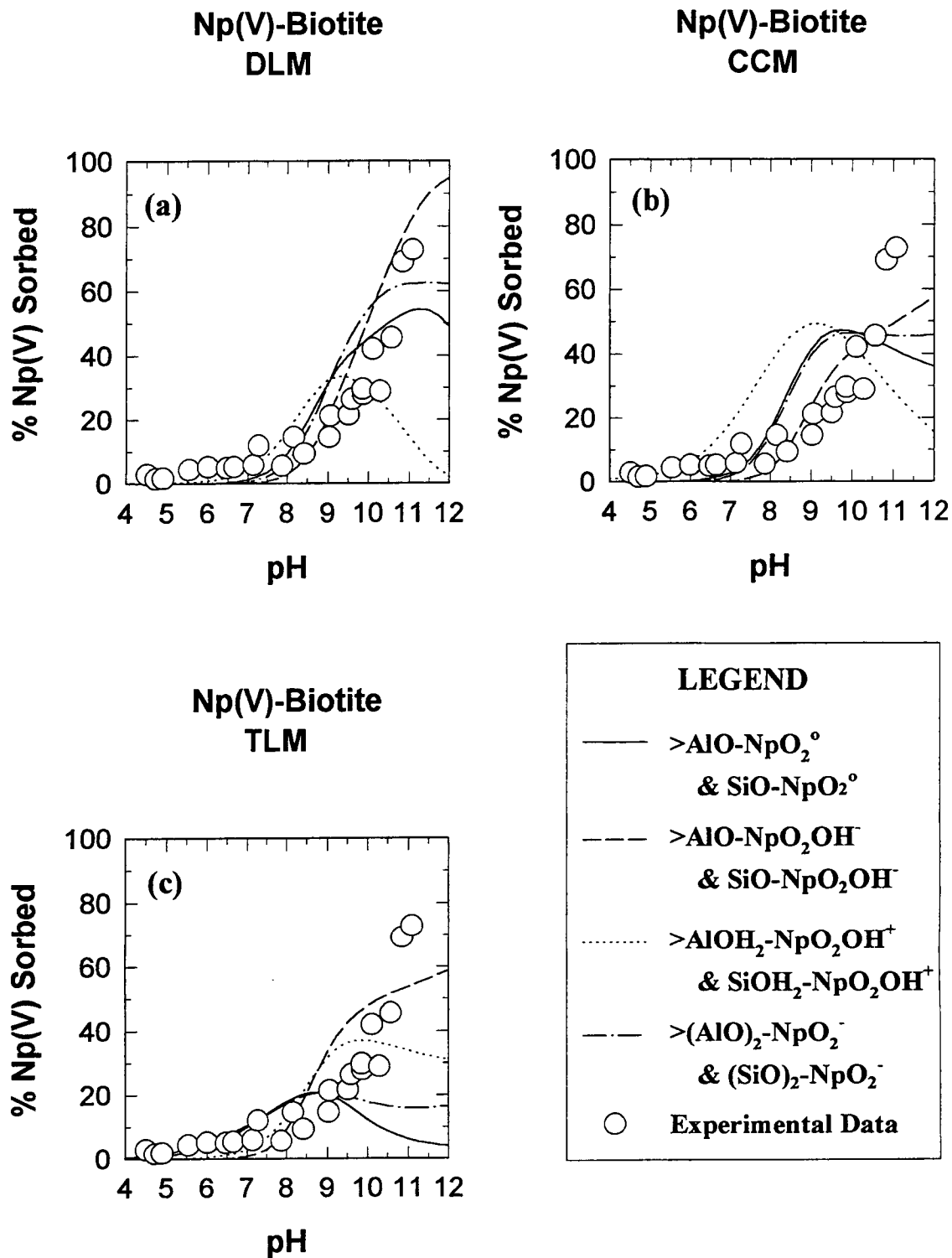


Figure 4-23. SCM predictions of Np(V) sorption on biotite (a) DLM; (b) CCM; and (c) TLM results. $Np(V)_T = 6 \times 10^{-6}$ M, 0.1 M $NaNO_3$, M/V=1 g/L. Model parameters from Tables 3-1 and B-23. Si:Al ratio of 3:1 assumed. Data from Nakayama and Sakamoto (1991).

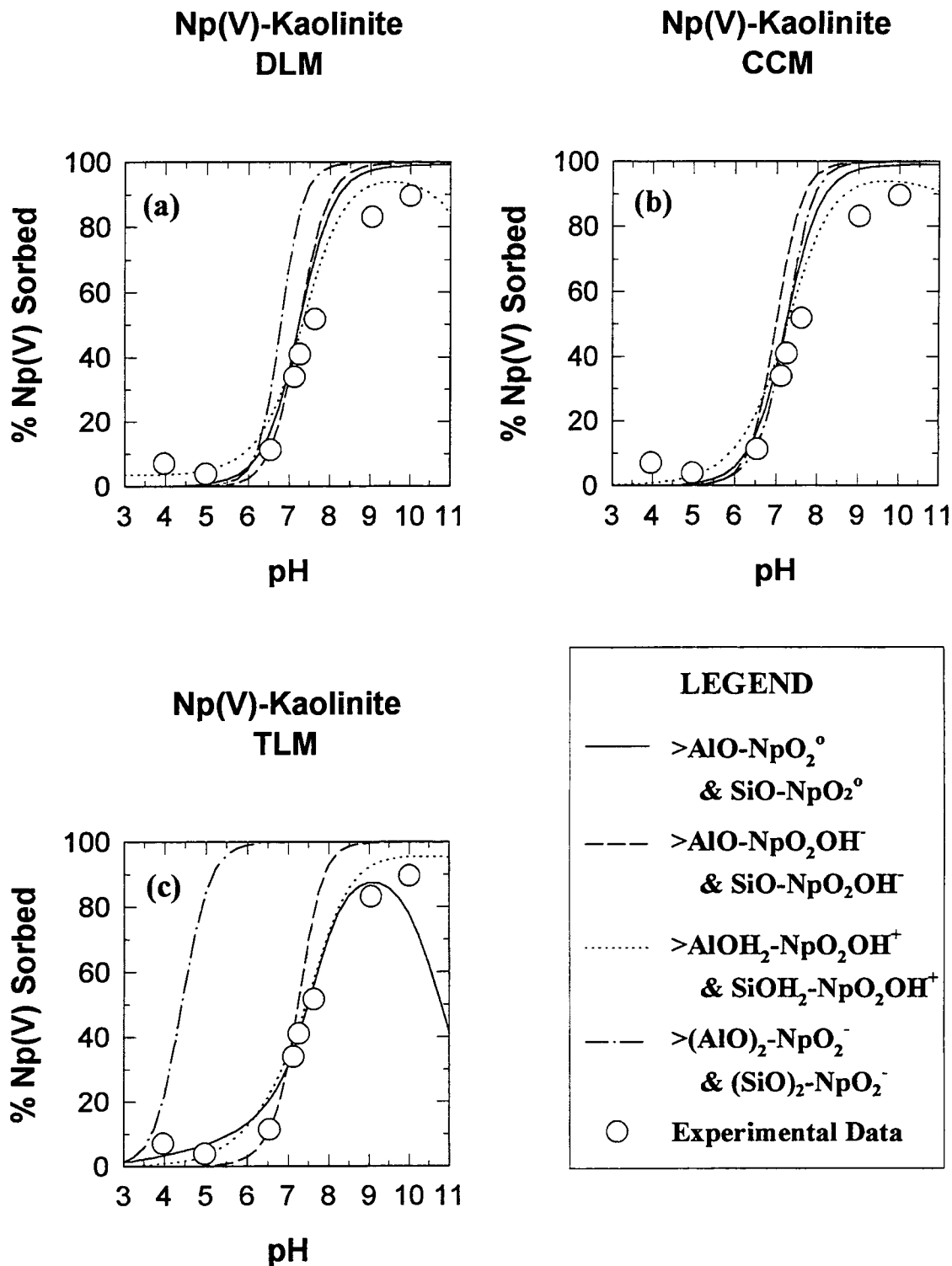


Figure 4-24. SCM predictions of Np(V) sorption on kaolinite (a) DLM; (b) CCM; and (c) TLM results. $Np(V)_T = 1.25 \times 10^{-7}$ M, 0.1 M $NaClO_4$, M/V = 5 g/L. Model parameters from Tables 3-1 and B-24. Si:Al ratio of 1:1 assumed. Data from Kohler et al. (1992).

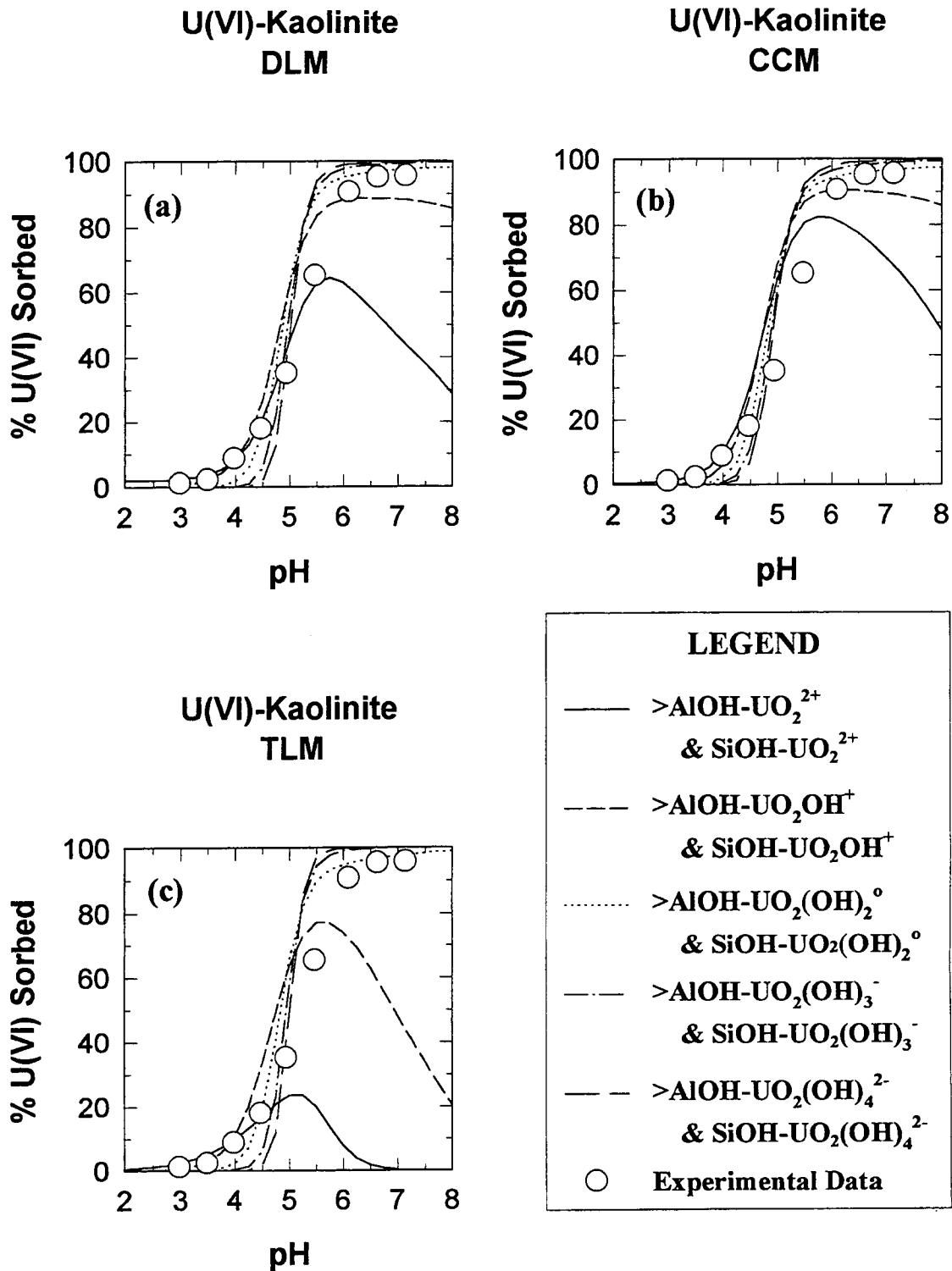


Figure 4-25. SCM predictions of U(VI) sorption on kaolinite (a) DLM; (b) CCM; and (c) TLM results. $U(VI)_T = 1 \times 10^{-6}$ M, 0.1 M $NaNO_3$, M/V=4 g/L. Model parameters from Tables 3-1 and B-25. Si:Al ratio of 1:1 assumed. Data from Payne et al. (1992).

4.3.2 Effect of Radionuclide Concentration

It is intuitive that in an experimental sorption study, because there are a finite number of available sorption sites, the radioelement concentration may affect the sorption behavior as sites are filled (Payne et al., 1992). In most of the experimental studies examined in this report, very dilute concentrations (10^{-10} to 10^{-14} M) have been used either due to safety concerns or to avoid complications due to precipitation effects. In natural systems, these dilute concentrations may be appropriate for many of the actinides considered here because solubility limits are typically low (U.S. Department of Energy, 1988). However, in most experimental systems the number of available sites is of the order 10^{-3} to 10^{-6} moles sites/L [Eq. (2-5)] and is far in excess of the radionuclide concentration. For this reason, the effect of increasing concentration in the ranges considered in the studies examined here has had relatively little effect on the sorption behavior. This small effect is reflected in both the experimental results and in the model predictions (Figure 4-26).

4.3.3 Effects of M/V Ratio

From Eq. (2-5), the total number of available sorption sites is directly proportional to the M/V ratio. Intuitively, the greater the number of available sites, the more effective the solid will be at sorbing trace concentrations of radionuclides. Such behavior has been demonstrated in several sets of sorption experiments (Pabalan and Turner, 1994, Payne et al., 1992); Zachara et al., 1987) (Figure 4-27). Using the binding constant derived at a single M/V ratio, the DLM (the simplest SCM) has proven to be able to predict the effects of changing M/V ratio quite well for both simple (hydr)oxides and aluminosilicates, predicting sorption behavior over a two order of magnitude range in M/V in the case of the U(VI)-montmorillonite sorption data of Pabalan et al. (1994).

Application of SCMs requires a single value for the M/V ratio to determine the total site concentration. Identifying the M/V ratio may be a large source of uncertainty in applying SCM approaches to field transport in natural systems. The M/V ratio is readily determined in experimental systems, but in a natural system such as a porous medium, this parameter may not be well constrained. Determining a value for M/V becomes even more problematic in fractures where mineral occurrences are sporadic, and fluid flow may be episodic. As is shown in Pabalan et al. (1994), sorption becomes relatively insensitive to increased M/V above a certain threshold value. This suggests that above a certain threshold value, the total number of available sites is in such excess relative to the radionuclide concentration that further increases in M/V have relatively little effect on total sorption. A similar relationship was observed by Rogers and Meijer (1993), where measured K_d values appeared to be relatively insensitive to specific surface area, another parameter affecting the number of available sites [Eq. (2-5)].

4.3.4 Effects of Carbon

Several studies have demonstrated that a desorption edge develops at high pH in actinide-solid- H_2O - CO_2 system (Tripathi, 1984; Hsi and Langmuir, 1985). This desorption has been attributed to both competition for sites by carbon species such as CO_3^{2-} and HCO_3^- (LaFlamme and Murray, 1987; Zachara et al., 1987; Bruno et al., 1992; van Geen et al., 1994), and competition for radioelements in solution by the formation of actinide-(hydroxy)-carbonate complexes (Tripathi, 1984; Kohler et al., 1992; Payne et al., 1992). In addition to its effect on sorption of actinides, the sorption of carbon species may contribute to the retardation of ^{14}C transport (Meijer, 1993).

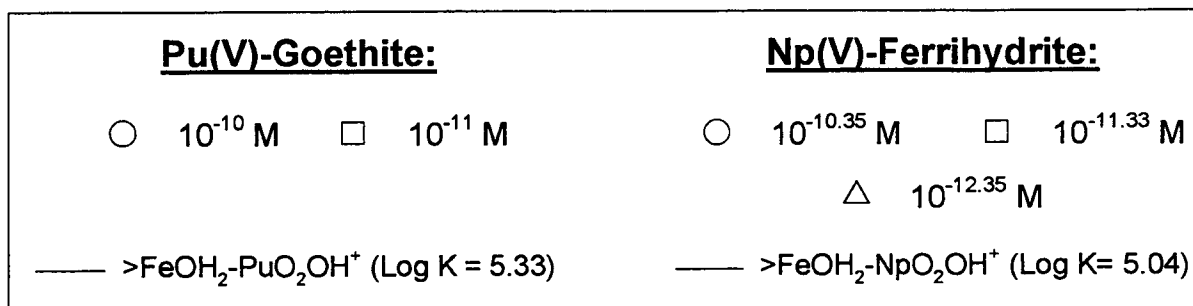
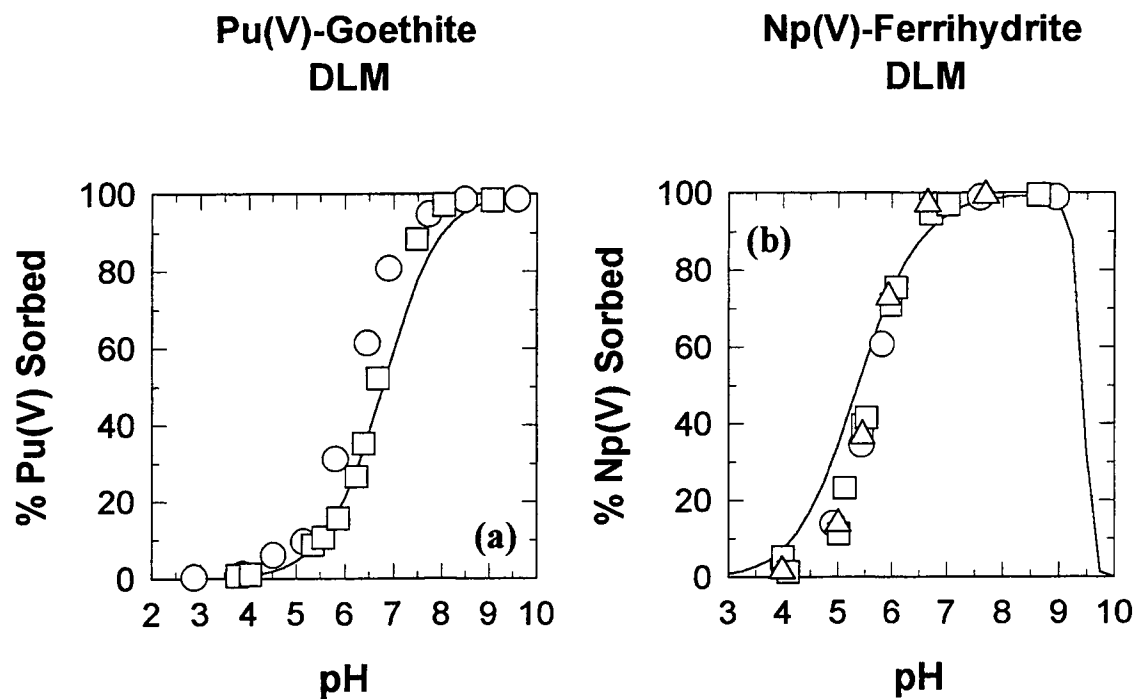
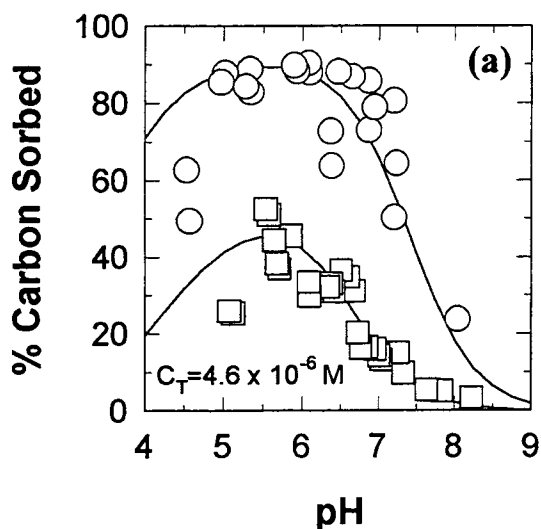
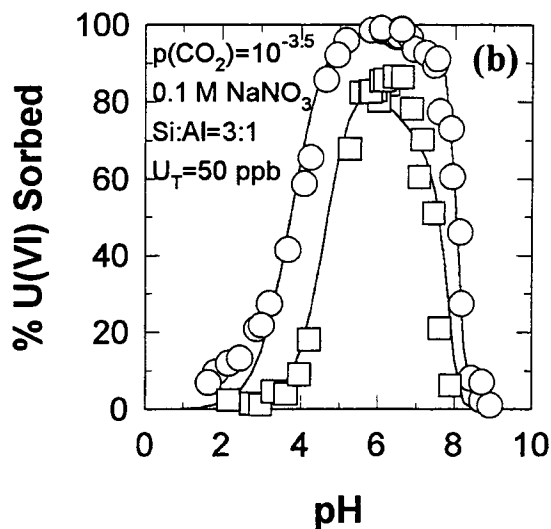


Figure 4-26. SCM predictions of the effects of changing radionuclide concentration. The SCM curves at different concentrations are indistinguishable (see text). (a) DLM results, Pu(V) sorption on goethite. Model parameters from Table B-13. Data from Sanchez et al. (1985); (b) DLM results, Np(V) sorption on ferrihydrite. Model parameters from Table B-10. Data from Girvin et al. (1991).

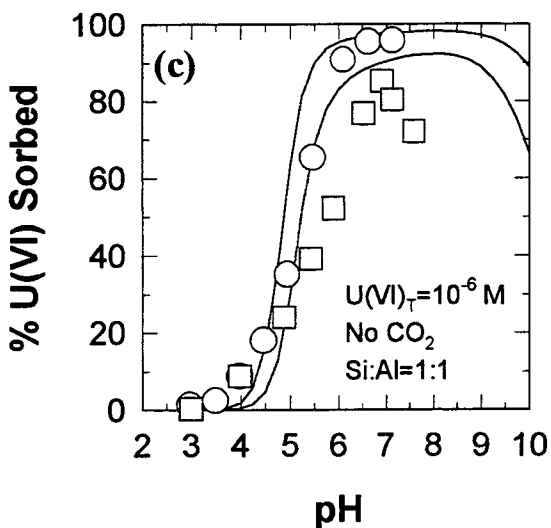
**Carbon-Ferrihydrite
DLM**



**U(VI)-Montmorillonite
DLM**



**U(VI)-Kaolinite
DLM**



Carbon-Ferrihydrite:

○ 0.77 g/L □ 0.077 g/L

— $>FeOH_2-HCO_3^{\circ}$ (Log K = 20.75)

U(VI)-Montmorillonite:

○ 2.5 g/L □ 0.25 g/L

— $>SiO-UO_2^+$ (Log K = 1.40)
& $>AlO-UO_2OH^{\circ}$ (Log K = -4.84)

U(VI)-Kaolinite:

○ 4 g/L □ 1 g/L

— $>SiOH-UO_2(OH)_2^{\circ}$ (Log K = -5.16)
& $>AlOH-UO_2(OH)_2^{\circ}$ (Log K = -3.85)

Figure 4-27. SCM predictions of the effects of changing M/V ratio. (a) DLM results, Carbon sorption on ferrihydrite. Model parameters from Table B-22. Data from Zachara et al. (1987); (b) DLM results, U(VI) sorption on montmorillonite. Model parameters as shown. Data from Pabalan et al. (1994); (c) DLM results, U(VI) sorption on kaolinite. Model parameters from Table B-25. Data from Payne et al. (1992).

Figure 4-28 shows the effect of changing total carbon on uranium sorption on goethite. As total carbon increases, a desorption edge begins to form at higher pH greater than six. The DLM results shown are calculated assuming the formation of a single surface complex, $>FeO-UO_2(OH)_2^-$, and agree with the observed data very well. The conceptual model does not explicitly invoke the formation of either uranium-carbonate surface species such as $>FeOH_2-UO_2(CO_3)_2^-$ or the competition for sites by carbon species (e.g., $>FeOH_2-CO_3^-$). Instead, in the model developed here, the desorption edge at higher pH is produced by more effective competition of carbonate ligand for the available uranium relative to the surface sites as total carbon concentration increases. At relatively low carbon concentrations, this assumption may be reasonable. At higher carbon concentrations, however, the coverage of surface sites by carbonate may become significant, leading to a reduction in sorption of radionuclides if they are more weakly sorbed than carbonate (van Geen et al., 1994). While this may not be a strictly accurate representation of the reactions occurring at the mineral-water interface, in the absence of definitive data on the surface complexes being formed, it was decided to use the simplest model capable of reproducing the observed sorption behavior.

4.4 IMPLEMENTATION OF SURFACE COMPLEXATION MODELS IN PERFORMANCE ASSESSMENT CALCULATIONS

The success of the DLM in predicting these experimental results suggests that it may be possible to use the simple conceptual model developed here to extrapolate to a variety of chemical conditions from a relatively limited data set. This extrapolation using SCM approaches based on geochemical principles is in contrast to typical empirical approaches, where the lack of a strong theoretical basis frequently makes extrapolation beyond experimental conditions uncertain. For these models, addressing the full range in expected chemical conditions may quickly lead to a considerable experimental burden. The mechanistic approach developed here also has the advantage of quantitatively evaluating critical chemical conditions that have the most effect on radionuclide sorption, and establishing those conditions where sorption is most limited.

There are several approaches to incorporating SCMs into transport calculations. The more exact method is to explicitly incorporate the SCM reactions into a coupled hydrogeochemical transport code such as HYDROGEOCHEM (Yeh and Tripathi, 1991). The coupling of geochemical and flow equations is computationally intensive (Tripathi and Yeh, 1993). For this reason, it may be difficult to use these codes extensively in PA calculations, particularly where multiple realizations are necessary for probabilistic models.

An alternative approach is to use the SCM to support ranges in K_d assigned to sorption in PA calculations. As discussed above, current efforts rely on empirical sorption models such as the K_d approach. For PA calculations, the K_d value for a given radioelement is typically assumed to be a property of the geologic medium, much like permeability and porosity. This property is assigned a range and a pdf, and sampled during multiple realizations to generate a family of Complementary Cumulative Distribution Functions (CCDF) for radionuclide release (Wilson et al., 1994). In actuality, the K_d value is derived property that is a function of system chemistry. SCM approaches may be used to represent K_d as a function of system properties such as pH and total carbon (Figure 4-29). As discussed above, although strongly influenced by pH, predicted K_d is relatively insensitive to increases in M/V above a threshold of about 1 g/L. At fairly low values for M/V, however, predicted values for K_d are sensitive to total carbon.

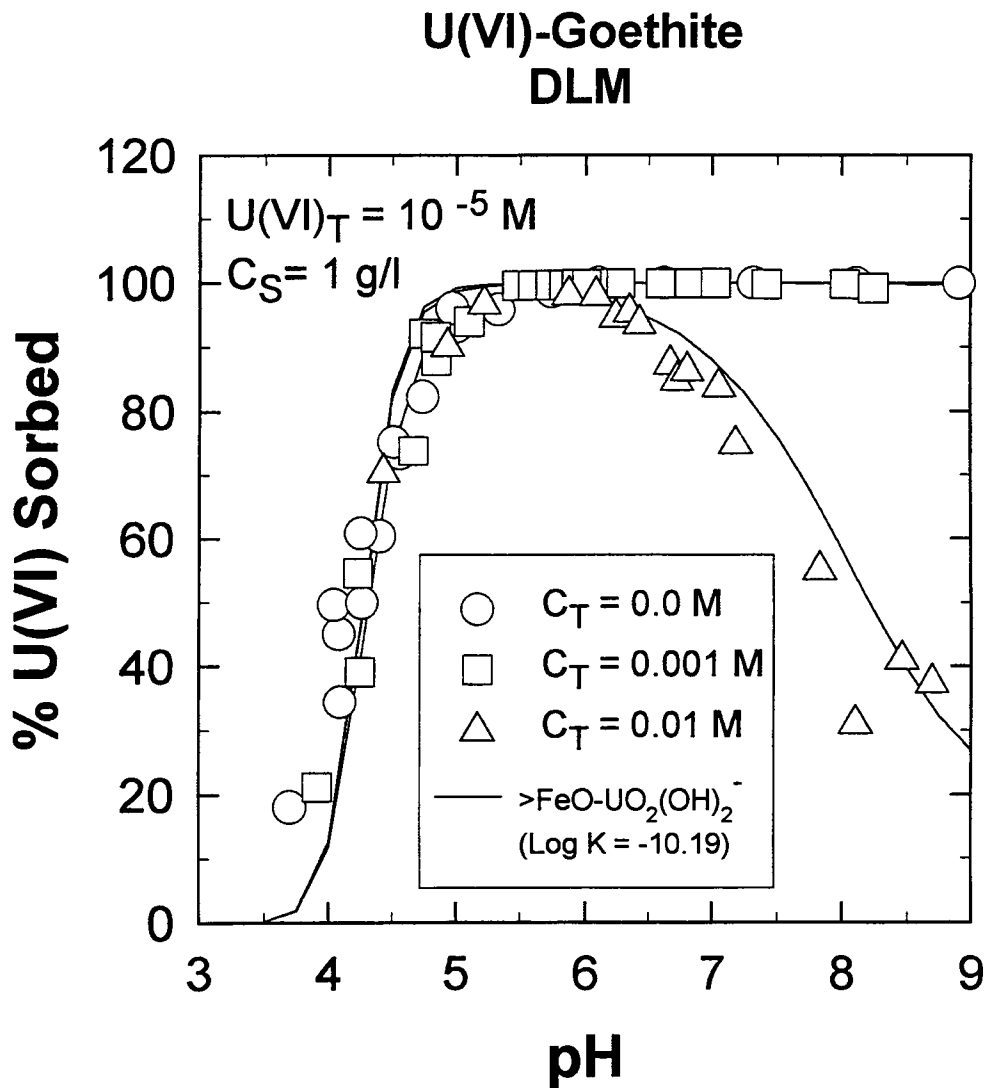


Figure 4-28. DLM predictions of the effects of changing carbon concentration. (a) Model results, U(VI) sorption on goethite. Model parameters from Table B-19. Data from Hsi and Langmuir (1985).

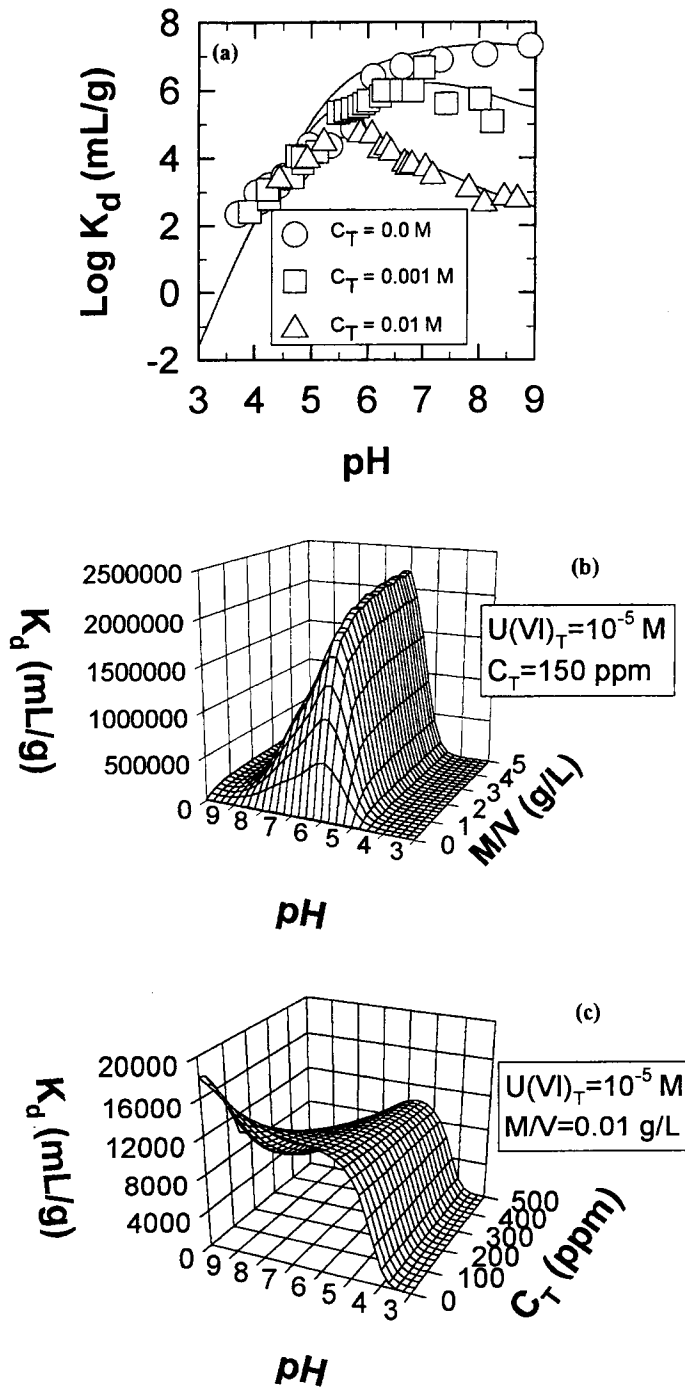


Figure 4-29. DLM predicted K_d for U(VI) sorption on goethite. Values plotted as a function of: (a) pH. Experimental data from Hsi and Langmuir (1985); (b) pH and M/V (in g/L), $C_T = 150$ ppm; and (c) pH and C_T (in ppm). All model results are calculated for $U(VI)_T = 1 \times 10^{-5}$ M assuming $>FeO-UO_2(OH)_2^-$ as a surface complex. Model parameters from Table B-19.

If these chemical variables can be measured and assigned ranges and pdfs, they can in turn be sampled, and the appropriate K_d , based on SCM calculations, assigned to the transport calculation in each realization. While this procedure is not an explicit incorporation of geochemistry in the transport calculations, it does provide a step toward a more theoretical basis for sorption modeling in PA.

One of the most difficult aspects of this type of approach, however, is in determining the appropriate values for these parameters in a natural groundwater system. While geochemical models can be used to limit likely pH and $p(\text{CO}_2)$ conditions, uncertainties remain in determining the effective solid concentration that is "seen" by groundwater containing dissolved radionuclides, particularly in the case of episodic fracture flow.

5 DISCUSSION AND SUMMARY

Current PA approaches tend to rely on empirical methods to model radioelement sorption. Because these models do not explicitly account for changes in system chemistry, however, extrapolation of laboratory data beyond experimental conditions is uncertain. Experimental sorption data indicate that radioelement (especially actinide) sorption is a complex function of the physical and chemical conditions of the system under consideration. Recent studies have provided data that demonstrate these dependencies, but in many cases these data have either not been examined quantitatively using a mechanistic approach, or have been interpreted on a case-by-case basis that makes model results difficult to compare and apply. The purpose of this study is to take advantage of existing sorption data and move toward a uniform mechanistic model for radioelement sorption that allows for prediction of complex sorption behavior.

SCMs represent one type of mechanistic approach to modeling sorption processes. Three models have been commonly used: DLMs, CCMs, and TLMs. These models use similar approaches to correct for electrostatic effects at the charged mineral-water interface, but differ in how the interface is represented. The complexity of these models varies, with the types of adjustable parameters ranging from four for the DLM to eight for the TLM. Traditional SCM applications rely on adjusting different parameters to match a given data set. Because of the number of parameters, this approach is likely to result in a nonunique fit and makes comparison between models and between studies difficult.

To minimize these problems, recent efforts have focused on developing a "standard" set of model parameters. This standard set has the benefit of maintaining a sorption model based on geochemical principles, while providing a set of uniform SCM parameters that share common reference values. Dzombak and Morel (1990) used such an approach for applying the DLM to ferrihydrite sorption data. To compare different models and to take advantage of the available radioelement sorption data (Table 3-2), this approach needs to be expanded to different minerals. In an effort to expand the mineral base, the current study has adopted many of the methods outlined in Dzombak and Morel (1990). Many simplifying assumptions have been made along the way (Turner, 1993) as a means of minimizing the amount of "tweaking" used in the modeling exercise.

The first step involved using numerical parameter optimization methods (Westall, 1982a,b) to interpret available potentiometric titration data to determine the acidity constants that are necessary to describe the acid-base behavior of the mineral surface (Turner, 1993). One simplifying step that has been taken here is to adopt the site density of 2.31 sites/nm² determined by Dzombak and Morel (1990) for ferrihydrite and recommended for all minerals by Davis and Kent (1990). With these parameters in place, it is possible to move to the next step of applying SCMs to radioelement sorption data.

A similar approach has been taken for interpreting radioelement sorption data. In the absence of independent evidence on specific surface complexes, a principle of parsimony has been adopted, using the simplest model capable of reproducing the observed sorption behavior. This approach involves using parameter optimization to determine binding constants for monodentate, mononuclear surface complexes to describe sorption in the radioelement-mineral systems listed in Table 3-2. Within this framework, the single-layer DLMs and CCMs were typically able to reproduce the general aspects of sorption behavior as well as the more complex TLMs while using a far simpler representation of the mineral-water interface. These simpler conceptual models may be preferred where it is desirable to strike a balance between accuracy of the conceptual model and the computational resources required by geochemistry in

PA calculations (Yeh and Tripathi, 1989). The different SCMs all proved capable of simulating the observed sorption behavior in most cases, although there is a tendency to predict overly steep sorption edges for highly charged actinides such as Am^{3+} . The fit to the data may be improved by invoking additional surface reactions, multidentate surface complexes, or heterogeneous site types as has been done in other studies (Hsi and Langmuir, 1985; Kohler et al., 1992). Without independent analysis (e.g., Manceau and Charlet, 1991) under relevant conditions, however, the validity of the postulated complexes remains uncertain. Additional EXAFS work will be required to ascertain the extent to which SCMs represent the mineral-water interface (Sposito, 1992).

As can be seen from examining the derived binding constants, different surface complexes result in identical values for binding constants in the DLM and CCM. For this reason, these models are not able to distinguish between like-charged surface complexes. It must also be stressed that the parameters calculated in the fitting exercise are dependent on the thermodynamic data used in the geochemical equilibrium model, and actinide data are notoriously uncertain. Even for the uranium data from the extensively evaluated Nuclear Energy Agency database (Grenthe et al., 1992), several studies (Tripathi, 1984; Fuger, 1992) suggest that there is some uncertainty in the value used for $\text{UO}_2(\text{OH})_2^0$.

As is apparent from this report, development of a uniform set of radionuclide binding constants proceeds through a logical progression of steps from potentiometric titration data (Turner, 1993) to radioelement sorption data. Radionuclide binding constants are dependent on the acidity constants used in the FITEQL optimization run; if these acidity constants are modified by the incorporation of new potentiometric titration data, all radionuclide binding constants must be reevaluated. In addition, the tabulated binding constants are dependent on the thermodynamic data available. Any significant changes in the data likewise require a recalculation of the necessary parameters.

Because much of the data is very recent, there is frequently only one data set available at a single set of experimental conditions for a given radioelement-mineral system (e.g., Np-biotite at a single Np_T). Additional data can be accommodated, using a weighting scheme like that proposed by Dzombak and Morel (1990), but combining data from different laboratories may be problematic, and deciding between data sets is not always straightforward. There are also possible complications to sorption data that are not always characterized in available radionuclide sorption data, including sorption on container walls and filtration apparatus that may be significant at the extremely dilute radioelement concentrations commonly used (Pabalan et al., 1994).

The success of the SCMs in predicting these experimental results suggests that it may be possible to use the simple conceptual models developed here to extrapolate to a variety of chemical conditions from a relatively limited data set. This approach, based on geochemical principles, is in contrast to typical empirical approaches where the lack of a strong theoretical basis frequently makes extrapolation beyond experimental conditions uncertain. For these models, addressing the full range in expected chemical conditions may quickly lead to a considerable experimental burden. The mechanistic approach developed here also has the advantage of identifying critical chemical conditions that have the most effect on radioelement sorption, and establishing those conditions where sorption is most limited. Experimental and modeling studies of actinide sorption indicate that sorption behavior is strongly dependent on several physical and chemical properties of the system, including pH, M/V, and total carbon (C_T). It may be possible to extrapolate beyond the experimental system, creating a "sorption surface" as a function of these parameters.

Ideally, mechanistic sorption models such as the SCM would be directly incorporated into reactive transport codes. While hydrogeochemical transport codes may be used to examine particular aspects of reactive transport, the additional computational burden that results from coupling equations for geochemistry and fluid flow may be excessive for the purposes of PA. This burden is even more important for stochastic approaches that rely on sampling techniques and many realizations to generate CCDFs and population statistics. It may be possible to use the DLM "off-line" to support K_d selection and to assess the effect of critical parameters such as pH, total carbon (C_T) and M/V ratios for conditions beyond the ranges used in sorption experiments. Unlike K_d , which is a derived value, these parameters are properties of the physical-chemical system that can either be measured or assigned bounding limits. The calculated sorbed and aqueous concentrations can be used to develop a range in K_d values predicted as a function of these variables. One of the most difficult aspects of this type of approach, however, is in determining the appropriate values for these parameters in the natural groundwater system at YM. While geochemical models can be used to limit likely pH and $p(\text{CO}_2)$ conditions, parameter uncertainty is particularly true in determining the effective solid concentration that is "seen" by groundwater containing dissolved radionuclides. For the purposes of PA calculations, the variables could be sampled over likely ranges, and the associated K_d used in transport calculations. While this approach is not an explicit incorporation of geochemistry in the transport calculations, it does provide a step towards a more theoretical basis for sorption modeling in PA.

6 REFERENCES

- Abendroth, R.P. 1970. Behavior of pyrogenic silica in aqueous electrolytes. *Journal of Colloid and Interface Science* 34: 591-596.
- Allard, B., M. Karlsson, E-L Tullborg, and S.A. Larson. 1983. *Ion Exchange Capacities and Surface Areas of Some Major Components and Common Fracture Filling Materials of Igneous Rocks*. Report KBS 83-64. Göteborg, Sweden: Chalmers University of Technology.
- Allison, J.D., D.S. Brown, and K.J. Novo-Gradac. 1991. *MINTEQA2/PRODEFA2, A Geochemical Assessment Model for Environmental Systems: Version 3.0 User's Manual*. EPA/600/3-91/021. Athens, GA: Environmental Protection Agency.
- Atkinson, R.J., A.M. Posner, and J.P. Quirk. 1967. Adsorption of potential determining ions at the ferric oxide-aqueous electrolyte interface. *Journal of Physical Chemistry* 71: 550-558.
- Balistrieri, L., and J.W. Murray. 1981. The surface chemistry of goethite (α -FeOOH) in major ion sea water. *American Journal of Science* 281: 788-806.
- Benjamin, M.M. 1980. *Effects of Competing Metals and Complexing Ligands on Trace Metal Adsorption at the Oxide/Solution Interface*. Ph.D. Dissertation. Stanford CA: Stanford University.
- Benjamin, M.M., and J.O. Leckie. 1980. Multiple-site adsorption of Cd, Cu, Zn, and Pb on amorphous iron oxyhydroxide. *Journal of Colloid and Interface Science* 79: 209-221.
- Berube, Y.G., and P.L. de Bruyn. 1968. Adsorption at the rutile-solution interface. 1. Thermodynamic and experimental study. *Journal of Colloid and Interface Science* 27: 305-318.
- Bolt, G.H. 1957. Determination of the charge density of silica soils. *Journal of Physical Chemistry* 61: 1,166-1,169.
- Bradbury, M.H., and B. Baeyens. 1992. A mechanistic approach to the generation of sorption databases. *Radionuclide Sorption From the Safety Evaluation Perspective. Proceedings of an NEA Workshop*. Nuclear Energy Agency. Paris: Organization for Economic Cooperation and Development: 121-162.
- Bradbury, M.H., and B. Baeyens. 1993. A general application of surface complexation to modeling radionuclide sorption in natural systems. *Journal of Colloid and Interface Science* 158: 364-371.
- Bruno, J., W. Stumm, P. Wersin, and F. Brandberg. 1992. On the influence of carbonate in mineral dissolution: I. The thermodynamic and kinetics of hematite dissolution in bicarbonate solutions at T = 25 °C. *Geochimica et Cosmochimica Acta* 56: 1,139-1,147.
- Catts, J.G., and D. Langmuir. 1986. Adsorption of Cu, Pb and Zn by δ -MnO₂: Applicability of the site binding surface complexation model. *Applied Geochemistry* 1: 255-264.

- Codell, R.B., and W.M. Murphy. 1992. Geochemical model for ^{14}C transport in unsaturated rock. *Proceedings of the Third International Conference on High-Level Radioactive Waste Management 2*. La Grange Park, IL: American Nuclear Society: 1,959–1,965.
- Davis, J.A. 1977. *Adsorption of Trace Metals and Complexing Ligands at the Oxide/Water Interface*. Ph.D. Dissertation. Stanford, CA: Stanford University.
- Davis, J.A., and J.O. Leckie. 1978. Surface ionization and complexation at the oxide/water interface 2. Surface properties of amorphous iron oxyhydroxide and adsorption of metal ions. *Journal of Colloid and Interface Science* 67: 90–107.
- Davis, J.A., R.O. James, and J.O. Leckie. 1978. Surface ionization and complexation at the oxide/water interface 1. Computation of electrical double layer properties in simple electrolytes. *Journal of Colloid and Interface Science* 63: 480–499.
- Davis, J.A., and D.B. Kent. 1990. Surface complexation modeling in aqueous geochemistry. *Reviews in Mineralogy: Volume 23. Mineral-Water Interface Geochemistry*. M.F. Hochella, Jr. and A.F. White, eds. Washington, DC: Mineralogical Society of America: 177–260.
- Della Mea, G., J.C. Dran, V. Moulin, J.C. Petit, J.D.F. Ramsay, and M. Theyssier. 1992. Scavenging properties of inorganic particles toward heavy elements. *Radiochimica Acta* 58/59: 219–223.
- Dzombak, D.A., and F.M.M. Morel. 1990. *Surface Complexation Modeling: Hydrous Ferric Oxide*. New York, NY: John Wiley and Sons.
- Fuger, J. 1992. Thermodynamic properties of actinide aqueous species relevant to geochemical problems. *Radiochimica Acta* 58/59: 81–91.
- Girvin, D.C., L.L. Ames, A.P. Schwab, and J.E. McGarrah. 1991. Neptunium adsorption on synthetic amorphous iron oxyhydroxide. *Journal of Colloid and Interface Science* 141: 67–78.
- Grenthe, I., J. Fuger, R.J. Lemire, A.B. Muller, C. Nguyen-Trung, and H. Wanner. 1992. *Chemical Thermodynamics Series, Volume 1: Chemical Thermodynamics of Uranium*. Nuclear Energy Agency, Organization for Economic Cooperation and Development. New York, NY: Elsevier.
- Hayes, K.F., and J.O. Leckie. 1987. Mechanism of lead ion adsorption at the goethite-water interface. *Geochemical Processes at Mineral Surfaces*. J.A. Davis and K.F. Hayes, eds. ACS Symposium Series 323. Washington, DC: American Chemical Society: 114–141.
- Hayes, K.F., G. Redden, W. Ela, and J.O. Leckie. 1990. *Application of Surface Complexation Models for Radionuclide Adsorption: Sensitivity Analysis of Model Input Parameters*. NUREG/CR-5547. Washington, DC: Nuclear Regulatory Commission.
- Hayes, K.F., G. Redden, W. Ela, and J.O. Leckie. 1991. Surface complexation models: An evaluation of model parameter estimation using FITEQL and oxide mineral titration data. *Journal of Colloid and Interface Science* 142: 448–469.

- Hsi, C-K.D. 1981. *Sorption of Uranium(VI) by Iron Oxides*. Ph.D. Dissertation. Golden, CO: Colorado School of Mines.
- Hsi, C-K.D., and D. Langmuir. 1985. Adsorption of uranyl onto ferric oxyhydroxides: Application of the surface complexation site-binding model. *Geochimica et Cosmochimica Acta* 49: 1,931-1,941.
- Huang, C.P., and W. Stumm. 1972. The specific surface area of γ -Al₂O₃. *Surface Science* 32: 287-296.
- Hunter, K.A., D.J. Hawke, and L.K. Choo. 1988. Equilibrium adsorption of thorium by metal oxides in marine electrolytes. *Geochimica et Cosmochimica Acta* 52: 627-636.
- Kent, D.B., V.S. Tripathi, N.B. Ball, J.O. Leckie, and M.D. Siegel. 1988. *Surface-Complexation Modeling of Radionuclide Adsorption in Subsurface Environments*. NUREG/CR-4807. Washington, DC: Nuclear Regulatory Commission.
- Kohler, M., E. Wieland, and J.O. Leckie. 1992. Metal-ligand-surface interactions during sorption of uranyl and neptunyl on oxides and silicates. *Proceedings of the 7th International Symposium on Water-Rock Interaction - WRI-7. Volume 1: Low Temperature Environments*. Y.K. Kharaka and A.S. Maest, eds. Rotterdam: A.A. Balkema.
- LaFlamme, B.D., and J.W. Murray. 1987. Solid/solution interaction: The effect of carbonate alkalinity on adsorbed thorium. *Geochimica et Cosmochimica Acta* 51: 243-250.
- Lieser, K.H., and B. Thybusch. 1988. Sorption of uranyl ions on hydrous titanium dioxide. *Fresenius Zeitschrift für Analytisch Chemie* 332: 351-357.
- Manceau, A., and L. Charlet. 1991. Sorption and speciation of heavy metals at the oxide/water interface: From microscopic to macroscopic. *Environmental Pollution* 1: 401-408.
- Matjevic, E., and P. Scheiner. 1978. Ferric hydrous oxide sols III. Preparation of uniform particles by hydrolysis of Fe(III)-chloride, -nitrate, and -perchlorate solutions. *Journal of Colloid and Interface Science* 63: 509-524.
- Meijer, A. 1993. Far-field transport of carbon dioxide: Retardation mechanisms and possible validation experiments. *Conference Proceedings FOCUS '93: Site Characterization and Model Validation*. La Grange Park, IL: American Nuclear Society: 110-112.
- Mesuere, K.L.G. 1992. *Adsorption and Dissolution Reactions Between Oxalate, Chromate, and an Iron Oxide Surface: Assessment of Current Modeling Concepts*. Ph.D. Dissertation. Beaverton, OR: Oregon Graduate Institute of Science and Technology.
- Moulin, V., D. Stammose, and G. Ouzounian. 1992. Actinide sorption at oxide-water interfaces: Application to α alumina and amorphous silica. *Applied Geochemistry Supplemental Issue* 1: 163-166.

- Murray, J.W. 1974. The surface chemistry of hydrous manganese dioxide. *Journal of Colloid and Interface Science* 46: 357-371.
- Nakayama, S., and Y. Sakamoto. 1991. Sorption of neptunium on naturally-occurring iron-containing minerals. *Radiochimica Acta* 52/53: 153-157.
- Pabalan, R.T., and D.R. Turner. 1992. Sorption modeling for HLW performance assessment. *Report on Research Activities for Calendar Year 1991*. W.C. Patrick, ed. CNWRA 91-01A. San Antonio, TX: Center for Nuclear Waste Regulatory Analyses: 8-1 to 8-66.
- Pabalan, R.T., and D.R. Turner. 1994. Sorption Modeling for HLW Performance Assessment. *NRC High-Level Radioactive Waste Research at CNWRA July-December 1993*. B. Sagar, ed. CNWRA 93-02S. San Antonio, TX: Center for Nuclear Waste Regulatory Analyses: 6-1 to 6-23.
- Pabalan, R.T., J.D. Prikryl, P.M. Muller, and T.B. Dietrich. 1993. Experimental study of uranium(6+) sorption on the zeolite mineral clinoptilolite. *Materials Research Society Symposium Proceedings: Scientific Basis for Nuclear Waste Management - XVI*. C. Interrante and R. Pabalan, eds. Pittsburgh, PA: Material Research Society: 777-782.
- Pabalan, R.T., D.R. Turner, and F.P. Bertetti. 1994. Sorption Modeling for HLW Performance Assessment. *NRC High-Level Radioactive Waste Research at CNWRA January-June 1994*. B. Sagar, ed. CNWRA 94-01S. San Antonio, TX: Center for Nuclear Waste Regulatory Analyses: 77-95.
- Payne, T.E., and T.D. Waite. 1991. Surface complexation modelling of uranium sorption data obtained by isotope exchange techniques. *Radiochimica Acta* 52/53: 487-493.
- Payne, T.E., K. Sekine, J.A. Davis, and T.D. Waite. 1992. Modeling of radionuclide sorption processes in the weathered zone of the Koongarra ore body. *Alligator Rivers Analogue Project Annual Report, 1990-1991*. P. Duerden, ed. Australian Nuclear Science and Technology Organization: 57-85.
- Rai, D., J.M. Zachara, L.E. Eary, C.C. Ainsworth, J.E. Amonette, C.E. Cowan, R.W. Szelmezcza, C.R. Resch, R.L. Schmidt, D.C. Girvin, and S.C. Smith. 1988. *Chromium Reactions in Geologic Materials*. EPRI-EA-5741, Palo Alto, CA: Electric Power Research Institute.
- Reardon, E.J. 1981. K_d 's - Can they be used to describe reversible ion sorption reactions in contaminant migration? *Groundwater* 19: 279-286.
- Regazzoni, A.E., M.A. Blesa, and A.J.G. Maroto. 1983. Interfacial properties of zirconium dioxide and magnetite. *Journal of Colloid and Interface Science* 91: 560-570.
- Riese, A.C. 1982. *Adsorption of Radium and Thorium onto Quartz and Kaolinite: A Comparison of Solution/Surface Equilibria Models*. Ph.D. Dissertation. Golden, CO: Colorado School of Mines.

- Righetto, L., G. Bidoglio, B. Marcandalli, and I.R. Bellobono. 1988. Surface interactions of actinides with alumina colloids. *Radiochimica Acta* 44/45: 73-75.
- Righetto, L., G. Bidoglio, G. Azimonti, and I.R. Bellobono. 1991. Competitive actinide interactions in colloidal humic acid-mineral oxide systems. *Environmental Science and Technology* 25: 1,913-1,919.
- Rogers, P.S.Z., and A. Meijer. 1993. Dependence of radionuclide sorption on sample grinding, surface area, and water composition. *Proceedings of the Fourth Annual International Conference on High-Level Radioactive Waste Management*. La Grange Park, IL: American Nuclear Society: 1,509-1,516.
- Sanchez, A.L., J.W. Murray, and T.H. Sibley. 1985. The adsorption of plutonium IV and V on goethite. *Geochimica et Cosmochimica Acta* 49: 2,297-2,307.
- Schulthess, C.P., and J.F. McCarthy. 1990. Competitive adsorption of aqueous carbonic and acetic acids by an aluminum oxide. *Soil Science Society of America Journal* 54: 688-694.
- Sposito, G. 1992. Experimental validation of surface speciation models. *American Geophysical Union 1992 Annual Meeting*. Washington, DC: American Geophysical Union: 597.
- Sprycha, R. 1984. Surface charge and adsorption of background electrolyte ions at anatase/electrolyte interface. *Journal of Colloid and Interface Science* 102: 173-185.
- Sprycha, R. 1989. Electrical double layer at alumina/electrolyte interface. *Journal of Colloid and Interface Science* 127: 1-11.
- Stammose, D., and J.M. Dolo. 1990. Sorption of americium at trace levels on a clay mineral. *Radiochimica Acta* 51: 189-193.
- Swallow, K.C. 1978. *Adsorption of Trace Metals by Hydrous Ferric Oxide*. Ph.D. Dissertation. Cambridge, MA: Massachusetts Institute of Technology.
- Tripathi, V.S. 1984. *Uranium(VI) Transport Modeling: Geochemical Data and Submodels*. Ph.D. Dissertation. Stanford, CA: Stanford University.
- Tripathi, V.S., and G.T. Yeh. 1993. A performance comparison of scalar, vector, and concurrent vector computers including supercomputers for modeling transport of reactive contaminants in groundwater. *Water Resources Research* 29: 1,819-1,823.
- Turner, D.R. 1993. *Mechanistic Approaches to Radionuclide Sorption Modeling*. CNWRA 93-019. San Antonio, TX: Center for Nuclear Waste Regulatory Analyses.
- U.S. Department of Energy. 1988. *Site Characterization Plan: Yucca Mountain Site, Nevada Research and Development Area, Nevada*. Office of Civilian Radioactive Waste Management, DOE/RW-0199. Washington, DC: U.S. Department of Energy.

- van Geen, A., A.P. Robertson, and J.O. Leckie. 1994. Complexation of carbonate species at the goethite surface: Implications for adsorption of metal ions in natural waters. *Geochimica et Cosmochimica Acta* 58: 2,073-2,086.
- Venkataramani, B., and A.R. Gupta. 1991. Effect of anions on the sorption of uranyl ions on hydrous oxides: Application of the surface hydrolysis model. *Colloids and Surfaces* 53: 1-19.
- Vochten, R.F., L. van Haverbeke, and F. Goovaerts. 1990. External surface adsorption of uranyl-hydroxo complexes on zeolite particles in relation to the double-layer potential. *Journal of the Chemical Society Faraday Transactions*. 86: 4,095-4,099.
- Waite, T.D., T.E. Payne, J.A. Davis, and K. Sekine. 1993. Uranium sorption modeling - A surface complexation approach. *5th Commission of the European Communities Natural Analogue Working Group Meeting and Alligator River Analogue Project (ARAP) Final Workshop*. H. von Maravic and J. Smellie, eds. Brussels, Belgium: Commission of the European Communities, Nuclear Science and Technology: 83-88.
- Westall, J.C. 1982a. *FITEQL: A Computer Program for Determination of Chemical Equilibrium Constants From Experimental Data, Version 1.2*. Rpt. 82-01. Corvallis, OR: Department of Chemistry, Oregon State University.
- Westall, J.C. 1982b. *FITEQL: A Computer Program for Determination of Chemical Equilibrium Constants From Experimental Data, Version 2.0*. Rpt. 82-02. Corvallis, OR: Department of Chemistry, Oregon State University.
- Westall, J.C., and H. Hohl. 1980. A comparison of electrostatic models for the oxide/solution interface. *Advances in Colloid and Interface Science* 12: 265-294.
- Wilson, M.L., J.H. Gauthier, R.W. Barnard, G.E. Barr, and H.A. Dockery. 1994. *Total System Performance Assessment for Yucca Mountain - SNL Second Iteration (TSPA-1993)*. SAND93-2675. Albuquerque, NM: Sandia National Laboratories.
- Yates, D.A. 1975. *The Structure of the Oxide/Aqueous Electrolyte Interface*. Ph.D. Dissertation. Melbourne, Australia: University of Melbourne.
- Yates, D.A., and T.W. Healy. 1975. Mechanism of anion adsorption at the ferric and chromic oxide/water interfaces. *Journal of Colloid and Interface Science* 52: 222-228.
- Yeh, G.T., and V.S. Tripathi. 1989. A critical evaluation of recent developments in hydrogeochemical transport models of reactive multichemical components. *Water Resources Research* 25: 93-108.
- Yeh, G.T., and V.S. Tripathi. 1991. A model for simulating transport of reactive multispecies components: Model development and demonstration. *Water Resources Research* 27: 3,075-3,094.

Zachara, J.M., D.C. Girvin, R.L. Schmidt, and C.T. Resch. 1987. Chromate adsorption on amorphous iron oxyhydroxide in the presence of major groundwater ions. *Environmental Science and Technology* 21: 589-594.

APPENDIX A

**SUMMARY OF RADIONUCLIDE SORPTION DATA:
EXPERIMENTAL CONDITIONS**

SUMMARY OF RADIONUCLIDE SORPTION DATA: EXPERIMENTAL CONDITIONS

Radionuclide sorption data for the actinides and carbon have become readily available in the open literature only relatively recently. The sources considered for U, Th, Np, Am, Pu, and C sorption are listed in Table 3-2 of this report. This appendix provides a summary of the reported experimental conditions. This appendix is intended only as a brief summary; readers are referred to the original work for more detailed descriptions of the quality and limitations of the experimental methods used.

The following notation is used throughout the appendix.

Solid Preparation. Includes both synthetic and natural mineral sources. Where noted, mineral sources and size fractions are given. The surface area and site density used in the modeling analyses are discussed in the text.

C_{RN}. Total radionuclide concentration reported in the experiment. In some experiments, more than one concentration has been investigated.

M/V. Solid-mass to solution-volume ratio (g/L). In some experiments, more than one ratio has been considered.

pH range. The range in pH is sometimes reported, but in most cases it has been read from graphical data.

T. Experimental temperature (°C).

CO₂. Carbon dioxide/carbonate can significantly affect the sorption behavior of radionuclides, particularly at higher pH. Many experiments have been performed in CO₂-free controlled environments, or have used variable amounts of total carbon (C_T) to examine these effects.

Reaction Vessel. Due to the potential for sorption to the vessel walls, this information is provided where it has been reported.

Equilibration Time. Typically based on kinetic experiments to determine the time necessary for the system to reach equilibrium.

Filtration/Phase Separation. Due to the potential for sorption to a filtration apparatus, this information is provided where it has been reported.

Measurement Techniques. Varying techniques such as alpha and gamma counting have been used to determine the amount of radionuclide sorbed on the solid under consideration. This information is provided where it has been reported.

n.r. Information not reported

Additional notes on experimental procedures and conditions are provided as appropriate.

AMERICIUM SORPTION

Moulin et al. (1992)

Experiment: Am(III) sorption on α -Al₂O₃

Solid preparation:	Commercial α -Al ₂ O ₃ (Ventron @ 0.063 to 0.125 mm)
C _{RN} =	10 ⁻⁸ M
M/V =	10 g/L
pH range =	3 to 10
Background Electrolyte =	0.01, 0.1 M NaClO ₄
T =	20 °C
Reaction vessel:	Polycarbonate
CO ₂ :	Atmospheric CO ₂
Equilibration time:	2 d
Filtration/Phase Separation:	Centrifuged for 15 min @ 4,000 rpm
Measurement techniques:	Liquid scintillation counting for ²⁴¹ Am

Notes: Results reported graphically as Log K_d, increasing the significance of the digitizing uncertainty

Moulin et al. (1992)

Experiment: Am(III) sorption on amorphous SiO₂

Solid preparation:	Commercial amorphous SiO ₂ (Merck @ 0.063 to 0.125 mm)
C _{RN} =	10 ⁻⁸ M
M/V =	10 g/L
pH range =	3 to 8
Background Electrolyte =	0.01, 0.1 M NaClO ₄
T =	20° C
Reaction vessel:	Polycarbonate
CO ₂ :	Atmospheric CO ₂
Equilibration time:	2 d
Filtration/Phase Separation:	Centrifuged for 15 min @ 4,000 rpm
Measurement techniques:	Liquid scintillation counting for ²⁴¹ Am

Notes: Results reported graphically as Log K_d, increasing the significance of the digitizing uncertainty

Righetto et al. (1988)

Experiment: Am(III) sorption on γ -Al₂O₃

Solid preparation:	Commercial γ -Al ₂ O ₃ (Aluminum Oxide C, Degussa @ 20 nm)
C _{RN} =	5 × 10 ⁻¹⁰ M
M/V =	0.01 and 0.2 g/L
pH range =	3.5 to 11.0
Background Electrolyte =	0.01, 0.1 M NaClO ₄
T =	n.r. (Presumably room temperature)
Reaction vessel:	Quick Seal ultracentrifuge tubes (Beckman - material not reported)
CO ₂ :	CO ₂ -free; C _T =0.05 M
Equilibration time:	7 d

Filtration/Phase Separation: Centrifuged for 1 hr @ 55,000 rpm
Measurement techniques: Gamma counting for ^{241}Am

Notes: Additional experiments to consider the effects of humic acids (5 ppm).

Righetto et al. (1991)

Experiment: Am(III) sorption on $\gamma\text{-Al}_2\text{O}_3$

Solid preparation: Commercial $\gamma\text{-Al}_2\text{O}_3$ (Aluminum Oxide C, Degussa @ 20 nm)
 $C_{\text{RN}} = 5 \times 10^{-10} \text{ M}$
 $M/V = 0.2 \text{ g/L}$
pH range = 3.5 to 7.0
Background Electrolyte = 0.1 M NaClO_4
 $T = 25 \pm 1 \text{ }^\circ\text{C}$
Reaction vessel: Polyallomer ultracentrifuge tubes
 CO_2 : CO_2 -free
Equilibration time: 7 d
Filtration/Phase Separation: Centrifuged for 1 hr @ 55,000 rpm
Measurement techniques: Gamma counting for ^{241}Am

Notes: Additional experiments to consider the effects of humic acids (1 to 50 ppm)

Righetto et al. (1991)

Experiment: Am(III) sorption on amorphous SiO_2

Solid preparation: Synthetic silica precipitated by addition of acid to Na-silicate under controlled conditions (unspecified) to give a hydrous sol
 $C_{\text{RN}} = 5 \times 10^{-10} \text{ M}$
 $M/V = 1.2 \text{ g/L}$
pH range = 4.0 to 10.0
Background Electrolyte = 0.1 M NaClO_4
 $T = 25 \pm 1 \text{ }^\circ\text{C}$
Reaction vessel: Polyallomer ultracentrifuge tubes
 CO_2 : CO_2 -free
Equilibration time: 7 d
Filtration/Phase Separation: Centrifuged for 1 hr @ 55,000 rpm
Measurement techniques: Gamma counting for ^{241}Am

Notes: Additional experiments to consider the effects of humic acids (1 to 30 ppm @ pH=5 to 10)

NEPTUNIUM SORPTION

Girvin et al. (1991)

Experiment: Np(V) sorption on ferrihydrite

Solid preparation:	Synthetic ferrihydrite prepared using method of Benjamin (1979)
$C_{RN} =$	4.5×10^{-11} M; 4.7×10^{-12} M; 4.5×10^{-13} M
M/V =	0.88 g/L; 0.33 g/L; 0.089 g/L
pH range =	5.0 to 9.5 (Adjusted with 0.1 M HNO ₃ or 0.1 M NaOH)
Background Electrolyte =	0.1 M NaNO ₃
T =	25 °C
Reaction vessel:	Polyethylene
CO ₂ :	Atmospheric CO ₂ , capped, 5 mL headspace ($C_T = 10^{-5}$ to 10^{-4} M)
Equilibration time:	3 to 4 hr
Filtration/Phase Separation:	0.18- μ m filter
Measurement techniques:	Liquid scintillation for ²³⁵ Np

Notes: Kinetic experiments run for 1 to 96 hr. After 3 to 4 hr, sorption reached 95 percent of the 96 hr value, with essentially no change occurring after 24 hr.

Kohler et al. (1992)

Experiment: Np(V) sorption on hematite

Solid preparation:	n.r.
$C_{RN} =$	1.2×10^{-7} M
M/V =	1 g/L
pH range =	4.0 to 10.0
Background Electrolyte =	0.005, 0.01, 0.05, 0.1 M NaClO ₄
T =	n.r.
Reaction vessel:	n.r.
CO ₂ :	n.r.
Equilibration time:	6 to 10 hr
Filtration/Phase Separation:	n.r.
Measurement techniques:	n.r.

Notes: Additional experiments to consider the effects of Na-EDTA (3.3×10^{-5} M) and Ca-EDTA (3.3×10^{-5} M)

Kohler et al. (1992)

Experiment: Np(V) sorption on kaolinite

Solid preparation:	n.r.
$C_{RN} =$	$(1.2-1.3) \times 10^{-7}$ M
M/V =	5 g/L
pH range =	4.0 to 10.5
Background Electrolyte =	0.1 M NaClO ₄
T =	n.r.
Reaction vessel:	n.r.

CO₂: n.r.
Equilibration time: n.r.
Filtration/Phase Separation: n.r.
Measurement techniques: n.r.

Notes: Additional experiments to consider the effects of EDTA (10⁻³, 10⁻⁴, 10⁻⁶ M). No form specified for EDTA

Nakayama and Sakamoto (1991)

Experiment: Np(V) sorption on natural goethite

Solid preparation: Natural goethite crushed to < 149 μm (Mongolia, China)
C_{RN} = 6 × 10⁻⁶ M
M/V = 1 g/L
pH range = 3.5 to 11.0 (adjusted using HNO₃ and NaOH)
Background Electrolyte = 0.1 M NaNO₃
T = 30 °C
Reaction vessel: Glass or polyethylene
CO₂: n.r., Capped vials
Equilibration time: 2 d
Filtration/Phase Separation: Filtered through 0.45-μm membrane filter
Measurement techniques: Liquid scintillation counting, alpha radioactivity for ²³⁷Np

Notes: Kinetic experiments conducted out to 6 days, with reversibility studies conducted by changing suspension pH

Nakayama and Sakamoto (1991)

Experiment: Np(V) sorption on natural biotite

Solid preparation: Natural biotite crushed to < 149 μm (Mongolia, China)
C_{RN} = 6 × 10⁻⁶ M
M/V = 1 g/L
pH range = 3.5 to 11.0 (adjusted using HNO₃ and NaOH)
Background Electrolyte = 0.1 M NaNO₃
T = 30 °C
Reaction vessel: Glass or polyethylene
CO₂: n.r., Capped vials
Equilibration time: 2 to 3 hr
Filtration/Phase Separation: Filtered through 0.45-μm membrane filter
Measurement techniques: Liquid scintillation counting, alpha radioactivity for ²³⁷Np

Notes: Kinetic experiments conducted out to 1 day, with reversibility studies conducted by changing suspension pH

Nakayama and Sakamoto (1991)**Experiment: Np(V) sorption on natural magnetite**

Solid preparation:	Natural magnetite crushed to < 149 μm (Mongolia, China)
$C_{\text{RN}} =$	6×10^{-6} M
M/V =	1 g/L
pH range =	3.5 to 11.0 (adjusted using HNO_3 and NaOH)
Background Electrolyte =	0.1 M NaNO_3
T =	30 $^\circ\text{C}$
Reaction vessel:	Glass or polyethylene
CO_2 :	n.r., Capped vials
Equilibration time:	2 to 3 hr
Filtration/Phase Separation:	Filtered through 0.45- μm membrane filter
Measurement techniques:	Liquid scintillation counting, alpha radioactivity for ^{237}Np

Notes: Kinetic experiments conducted out to 1 day, with reversibility studies conducted by changing suspension pH

Nakayama and Sakamoto (1991)**Experiment: Np(V) sorption on natural hematite**

Solid preparation:	Natural hematite crushed to < 149 μm (Mongolia, China)
$C_{\text{RN}} =$	6×10^{-6} M
M/V =	1 g/L
pH range =	3.5 to 11.0 (adjusted using HNO_3 and NaOH)
Background Electrolyte =	0.1 M NaNO_3
T =	30 $^\circ\text{C}$
Reaction vessel:	Glass or polyethylene
CO_2 :	n.r., Capped vials
Equilibration time:	2 to 3 hr
Filtration/Phase Separation:	Filtered through 0.45- μm membrane filter
Measurement techniques:	Liquid scintillation counting, alpha radioactivity for ^{237}Np

Notes: Kinetic experiments conducted out to 1 day

Nakayama and Sakamoto (1991)**Experiment: Np(V) sorption on synthetic magnetite**

Solid preparation:	Reagent-grade magnetite (Wako Pure Chemical Industries, Osaka, Japan)
$C_{\text{RN}} =$	6×10^{-6} M
M/V =	1 g/L
pH range =	3.5 to 11.0 (adjusted using HNO_3 and NaOH)
Background Electrolyte =	0.1 M NaNO_3
T =	30 $^\circ\text{C}$
Reaction vessel:	Glass or polyethylene
CO_2 :	n.r., Capped vials
Equilibration time:	2 to 3 hr
Filtration/Phase Separation:	Filtered through 0.45- μm membrane filter
Measurement techniques:	Liquid scintillation counting, alpha radioactivity for ^{237}Np

Nakayama and Sakamoto (1991)**Experiment: Np(V) sorption on synthetic hematite**

Solid preparation:	Reagent-grade hematite (Wako Pure Chemical Industries, Osaka, Japan)
$C_{RN} =$	6×10^{-6} M
M/V =	1 g/L
pH range =	3.5 to 11.0 (adjusted using HNO ₃ and NaOH)
Background Electrolyte =	0.1 M NaNO ₃
T =	30 °C
Reaction vessel:	Glass or polyethylene
CO ₂ :	n.r., Capped vials
Equilibration time:	2 to 3 hr
Filtration/Phase Separation:	Filtered through 0.45- μ m membrane filter
Measurement techniques:	Liquid scintillation counting, alpha radioactivity for ²³⁷ Np

Nakayama and Sakamoto (1991)**Experiment: Np(V) sorption on synthetic α -Al₂O₃**

Solid preparation:	Reagent-grade α -Al ₂ O ₃ (Wako Pure Chemical Industries, Osaka, Japan)
$C_{RN} =$	6×10^{-6} M
M/V =	1 g/L
pH range =	3.5 to 11.0 (adjusted using HNO ₃ and NaOH)
Background Electrolyte =	0.1 M NaNO ₃
T =	30 °C
Reaction vessel:	Glass or polyethylene
CO ₂ :	n.r., Capped vials
Equilibration time:	2 to 3 hr
Filtration/Phase Separation:	Filtered through 0.45- μ m membrane filter
Measurement techniques:	Liquid scintillation counting, alpha radioactivity for ²³⁷ Np

Notes: Kinetic experiments conducted out to 1 day

Nakayama and Sakamoto (1991)**Experiment: Np(V) sorption on synthetic boehmite (γ -AlOOH)**

Solid preparation:	Reagent-grade γ -AlOOH (Wako Pure Chemical Industries, Osaka, Japan)
$C_{RN} =$	6×10^{-6} M
M/V =	1 g/L
pH range =	3.5 to 11.0 (adjusted using HNO ₃ and NaOH)
Background Electrolyte =	0.1 M NaNO ₃
T =	30 °C
Reaction vessel:	Glass or polyethylene
CO ₂ :	n.r., Capped vials
Equilibration time:	1 d
Filtration/Phase Separation:	Filtered through 0.45- μ m membrane filter
Measurement techniques:	Liquid scintillation counting, alpha radioactivity for ²³⁷ Np

Notes: Kinetic experiments conducted out to 6 days

Nakayama and Sakamoto (1991)**Experiment: Np(V) sorption on synthetic lepidocrocite (γ -FeOOH)**

Solid preparation:	Reagent-grade γ -FeOOH (Wako Pure Chemical Industries, Osaka, Japan)
C_{RN} =	6×10^{-6} M
M/V =	1 g/L
pH range =	3.5 to 11.0 (adjusted using HNO ₃ and NaOH)
Background Electrolyte =	0.1 M NaNO ₃
T =	30 °C
Reaction vessel:	Glass or polyethylene
CO ₂ :	n.r., Capped vials
Equilibration time:	1 d
Filtration/Phase Separation:	Filtered through 0.45- μ m membrane filter
Measurement techniques:	Liquid scintillation counting, alpha radioactivity for ²³⁷ Np

Notes: Kinetic experiments conducted out to 6 days

Righetto et al. (1988)**Experiment: Np(V) sorption on γ -Al₂O₃**

Solid preparation:	Commercial γ -Al ₂ O ₃ (Aluminum Oxide C, Degussa @ 20 nm)
C_{RN} =	10^{-14} M
M/V =	0.2 g/L
pH range =	5.0 to 11.0
Background Electrolyte =	0.1 M NaClO ₄
T =	n.r. (Presumably room temperature)
Reaction vessel:	Quick Seal ultracentrifuge tubes (Beckman - material not reported)
CO ₂ :	CO ₂ -free; CT=0.05 M
Equilibration time:	4 d
Filtration/Phase Separation:	Centrifuged for 1 hr @ 55,000 rpm
Measurement techniques:	Gamma counting for ²³⁹ Np

Notes: Additional experiments to consider the effects of humic acids (5 and 50 ppm)

Righetto et al. (1991)**Experiment: Np(V) sorption on γ -Al₂O₃**

Solid preparation:	Commercial γ -Al ₂ O ₃ (Aluminum Oxide C, Degussa @ 20 nm)
C_{RN} =	10^{-14} M
M/V =	0.2 g/L
pH range =	5.0 to 11.5
Background Electrolyte =	0.1 M NaClO ₄
T =	25 ± 1 °C
Reaction vessel:	Polyallomer ultracentrifuge tubes
CO ₂ :	CO ₂ -free
Equilibration time:	4 d
Filtration/Phase Separation:	Centrifuged for 1 hr @ 55,000 rpm
Measurement techniques:	Gamma counting for ²³⁹ Np

Notes: Additional experiments to consider the effects of humic acids (1 to 50 ppm)

Righetto et al. (1991)

Experiment: Np(V) sorption on amorphous SiO₂

Solid preparation:	Synthetic silica precipitated by addition of acid to Na-silicate under controlled conditions (unspecified) to give a hydrous sol
C _{RN} =	10 ⁻¹⁴ M
M/V =	1.2 g/L
pH range =	6.0 to 10.5
Background Electrolyte =	0.1 M NaClO ₄
T =	25 ± 1 °C
Reaction vessel:	Polyallomer ultracentrifuge tubes
CO ₂ :	CO ₂ -free
Equilibration time:	4 d
Filtration/Phase Separation:	Centrifuged for 1 hr @ 55,000 rpm
Measurement techniques:	Gamma counting for ²³⁹ Np

Notes: Additional experiments to consider the effects of humic acids (1 to 10 ppm @ pH=7 to 10)

PLUTONIUM SORPTION:

Righetto et al. (1991)

Experiment: Np(V) sorption on $\gamma\text{-Al}_2\text{O}_3$

Solid preparation:	Commercial $\gamma\text{-Al}_2\text{O}_3$ (Aluminum Oxide C, Degussa @ 20 nm)
$C_{\text{RN}} =$	2×10^{-10} M
M/V =	0.2 g/L
pH range =	6.0 to 11.0
Background Electrolyte =	0.1 M NaClO_4
T =	25 ± 1 °C
Reaction vessel:	Polyallomer ultracentrifuge tubes
CO_2 :	CO_2 -free
Equilibration time:	7 d
Filtration/Phase Separation:	Centrifuged for 1 hr @ 55,000 rpm
Measurement techniques:	Gamma counting for ^{238}Pu

Notes: Oxidation state of Pu uncertain, but authors suggest that Pu(V) may be dominant oxidation state.
Additional experiments to consider the effects of humic acids (5 and 50 ppm).

Sanchez et al. (1985)

Experiment:

Pu(IV) sorption on goethite

Pu(V) sorption on goethite

Solid preparation:	Synthetic goethite prepared using method of Atkinson et al. (1967)
$C_{\text{RN}} =$	10^{-10} M; 10^{-11} M
M/V =	0.55 g/L
pH range =	2.0 to 9.0 (Adjusted with 0.1 N HCl or 0.1 N NaOH)
Background Electrolyte =	0.1 M NaNO_3 0.1 M, 0.5 M, 1.0 M, 3.0 M NaNO_3 (@ pH=7.0; $C_{\text{RN}}=10^{-11}$ M) 0.5 M, 3.0 M NaCl (@ pH=7.0; $C_{\text{RN}}=10^{-11}$ M) 0.03 M, 0.15 M, 0.30 M Na_2SO_4 (@ pH=7.0; $C_{\text{RN}}=10^{-11}$ M)
T =	20 ± 2 °C
Reaction vessel:	Borosilicate Glass
CO_2 :	CO_2 -free; 10, 30, 100, 200, 400, 1000 meq/l @ pH=8.6
Equilibration time:	Pu(IV) - 1 to 96 hr; Pu(V) - 1 hr to 20 d
Filtration/Phase Separation:	Filter not specified
Measurement techniques:	Liquid scintillation spectrometry for ^{238}Pu

THORIUM SORPTION:

Hunter et al. (1988)

Experiment: Th(IV) sorption on goethite

Solid preparation:	Synthetic goethite prepared using method of Atkinson et al. (1967)
$C_{RN} =$	4.5×10^{-5} M; 9.0×10^{-6} M
M/V =	0.54 g/L, 8.60 g/L
pH range =	2.0 to 8.0
Background Electrolyte =	0.422 M NaCl; 0.422 M NaCl+0.054 MgCl ₂ ; 0.422 M NaCl+0.010 M CaCl ₂ ; 0.422 M NaCl+0.028 M Na ₂ SO ₄ ; UV irradiated seawater
T =	20±2 °C
Reaction vessel:	Pyrex
CO ₂ :	n.r.
Equilibration time:	3 hr
Filtration/Phase Separation:	Centrifuge for 15 min @ 4,500 rpm
Measurement techniques:	Colorimetry using Th-Arsenazo complex

Notes: Also conducted experiments using competing ligands EDTA and CDTA (8.3×10^{-6} M)

Hunter et al. (1988)

Experiment: Th(IV) sorption on δ -MnO₂

Solid preparation:	Synthetic δ -MnO ₂ prepared using method of Murray (1974) and Balistrieri and Murray (1981)
$C_{RN} =$	4.5×10^{-5} M; 9.0×10^{-6} M
M/V =	8.3×10^{-3} g/L
pH range =	2.0 to 8.0
Background Electrolyte =	0.422 M NaCl; 0.422 M NaCl+0.054 MgCl ₂ ; 0.422 M NaCl+0.010 M CaCl ₂ ; 0.422 M NaCl+0.028 M Na ₂ SO ₄ ; UV irradiated seawater
T =	20±2 °C
Reaction vessel:	Pyrex
CO ₂ :	n.r.
Equilibration time:	6 hr
Filtration/Phase Separation:	Centrifuge for 15 min @ 4,500 rpm
Measurement techniques:	Colorimetry using Th-Arsenazo complex

Notes: Also conducted experiments using complexing ligands EDTA and CDTA (8.3×10^{-6} M)

LaFlamme and Murray (1987)**Experiment: Th(IV) sorption on goethite**

Solid preparation:	Synthetic goethite prepared using method of Atkinson et al. (1967)
$C_{RN} =$	10^{-13} M
M/V =	5.22×10^{-3} g/L
pH range =	1.8 to 10.5 (Adjusted with HCl or NaOH)
Background Electrolyte =	0.1 M NaNO ₃
	0.01 M, 0.1 M, 1.0 M, 2.0 M NaNO ₃ (@ pH=8.9)
T =	20 ± 2 °C
Reaction vessel:	Glass
CO ₂ :	CO ₂ free; 15 to 1788 meq/L (@ pH=9.0)
Equilibration time:	24 hr
Filtration/Phase Separation:	0.45- μ m Millipore filter
Measurement techniques:	Alpha counting for ²²⁹ Th

Righetto et al. (1988)**Experiment: Th(IV) sorption on γ -Al₂O₃**

Solid preparation:	Commercial γ -Al ₂ O ₃ (Aluminum Oxide C, Degussa @ 20nm)
$C_{RN} =$	10^{-11} M
M/V =	0.01 g/L
pH range =	1.0 to 10.0
Background Electrolyte =	0.1 M NaClO ₄
T =	n.r. (Presumably room temperature)
Reaction vessel:	Quick Seal ultracentrifuge tubes (Beckman - material not reported)
CO ₂ :	CO ₂ -free; C _T =0.05 M
Equilibration time:	7 d
Filtration/Phase Separation:	Centrifuged for 1 hr @ 55,000 rpm
Measurement techniques:	Gamma counting for ²²⁸ Th

Notes: Additional experiments to consider the effects of humic acids (5 to 50 ppm)

Righetto et al. (1991)**Experiment: Th(IV) sorption on amorphous SiO₂**

Solid preparation:	Synthetic silica precipitated by addition of acid to Na-silicate under controlled conditions (unspecified) to give a hydrous sol
$C_{RN} =$	10^{-11} M
M/V =	0.06 g/L
pH range =	0 to 3.5
Background Electrolyte =	0.1 M NaClO ₄
T =	25 ± 1 °C
Reaction vessel:	Polyallomer ultracentrifuge tubes
CO ₂ :	CO ₂ -free
Equilibration time:	7 d
Filtration/Phase Separation:	Centrifuged for 1 hr @ 55,000 rpm
Measurement techniques:	Gamma counting for ²²⁸ Th

URANIUM SORPTION:

Hsi (1981)

Experiment: U(VI) sorption on goethite

Solid preparation: Synthetic goethite prepared using method of Atkinson et al. (1967)
 $C_{RN} =$ Conducted experiments at 10^{-5} to 10^{-8} M. Only 10^{-5} M results reported
M/V = 1 g/L
pH range = 4.0 to 9.0 (Adjusted with 0.1 N HNO₃ or 0.1 N NaOH)
Background Electrolyte = 0.1 M NaNO₃
T = 25 °C
Reaction vessel: Polycarbonate
CO₂: CO₂-free; C_T=0.01 M and 0.001 M
Equilibration time: 4 hr
Filtration/Phase Separation: Centrifuge for 15 min @ 3,000 rpm
Measurement techniques: SINTREX UA-3 uranium analyzer (laser-induced fluorescence)

Notes: Experiments to determine the effects of competing cations (Ca²⁺ and Mg²⁺ @ 10^{-3} M)

Hsi (1981)

Experiment: U(VI) sorption on ferrihydrite (amorphous ferric oxyhydroxide - Fe(OH)₃)

Solid preparation: Synthetic ferrihydrite prepared using method of Davis and Leckie (1978)
 $C_{RN} =$ Conducted experiments at 10^{-5} to 10^{-8} M. Only 10^{-5} M results reported
M/V = 1 g/L
pH range = 4.0 to 9.0 (Adjusted with 0.1 N HNO₃ or 0.1 N NaOH)
Background Electrolyte = 0.1 M NaNO₃
T = 25 °C
Reaction vessel: Polycarbonate
CO₂: CO₂-free; C_T=0.01 M and 0.001 M
Equilibration time: 4 hr
Filtration/Phase Separation: Centrifuge for 15 min @ 3,000 rpm
Measurement techniques: SINTREX UA-3 uranium analyzer (laser-induced fluorescence)

Notes: Experiments to determine the effects of competing cations (Ca²⁺ and Mg²⁺ @ 10^{-3} M), as well as complexing ligands (PO₄³⁻ @ 10^{-3} and 10^{-5} M)

Hsi (1981)

Experiment: U(VI) sorption on synthetic hematite

Solid preparation: Synthetic hematite prepared using method of Matjevic and Scheiner (1978)
 $C_{RN} =$ Conducted experiments at 10^{-5} to 10^{-8} M. Only 10^{-5} M results reported
M/V = 1 g/L
pH range = 4.0 to 9.0 (Adjusted with 0.1 N HNO₃ or 0.1 N NaOH)

Background Electrolyte = 0.1 M NaNO₃
 T = 25 °C
 Reaction vessel: Polycarbonate
 CO₂: CO₂-free; C_T=0.01 M and 0.001 M
 Equilibration time: 4 hr
 Filtration/Phase Separation: Centrifuge for 15 min @ 3,000 rpm
 Measurement techniques: SINTREX UA-3 uranium analyzer (laser-induced fluorescence)

Notes: Experiments to determine the effects, as well as complexing ligands (PO₄³⁻ @ 10⁻³ and 10⁻⁵ M)

Hsi (1981)

Experiment: U(VI) sorption on natural hematite

Solid preparation: Natural specular hematite ground and sieved to <45 μm. No source given.
 C_{RN} = Conducted experiments at 10⁻⁵ to 10⁻⁸ M. Only 10⁻⁵ M results reported
 M/V = 1 g/L
 pH range = 4.0 to 9.0 (Adjusted with 0.1 N HNO₃ or 0.1 N NaOH)
 Background Electrolyte = 0.1 M NaNO₃
 T = 25 °C
 Reaction vessel: Polycarbonate
 CO₂: CO₂-free; C_T=0.01 M and 0.001 M
 Equilibration time: 4 hr
 Filtration/Phase Separation: Centrifuge for 15 min @ 3,000 rpm
 Measurement techniques: SINTREX UA-3 uranium analyzer (laser-induced fluorescence)

Notes: Experiments to determine effects of competing cations (Ca²⁺ and Mg²⁺ @ 10⁻³ M), as well as complexing ligands (PO₄³⁻ @ 10⁻³ and 10⁻⁵ M)

Hsi and Langmuir (1985)

Experiment: U(VI) sorption on goethite

Solid preparation: Synthetic goethite prepared using method of Atkinson et al. (1967).
 C_{RN} = 10⁻⁵ M
 M/V = 1 g/L
 pH range = 4.0 to 9.0 (Adjusted with 0.1 N HNO₃ or 0.1 N NaOH)
 Background Electrolyte = 0.1 M NaNO₃
 T = 25 °C
 Reaction vessel: Polycarbonate
 CO₂: CO₂-free; C_T=0.01 M and 0.001 M
 Equilibration time: 4 hr
 Filtration/Phase Separation: Centrifuge for 15 min @ 3,000 rpm
 Measurement techniques: SINTREX UA-3 uranium analyzer (laser-induced fluorescence)

Notes: Experimental data are the same as Hsi (1981)

Hsi and Langmuir (1985)**Experiment: U(VI) sorption on ferrihydrite (amorphous ferric oxyhydroxide - Fe(OH)₃)**

Solid preparation: Synthetic ferrihydrite prepared using method of Davis and Leckie (1978)
 $C_{RN} = 10^{-5}$ M
 $M/V = 1$ g/L
pH range = 4.0 to 9.0 (Adjusted with 0.1 N HNO₃ or 0.1 N NaOH)
Background Electrolyte = 0.1 M NaNO₃
T = 25 °C
Reaction vessel: Polycarbonate
CO₂: CO₂-free; $C_T = 0.01$ M and 0.001 M
Equilibration time: 4 hr
Filtration/Phase Separation: Centrifuge for 15 min @ 3,000 rpm
Measurement techniques: SINTREX UA-3 uranium analyzer (laser-induced fluorescence)

Notes: Experimental data are the same as Hsi (1981)

Hsi and Langmuir (1985)**Experiment: U(VI) sorption on synthetic hematite**

Solid preparation: Synthetic hematite prepared using method of Matjevic and Scheiner (1978)
 $C_{RN} = 10^{-5}$ M
 $M/V = 1$ g/L
pH range = 4.0 to 9.0 (Adjusted with 0.1 N HNO₃ or 0.1 N NaOH)
Background Electrolyte = 0.1 M NaNO₃
T = 25 °C
Reaction vessel: Polycarbonate
CO₂: CO₂-free; $C_T = 0.01$ M and 0.001 M
Equilibration time: 4 hr
Filtration/Phase Separation: Centrifuge for 15 min @ 3,000 rpm
Measurement techniques: SINTREX UA-3 uranium analyzer (laser-induced fluorescence)

Notes: Experimental data are the same as Hsi (1981)

Hsi and Langmuir (1985)**Experiment: U(VI) sorption on natural hematite**

Solid preparation: Natural specular hematite ground and sieved to <45 μm. No source given.
 $C_{RN} = 10^{-5}$ M
 $M/V = 1$ g/L
pH range = 4.0 to 9.0 (Adjusted with 0.1 N HNO₃ or 0.1 N NaOH)
Background Electrolyte = 0.1 M NaNO₃
T = 25 °C
Reaction vessel: Polycarbonate
CO₂: CO₂-free; $C_T = 0.01$ M and 0.001 M
Equilibration time: 4 hr

Filtration/Phase Separation: Centrifuge for 15 min @ 3,000 rpm
Measurement techniques: SINTREX UA-3 uranium analyzer (laser-induced fluorescence)

Notes: Experimental data are the same as Hsi (1981)

Lieser and Thybusch (1988)

Experiment: U(VI) sorption on hydrous TiO₂

Solid preparation: Analytical grade TiO₂•H₂O (0.5 to 1 mm)
C_{RN} = 2.1 × 10⁻⁶ M
M/V = 1 g/L
pH range = 2.0 to 11.0 (Adjusted with N HCl or NaOH)
Background Electrolyte = 0.5 M NaCl
T = Room temperature (not specified)
Reaction vessel: Polyethylene
CO₂: CO₂-free; C_T=0.1 M and 0.0001 M
Equilibration time: 17 hr
Filtration/Phase Separation: Centrifuge for 15 min @ 3,000 rpm
Measurement techniques: Chelation with cellulose exchanger and XRF

Payne et al. (1992)

Experiment: U(VI) sorption on ferrihydrite (amorphous ferric oxyhydroxide - Fe(OH)₃)

Solid preparation: Synthetic ferrihydrite formed by raising the pH of a Fe³⁺/HNO₃ solution to 6.0, aged for 65 hr @ 25 °C
C_{RN} = 10⁻⁴, 10⁻⁵, 10⁻⁶, and 10⁻⁸ M
M/V = 0.11 and 1.78 g/L (10⁻³ M and 2 × 10⁻² M Fe)
pH range = 2.5 to 10.0 (Adjusted with HNO₃ or NaHCO₃)
Background Electrolyte = 0.1 M NaNO₃
T = 25 °C
Reaction vessel: Polypropylene
CO₂: Atmospheric (0.03 percent) and 1 percent CO₂
Equilibration time: 48 hr
Filtration/Phase Separation: Centrifugation
Measurement techniques: Kinetic phosphorescence analysis

Payne et al. (1992)

Experiment: U(VI) sorption on kaolinite

Solid preparation: Commercial natural kaolinites (Clay Minerals Society standard KGa-1, and a Japanese standard Nichika #15-27-2)
C_{RN} = 10⁻⁶ M
M/V = 1, 4, and 16 g/L
pH range = 2.5 to 10.0 (Adjusted with HNO₃ or NaHCO₃)
Background Electrolyte = 0.1 M NaNO₃
T = 25 °C
Reaction vessel: Polypropylene
CO₂: Atmospheric CO₂

Equilibration time: 48 hr
Filtration/Phase Separation: Centrifugation
Measurement techniques: Kinetic phosphorescence analysis

Tripathi (1984)

Experiment: U(VI) sorption on goethite

Solid preparation: Synthetic goethite prepared by hydrolysis and aging of ferric nitrate solution using method of Atkinson et al. (1967)
 $C_{RN} = 10^{-5.4}, 10^{-5.8}, 10^{-6}, 10^{-6.4}, 10^{-6.7}, \text{ and } 10^{-7.1} \text{ M}$
 $M/V = 0.1, 0.41, 0.96, 2.10 \text{ g/L}$
pH range = 5.0 to 9.0 (Adjusted with HNO_3 or NaOH)
Background Electrolyte = 0.1, 0.5, 0.7 M NaNO_3
T = 25 °C
Reaction vessel: Nalgene
 CO_2 : CO_2 -free; Atmospheric CO_2
Equilibration time: CO_2 -free: 6 hr (8 hr for experiments with $I > 0.1 \text{ M}$ and PO_4^{3-})
Atmospheric CO_2 : 12 hr
Filtration/Phase Separation: Centrifugation and 0.2- μm Nucleopore filter
Measurement techniques: Spectrophotometry using Rhodamine-B, Bromo-PADAP, Arsenazo III methods

Notes: Additional experiments to determine the effects of competing ligands (F^- @ 50 ppb to 5 ppm, and PO_4^{3-} @ 40 to 100 ppb).

Venkataramani and Gupta (1991)

Experiment: U(VI) sorption on hydrous titanium oxide (HTiO)

Solid preparation: Synthetic HTiO.
 $C_{RN} = 10^{-4} \text{ M}$
 $M/V = 8 \text{ g/L}$
pH range = 1.5 to 7.0
Background Electrolyte = 0.1 M NaClO_4 ; 0.1 M NaNO_3 ; 0.1 M NaCl ; 0.1 M Na_2SO_4
T = 25 ± 1 °C
Reaction vessel: n.r.
 CO_2 : n.r.
Equilibration time: 4 hr
Filtration/Phase Separation: n.r.
Measurement techniques: n.r.

Notes: Investigated the effects of different anions. Background electrolyte set at 0.1 M ($\text{NaClO}_4 + \text{NaX}$), where X represents ClO_4^- , Cl^- , NO_3^- , or SO_4^{2-} . Presumably two sets of experiments performed to investigate the effects of carbonate: CO_2 -free, and CO_3^{2-} added (no concentration specified).

Notes: Investigated effects of different anions. Background electrolyte set at 0.1 M (NaClO₄+NaX), where X represents ClO₄⁻, Cl⁻, NO₃⁻, or SO₄²⁻. Presumably two sets of experiments performed to investigate the effects of carbonate: CO₂-free, and CO₃²⁻ added (no concentration specified).

Vochten et al. (1990)

Experiment: U(VI) sorption on zeolites

Solid preparation: Stilbite - Deacon basalt formation, India (35-75 μm)
Scolecite - Deacon basalt formation, India (35-75 μm)
Heulandite - Deacon basalt formation, India (35-75 μm)
Chabazite - Freisen, Germany (35-75 μm)

C_{RN} = 2 × 10⁻⁵ M
M/V = 2 g/L
pH range = 4.0 to 7.0
Background Electrolyte = n.r.
T = 25° C
Reaction vessel: n.r.
CO₂: CO₂-free
Equilibration time: 1 week
Filtration/Phase Separation: Centrifugation
Measurement techniques: Spectrophotometry with Arsenazo III

Waite et al. (1993)

Experiment: U(VI) sorption on ferrihydrite (amorphous ferric oxyhydroxide - Fe(OH)₃)

Solid preparation: Synthetic ferrihydrite formed by raising the pH of a Fe³⁺/HNO₃ solution to 6.0, aged for 65 hr @ 25 °C

C_{RN} = 10⁻⁴, 10⁻⁶ M
M/V = 0.09 g/L (10⁻³ M Fe)
pH range = 3.5 to 9.0 (Adjusted with HNO₃ or NaHCO₃)
Background Electrolyte = 0.1 M NaNO₃
T = 25 °C
Reaction vessel: Polypropylene
CO₂: Atmospheric CO₂
Equilibration time: 48 hr
Filtration/Phase Separation: Centrifugation @ 15,000 rpm
Measurement techniques: Kinetic phosphorescence analysis and alpha spectrometry for ²³⁶U

Notes: Appears to be same experimental data reported in Payne et al. (1992)

Waite et al. (1993)

Experiment: U(VI) sorption on quartz

Solid preparation: Commercial quartz (8-15 μm)

C_{RN} = 10⁻⁶ M
M/V = 100 g/L
pH range = 3.5 to 6.0 (Adjusted with HNO₃ or NaHCO₃)
Background Electrolyte = 0.1 M KNO₃
T = 25 °C

Reaction vessel: Polypropylene
 CO₂: Atmospheric CO₂
 Equilibration time: 48 hr
 Filtration/Phase Separation: Centrifugation @ 15,000 rpm
 Measurement techniques: Kinetic phosphorescence analysis and alpha spectrometry for ²³⁶U

Notes: Additional experiments to determine effects of competing ligands (F⁻ @ 10⁻⁴ and 6 × 10⁻⁴ M)

CARBON SORPTION

Zachara et al. (1987)

Experiment: Carbon sorption on ferrihydrite

Solid preparation: Synthetic ferrihydrite formed by raising the pH of a 0.1 M Fe(NO₃)₃ solution to 7.25, aged under a N₂ atmosphere for 14 hr @ 25 °C
 C_{RN} = 4.6 × 10⁻⁶ M
 M/V = 0.077 g/L, 0.77 g/L
 pH range = 5.5 to 9.0 (Adjusted with HNO₃ or NaHCO₃)
 Background Electrolyte = 0.1 M NaNO₃
 T = 25 °C
 Reaction vessel: Corex (Corning Glass Works, Houghton Park, NY)
 CO₂: Capped, zero headspace. Spiked with NaHCO₃-NaH¹⁴CO₃
 Equilibration time: 24 hr
 Filtration/Phase Separation: n.r.
 Measurement techniques: ¹⁴C scintillation counting

van Geen et al. (1994)

Experiment: Carbon sorption on goethite

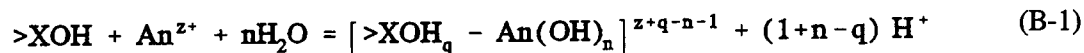
Solid preparation: Synthetic goethite prepared using method of Atkinson et al. (1967).
 C_{RN} = Total of 1.26 × 10⁻⁵ moles CO₂ added to system. Headspace p(CO₂) from 2,000 μatm to < 5 μatm. Approximately 50 μM CO₂ in suspension
 M/V = 2 g/L, 10 g/L
 pH range = 3.0 to 8.0 (Adjusted with HNO₃ or NaHCO₃)
 Background Electrolyte = 0.1 N NaClO₄
 T = 25 °C
 Reaction vessel: Glass
 CO₂: Controlled atmosphere with headspace equilibration system
 Equilibration time: 5 min
 Filtration/Phase Separation: Gas measurement, no phase separation required
 Measurement techniques: IR absorption

APPENDIX B

SURFACE COMPLEXATION MODEL BINDING CONSTANTS

SCM BINDING CONSTANTS

The following tables contain the binding constants calculated for the indicated surface complex using the numerical parameter optimization code FITEQL, Version 2.0 (Westall, 1982b). The surface reactions are written in the general form



where $q = 0, 1, \text{ or } 2$ and An represents the radioelement (actinide) of choice.

Additional abbreviations include:

A_{SP}	=	Specific surface area (in m^2/g).
Error	=	Error estimates used in FITEQL calculations. (See text and Westall, 1982a for detailed discussion of error propagation and uncertainty calculations).
N_{S}	=	Site density. Fixed at $2.31 \text{ sites}/\text{nm}^2$ based on work of Dzombak and Morel (1990) and recommendations of Davis and Kent (1990).
M/V	=	Solid-mass to solution-volume ratio (in g/L).
K_+, K_-	=	Acidity constants for mineral-water interface. (See Turner, 1993) for detailed discussion).
$K_{\text{Cat}}, K_{\text{An}}$	=	Binding constants for background electrolytes, triple layer model only. (See Turner, 1993 for detailed discussion).
V_Y	=	Goodness-of-fit estimate calculated by FITEQL based on error estimates and size of data set. Smaller values indicate better fit to sorption data (See Westall, 1982a for detailed discussion of calculations).
$\sigma_{\text{Log K}}$	=	Standard deviation for binding constant calculated by FITEQL based on error estimates and size of data set. (See Westall, 1982a for detailed discussion of calculations).

Table B-1. Americium (III)- γ -Al₂O₃ sorption binding constants: monodentate, mononuclear compounds

Solid: γ -Al ₂ O ₃ A _{Sp} : 130 m ² /g Data Source: Righetto et al. (1988) Concentration: [Am(III)] = 5E-10 M			Rel Error (pH): (a) Abs Error (pH): (a) Rel Error (radionuclide): 0.10 Abs Error (radionuclide): 5.0E-14			Ionic Strength (electrolyte): 0.1 M NaClO ₄ N _S = 2.31 sites/nm ² M/V = 0.01 g/L			
No CO ₂	DLM			CCM			TLM		
	Log K ₊ = 6.85 Log K ₋ = -9.05			Log K ₊ = 6.92 Log K ₋ = -9.00			Log K ₊ = 6.40 Log K ₋ = -10.40 Log K _{Cat} = -7.95 Log K _{An} = 8.28		
	Log K	V _Y	$\sigma_{\text{Log K}}$	Log K	V _Y	$\sigma_{\text{Log K}}$	Log K	V _Y	$\sigma_{\text{Log K}}$
XO-Am ²⁺	3.65	14.6	.0399	4.02	20.7	.0449	-1.50	75.7	.0299
XO-AmOH ⁺	-3.59	22.5	.0464	-3.41	24.2	.0481	-6.81	1.7	.0267
XO-Am(OH) ₂ ⁰	-10.84	28.0	.0519	-10.83	27.2	.0510	-12.71	13.5	.0391
XOH-Am(OH) ₂ ⁺	-3.59	22.5	.0464	-3.41	24.2	.0481	-4.65	11.4	.0376
XO-Am(OH) ₃ ⁻	-18.09	32.0	.0561	-18.26	29.8	.0535	-18.91	28.1	.0518
XOH-Am(OH) ₃ ⁰	-10.84	28.0	.0519	-10.83	27.2	.0510	-10.83	27.0	.0507
XOH ₂ -Am(OH) ₃ ⁺	-3.59	22.5	.0464	-3.41	24.2	.0481	-2.76	25.8	.0496

(a) No error assigned to pH to allow convergence for extremely low radionuclide concentrations.

Table B-2. Americium (III)- α -Al₂O₃ sorption binding constants: monodentate, mononuclear compounds

Solid: α -Al ₂ O ₃ A _{sp} : 0.07 m ² /g Data Source: Moulin et al. (1992) Concentration: [Am(III)] = 1E-8 M			Rel Error (pH): 0.05 Abs Error (pH): 0.0 Rel Error (radionuclide): 0.10 Abs Error (radionuclide): 1.0E-11			Ionic Strength (electrolyte): 0.01 M NaClO ₄ N _S = 2.31 sites/nm ² M/V = 10 g/L			
p(CO ₂) = 1E-3.5 atm	DLM			CCM			TLM		
	Log K ₊ = 8.33 Log K ₋ = -9.73			Log K ₊ = 8.18 Log K ₋ = -9.62			Log K ₊ = 6.90 Log K ₋ = -10.90 Log K _{Cat} = -7.73 Log K _{An} = 10.12		
	Log K	V _Y	$\sigma_{\text{Log K}}$	Log K	V _Y	$\sigma_{\text{Log K}}$	Log K	V _Y	$\sigma_{\text{Log.06036 K}}$
XO-Am ²⁺	8.54	21.1	.0707	8.91	21.3	.0797	-1.32	65.1	.0378
XO-AmOH ⁺	0.86	21.3	.0823	0.89	21.3	.0831	-6.32	18.9	.0618
XO-Am(OH) ₂ ⁰	-6.81	21.3	.0949	-7.13	21.3	.0867	-11.07	21.2	.0727
XOH-Am(OH) ₂ ⁺	0.86	21.3	.0823	0.89	21.3	.0831	-2.49	21.1	.0722
XO-Am(OH) ₃ ⁻	-14.47	21.3	.1084	-15.10	21.3	.0905	-15.79	21.3	.0883
XOH-Am(OH) ₃ ⁰	-6.81	21.3	.0949	-7.13	21.3	.0867	-7.24	21.3	.0859
XOH ₂ -Am(OH) ₃ ⁺	0.86	21.3	.0823	0.89	21.3	.0831	1.33	21.3	.0850
XO-AmCO ₃ ⁰	12.88	19.7	.0670	12.55	19.7	.0612	8.62	19.5	.0513
XOH-AmCO ₃ ⁺	16.48	27.0	.0830	16.28	27.0	.0834	17.19	19.5	.0509
XOH ₂ -Am(CO ₃) ₂ ⁰	32.56	12.4	.0765	32.23	12.4	.0709	35.92	12.4	.0803
XOH ₂ -Am(CO ₃) ₃ ²⁻	n.c.	n.c.	n.c.	33.05	23.2	.0949	36.86	15.2	.1417
n.c. FITEQL optimization did not converge.									

Table B-3. Americium (III)-amorphous SiO₂ sorption binding constants: monodentate, mononuclear compounds

Solid: amorphous SiO ₂ A _{SP} : 175 m ² /g Data Source: Righetto et al. (1991) Concentration: [Am(III)] = 5E-10 M			Rel Error (pH): (a) Abs Error (pH): (a) Rel Error (radionuclide): 0.10 Abs Error (radionuclide): 5.0E-14			Ionic Strength (electrolyte): 0.1 M NaClO ₄ N _S = 2.31 sites/nm ² M/V = 1.2 g/L			
No CO ₂	DLM			CCM			TLM		
	Log K ₊ = (b) Log K ₋ = -7.20			Log K ₊ = (b) Log K ₋ = -7.04			Log K ₊ = 0.90 Log K ₋ = -4.90 Log K _{Cat} = -6.22 Log K _{An} = (b)		
	Log K	V _Y	σ _{Log K}	Log K	V _Y	σ _{Log K}	Log K	V _Y	σ _{Log K}
XO-Am ²⁺	-1.71	26.5	.0461	-1.72	28.1	.0320	-3.37	41.5	.0461
XO-AmOH ⁺	-7.57	33.8	.0596	-7.59	33.6	.0604	-8.30	36.2	.0632
XO-Am(OH) ₂ ⁰	-13.20	39.3	.0657	-13.19	39.3	.0657	-12.87	38.6	.0651
XOH-Am(OH) ₂ ⁺	-7.57	33.8	.0596	-7.59	33.6	.0604	-8.49	37.1	.0633
XO-Am(OH) ₃ ⁻	-21.16	38.0	.0811	-21.17	38.1	.0812	-19.42	36.8	.0761
XOH-Am(OH) ₃ ⁰	-13.20	39.3	.0657	-13.19	39.3	.0657	-13.09	39.2	.0654
XOH ₂ -Am(OH) ₃ ⁺	-7.57	33.8	.0596	-7.59	33.6	.0604	-10.30	35.0	.0698

(a) No error assigned to pH to allow convergence for extremely low radionuclide concentrations.
 (b) Due to low zero-point of charge (pH_{ZPC}=2.1 for SiO₂), XOH₂⁺ (DLM, CCM) and XOH₂-An (TLM only) are assumed to be insignificant at slightly acid to basic pH [see discussion in Turner (1993)].

Table B-4. Neptunium (V)- γ -Al₂O₃ sorption binding constants: monodentate, mononuclear compounds

Solid: γ -Al ₂ O ₃ A _{SP} : 130 m ² /g Data Source: Righetto et al. (1988) Concentration: [Np(V)] = 1E-14 M			Rel Error (pH): (a) Abs Error (pH): (a) Rel Error (radionuclide): 0.10 Abs Error (radionuclide): 1.0E-18			Ionic Strength (electrolyte): 0.1 M NaClO ₄ N _S = 2.31 sites/nm ² M/V = 0.2 g/L			
No CO ₂	DLM			CCM			TLM		
	Log K ₊ = 6.85 Log K ₋ = -9.05			Log K ₊ = 6.92 Log K ₋ = -9.00			Log K ₊ = 6.40 Log K ₋ = -10.40 Log K _{Cat} = -7.95 Log K _{An} = 8.28		
	Log K	V _Y	$\sigma_{\text{Log K}}$	Log K	V _Y	$\sigma_{\text{Log K}}$	Log K	V _Y	$\sigma_{\text{Log K}}$
XO-NpO ₂ ⁰	-3.42	2.7	.0167	-3.42	3.2	.0166	-5.66	87.7	.0300
XOH-NpO ₂ ⁺	3.86	42.5	.0159	4.08	28.9	.0153	2.34	89.5	.0324
XO-NpO ₂ OH ⁻	-10.98	3.5	.0203	-11.05	1.8	.0195	-11.54	1.2	.0173
XOH-NpO ₂ OH ⁰	-3.42	2.7	.0167	-3.42	3.2	.0166	-3.41	3.8	.0165
XOH ₂ -NpO ₂ OH ⁺	3.86	42.5	.0159	4.08	28.9	.0153	4.70	9.2	.0161
OTHER SPECIES:									
(XO) ₂ -NpO ₂ ⁻	-6.91	4.7	.0209	-6.95	2.6	.0200	-9.47	83.7	.0260

(a) No error assigned to pH to allow convergence for extremely low radionuclide concentrations.

Table B-5. Neptunium (V)-goethite sorption binding constants: monodentate, mononuclear compounds

Solid: Natural Goethite A _{sp} : 15.7 m ² /g Data Source: Nakayama and Sakamoto (1991) Concentration: [Np(V)] = 6E-6 M			Rel Error (pH): 0.05 Abs Error (pH): 0.0 Rel Error (radionuclide): 0.10 Abs Error (radionuclide): 1.0E-9			Ionic Strength (electrolyte): 0.1 M NaNO ₃ N _S = 2.31 sites/nm ² M/V = 1 g/L			
No CO ₂	DLM			CCM			TLM		
	Log K ₊ = 7.35 Log K ₋ = -9.17			Log K ₊ = 6.47 Log K ₋ = -9.03			Log K ₊ = 6.00 Log K ₋ = -10.00 Log K _{Cat} = -7.64 Log K _{An} = 8.78		
	Log K	V _Y	σ _{Log K}	Log K	V _Y	σ _{Log K}	Log K	V _Y	σ _{Log K}
XO-NpO ₂ ⁰	-2.54	16.7	.0253	-2.60	14.6	.0242	-5.43	93.4	.0401
XOH-NpO ₂ ⁺	5.21	8.4	.0195	4.75	6.3	.0189	2.34	95.1	.0472
XO-NpO ₂ OH ⁻	-10.39	23.4	.0312	-9.92	21.5	.0305	-9.98	6.3	.0283
XOH-NpO ₂ OH ⁰	-2.54	16.7	.0253	-2.60	14.6	.0242	-2.44	14.1	.0239
XOH ₂ -NpO ₂ OH ⁺	5.21	8.4	.0195	4.75	6.3	.0189	5.86	6.9	.0257
OTHER SPECIES									
(XO) ₂ -NpO ₂ ⁻	-5.96	23.0	.0334	-5.54	20.7	.0320	-8.61	88.8	.0335

Table B-6. Neptunium (V)-synthetic magnetite sorption binding constants: monodentate, mononuclear compounds

Solid: Synthetic Magnetite A _{sp} : 5.5 m ² /g Data Source: Nakayama and Sakamoto (1991) Concentration: [Np(V)] = 6E-6 M			Rel Error (pH): 0.05 Abs Error (pH): 0.0 Rel Error (radionuclide) 0.10 Abs Error (radionuclide): 1.0E-9			Ionic Strength (electrolyte): 0.1 M NaNO ₃ N _S = 2.31 sites/nm ² M/V = 1 g/L			
No CO ₂	DLM			CCM			TLM		
	Log K ₊ = 6.72 Log K ₋ = -6.37			Log K ₊ = 6.26 Log K ₋ = -7.32			Log K ₊ = 4.70 Log K ₋ = -8.70 Log K _{Cat} = -5.47 Log K _{An} = 7.95		
	Log K	V _Y	σ _{Log K}	Log K	V _Y	σ _{Log K}	Log K	V _Y	σ _{Log K}
XO-NpO ₂ ⁰	-3.42	47.8	.0195	-3.97	48.1	.0202	-2.32	33.7	.0139
XOH-NpO ₂ ⁺	3.55	44.9	.0198	3.49	35.8	.0203	4.83	42.5	.0276
XO-NpO ₂ OH ⁻	-10.53	56.2	.0229	-11.25	54.7	.0235	-8.95	23.7	.0311
XOH-NpO ₂ OH ⁰	-3.42	47.8	.0195	-3.97	48.1	.0202	-3.65	49.1	.0205
XOH ₂ -NpO ₂ OH ⁺	3.55	44.9	.0198	3.49	35.8	.0203	4.55	21.9	.0299
OTHER SPECIES:									
(XO) ₂ -NpO ₂ ⁻	-4.82	49.1	.0231	-6.17	50.7	.0249	-3.11	31.1	.0284

B-7

Table B-7. Neptunium (V)-boehmite (γ -AlOOH) sorption binding constants: monodentate, mononuclear compounds

Solid: Boehmite (γ -AlOOH) A _{SP} : 175 m ² /g Data Source: Nakayama and Sakamoto (1991) Concentration: [Np(V)] = 6E-6 M			Rel Error (pH): 0.05 Abs Error (pH): 0.0 Rel Error (radionuclide): 0.10 Abs Error (radionuclide): 1.0E-9			Ionic Strength (electrolyte): 0.1 M NaNO ₃ N _S = 2.31 sites/nm ² M/V = 1 g/L			
No CO ₂	DLM (a)			CCM (a)			TLM (a)		
	Log K ₊ = 6.85 Log K ₋ = -9.05			Log K ₊ = 6.92 Log K ₋ = -9.00			Log K ₊ = 6.40 Log K ₋ = -10.40 Log K _{Cat} = -7.95 Log K _{An} = 8.28		
	Log K	V _Y	$\sigma_{\text{Log K}}$	Log K	V _Y	$\sigma_{\text{Log K}}$	Log K	V _Y	$\sigma_{\text{Log K}}$
XO-NpO ₂ ⁰	-3.36	15.7	.0480	-3.34	15.3	.0472	-5.03	43.0	.0241
XOH-NpO ₂ ⁺	4.09	8.0	.0351	4.23	9.1	.0376	3.17	52.4	.0259
XO-NpO ₂ OH ⁻	-10.84	22.9	.0610	-10.88	20.9	.0551	-11.46	15.4	.0496
XOH-NpO ₂ OH ⁰	-3.36	15.7	.0480	-3.34	15.3	.0472	-3.28	15.0	.0466
XOH ₂ -NpO ₂ OH ⁺	4.09	8.0	.0351	4.23	9.1	.0376	4.98	11.8	.0440
OTHER SPECIES:									
(XO) ₂ -NpO ₂ ⁻	-7.60	23.8	.0643	-7.58	21.7	.0571	9.79	32.8	.0261

(a) Surface constants for γ -Al₂O₃ used.

Table B-8. Neptunium (V)-lepidocrocite (γ -FeOOH) sorption binding constants: monodentate, mononuclear compounds

Solid: Lepidocrocite (γ -FeOOH) A _{sp} : 36 m ² /g Data Source: Nakayama and Sakamoto (1991) Concentration: [Np(V)] = 6E-6 M			Rel Error (pH): 0.05 Abs Error (pH): 0.0 Rel Error (radionuclide): 0.10 Abs Error (radionuclide): 1.0E-9			Ionic Strength (electrolyte): 0.1 M NaNO ₃ N _S = 2.31 sites/nm ² M/V = 1 g/L			
No CO ₂	DLM (a)			CCM (a)			TLM (a)		
	Log K ₊ = 7.35 Log K ₋ = -9.17			Log K ₊ = 6.47 Log K ₋ = -9.03			Log K ₊ = 6.00 Log K ₋ = -10.00 Log K _{Cat} = -7.64 Log K _{An} = 8.78		
	Log K	V _Y	$\sigma_{\text{Log K}}$	Log K	V _Y	$\sigma_{\text{Log K}}$	Log K	V _Y	$\sigma_{\text{Log K}}$
XO-NpO ₂ ⁰	-3.53	34.8	.0360	-3.59	34.4	.03576	-4.39	40.4	.0217
XOH-NpO ₂ ⁺	4.51	30.3	.0303	4.05	32.6	.02809	3.71	39.0	.0261
XO-NpO ₂ OH ⁻	-11.51	38.2	.0407	-11.11	38.7	.04175	-11.25	32.4	.0422
XOH-NpO ₂ OH ⁰	-3.53	34.8	.0360	-3.59	34.4	.03576	-3.43	34.3	.0356
XOH ₂ -NpO ₂ OH ⁺	4.51	30.3	.0303	4.05	32.6	.02809	4.81	30.9	.0395
OTHER SPECIES:									
(XO) ₂ -NpO ₂ ⁻	-7.52	38.4	.0420	-7.17	38.8	.04287	-7.82	40.2	.0289

(a) Surface constants for goethite (α -FeOOH).

Table B-9. Neptunium (V)- α -Al₂O₃ sorption binding constants: monodentate, mononuclear compounds

Solid: α -Al ₂ O ₃ A _{SP} : 2.5 m ² /g Data Source: Nakayama and Sakamoto (1991) Concentration: [Np(V)] = 6E-6 M			Rel Error (pH): 0.05 Abs Error (pH): 0.0 Rel Error (radionuclide): 0.10 Abs Error (radionuclide): 1.0E-9			Ionic Strength (electrolyte): 0.1 M NaNO ₃ N _S = 2.31 sites/nm ² M/V = 1 g/L			
No CO ₂	DLM			CCM			TLM		
	Log K ₊ = 8.33 Log K ₋ = -9.73			Log K ₊ = 8.12 Log K ₋ = -9.56			Log K ₊ = 6.90 Log K ₋ = -10.90 Log K _{Cat} = -7.73 Log K _{An} = 10.12		
	Log K	V _Y	$\sigma_{\text{Log K}}$	Log K	V _Y	$\sigma_{\text{Log K}}$	Log K	V _Y	$\sigma_{\text{Log K}}$
XO-NpO ₂ ⁰	-4.26	42.1	.0231	-4.26	41.9	.0231	-3.97	36.0	.0222
XOH-NpO ₂ ⁺	5.07	32.9	.0256	5.00	32.3	.0255	6.03	27.5	.0442
XO-NpO ₂ OH ⁻	-13.37	46.9	.0293	-13.31	47.3	.0297	-11.20	21.6	.0440
XOH-NpO ₂ OH ⁰	-4.26	42.3	.0231	-4.26	41.9	.0231	-3.88	41.5	.0230
XOH ₂ -NpO ₂ OH ⁺	5.07	32.9	.0256	5.00	32.3	.0255	6.46	20.6	.0424
OTHER SPECIES:									
(XO) ₂ -NpO ₂ ⁻	-7.99	43.7	.0352	-7.95	44.5	.0354	-5.74	22.2	.0536

B-10

Table B-10. Neptunium (V)-ferrihydrate sorption binding constants: monodentate, mononuclear compounds

Solid: Ferrihydrate A _{sp} : 600 m ² /g Data Source: Girvin et al. (1991) Concentration: [Np(V)] = 4.7E-12 M			Rel Error (pH): (a) Abs Error (pH): (a) Rel Error (radionuclide): 0.10 Abs Error (radionuclide): 4.7E-16			Ionic Strength (electrolyte): 0.1 M NaNO ₃ N _S = 2.31 sites/nm ² M/V = 0.89 g/L			
p(CO ₂) = 1E-3.5 atm	DLM			CCM			TLM		
	Log K ₊ = 7.29 Log K ₋ = -8.93			Log K ₊ = 7.35 Log K ₋ = -8.45			Log K ₊ = 6.00 Log K ₋ = -10.00 Log K _{Cat} = -7.66 Log K _{An} = 8.43		
	Log K	V _Y	σ _{Log K}	Log K	V _Y	σ _{Log K}	Log K	V _Y	σ _{Log K}
XO-NpO ₂ ⁰	-3.02	8.9	.0219	-2.83	7.9	.0225	-5.97	77.0	.0256
XOH-NpO ₂ ⁺	5.04	9.8	.0216	4.65	12.2	.0211	1.71	81.9	.0277
XO-NpO ₂ OH ⁻	-11.08	8.3	.0222	-10.35	8.1	.0242	-10.68	7.5	.0231
XOH-NpO ₂ OH ⁰	-3.02	8.9	.0219	-2.83	7.9	.0225	-2.90	8.1	.0223
XOH ₂ -NpO ₂ OH ⁺	5.04	9.8	.0216	4.65	12.2	.0211	4.87	9.7	.0216
OTHER SPECIES:									
(XO) ₂ -NpO ₂ ⁻	-8.28	8.3	.0222	-7.37	9.0	.0250	-10.69	65.3	.0226
(a) No error assigned to pH to allow convergence for extremely low radionuclide concentrations.									

B-11

Table B-11. Neptunium (V)-amorphous SiO₂ sorption binding constants: monodentate, mononuclear compounds

Solid: Amorphous SiO ₂ A _{SP} : 175 m ² /g Data Source: Righetto et al. (1991) Concentration:[Np(V)] = 1E-14 M			Rel Error (pH): (a) Abs Error (pH): (a) Rel Error (radionuclide): 0.10 Abs Error (radionuclide): 1.0E-18			Ionic Strength (electrolyte): 0.1 M NaClO ₄ N _S = 2.31 sites/nm ² M/V = 1.2 g/L			
No CO ₂	DLM			CCM			TLM		
	Log K ₊ = (b) Log K ₋ = -7.20			Log K ₊ = (b) Log K ₋ = -7.04			Log K ₊ = 0.90 Log K ₋ = -4.90 Log K _{Cat} = -6.22 Log K _{An} = (b)		
	Log K	V _Y	σ _{Log K}	Log K	V _Y	σ _{Log K}	Log K	V _Y	σ _{Log K}
XO-NpO ₂ ⁰	-5.39	24.9	.0179	-5.49	16.9	.0188	-3.89	50.3	.0174
XOH-NpO ₂ ⁺	1.30	41.1	.0168	1.18	17.4	.0161	-0.14	55.4	.0179
XO-NpO ₂ OH ⁻	-11.89	22.1	.0215	-12.27	21.1	.0221	-9.43	17.8	.0202
XOH-NpO ₂ OH ⁰	-5.39	24.9	.0179	-5.49	16.9	.0188	-5.52	16.8	.0191
XOH ₂ -NpO ₂ OH ⁺	1.30	41.1	.0168	1.18	17.4	.0161	-1.63	16.5	.0181
OTHER SPECIES:									
(XO) ₂ -NpO ₂ ⁻	-12.53	23.3	.0235	-12.27	21.1	.0221	-12.25	22.0	.0225

(a) No error assigned to pH to allow convergence for extremely low radionuclide concentrations.
 (b) Due to low zero-point of charge (pH_{ZPC}=2.1 for SiO₂), XOH₂⁺ (DLM, CCM) and XOH₂-An (TLM only) are assumed to be insignificant at slightly acid to basic pH [see discussion in Turner (1993)].

Table B-12. Plutonium (IV)-goethite sorption binding constants: monodentate, mononuclear compounds

Solid: Goethite A _{SP} : 50 m ² /L Data Source: Sanchez et al. (1985) Concentration: [Pu(IV)] = 1E-11 M			Rel Error (pH): (a) Abs Error (pH): (a) Rel Error (radionuclide): 0.10 Abs Error (radionuclide): 1.0E-14			Ionic Strength (electrolyte): 0.1 M NaNO ₃ N _S = 2.31 sites/nm ² M/V = 0.55 g/L			
No CO ₂	DLM			CCM			TLM		
	Log K ₊ = 7.35 Log K ₋ = -9.17			Log K ₊ = 6.47 Log K ₋ = -9.03			Log K ₊ = 6.00 Log K ₋ = -10.00 Log K _{Cat} = -7.64 Log K _{An} = 8.78		
	Log K	V _Y	σ _{Log K}	Log K	V _Y	σ _{Log K}	Log K	V _Y	σ _{Log K}
XO-Pu ³⁺	14.42	52.9	.0241	16.08	46.5	.0313	0.54	76.7	.0303
XO-PuOH ²⁺	9.10	44.3	.0277	9.65	43.2	.0333	-2.09	65.6	.0263
XO-Pu(OH) ₂ ⁺	3.84	39.9	.0356	3.25	39.2	.0355	-4.86	49.1	.0241
XOH-Pu(OH) ₂ ²⁺	9.10	44.3	.0277	9.65	43.2	.0333	2.80	50.9	.0241
XO-Pu(OH) ₃ ⁰	-2.37	30.6	.0455	-3.10	30.6	.0365	-7.87	46.9	.0301
XOH-Pu(OH) ₃ ⁺	3.84	39.9	.0356	3.25	39.2	.0355	-0.20	46.2	.0291
XO-Pu(OH) ₄ ⁻	-8.33	30.4	.0515	-10.12	23.7	.0435	-10.72	29.2	.0374
XOH-Pu(OH) ₄ ⁰	-2.37	30.6	.0455	-3.10	30.6	.0365	-3.04	31.0	.0361
XOH ₂ -Pu(OH) ₄ ⁺	3.84	39.9	.0356	3.25	39.2	.0355	4.62	33.0	.0351
XOH-Pu(OH) ₅ ⁻	-8.33	30.4	.0515	-10.12	23.7	.0435	n.c.	n.c.	n.c.
XOH ₂ -Pu(OH) ₅ ⁰	-2.37	30.6	.0455	-3.10	30.6	.0365	n.c.	n.c.	n.c.

n.c. FITEQL did not converge
(a) No error assigned to pH to allow convergence for extremely low radionuclide concentrations.

Table B-13. Plutonium (V)-goethite sorption binding constants: monodentate, mononuclear compounds

Solid: Goethite A _{sp} : 50 m ² /g Data Source: Sanchez et al. (1985) Concentration: [Pu(V)] = 1E-11 M			Rel Error (pH): (a) Abs Error (pH): (a) Rel Error (radionuclide): 0.10 Abs Error (radionuclide): 1.0E-16			Ionic Strength (electrolyte): 0.1 M NaNO ₃ N _S = 2.31 sites/nm ² M/V = 0.55 g/L			
No CO ₂	DLM			CCM			TLM		
	Log K ₊ = 7.35 Log K ₋ = -9.17			Log K ₊ = 6.47 Log K ₋ = -9.03			Log K ₊ = 6.00 Log K ₋ = -10.00 Log K _{Cat} = -7.64 Log K _{An} = 8.78		
	Log K	V _Y	σ _{Log K}	Log K	V _Y	σ _{Log K}	Log K	V _Y	σ _{Log K}
XO-PuO ₂ ⁰	-1.25	43.1	.0269	-1.98	30.0	.0219	-4.11	82.7	.0182
XOH-PuO ₂ ⁺	5.33	3.3	.0188	4.83	5.5	.0190	4.00	92.5	.0192
XO-PuO ₂ OH ⁻	-7.52	42.1	.0310	-8.65	39.6	.0255	-9.74	33.6	.0225
XOH-PuO ₂ OH ⁰	-1.25	43.1	.0269	-1.98	30.0	.0219	-1.85	27.7	.0216
XOH ₂ -PuO ₂ OH ⁺	5.33	3.3	.0188	4.83	5.5	.0190	6.05	20.3	.0207
(a) No error assigned to pH to allow convergence for extremely low radionuclide concentrations.									

Table B-14. Plutonium (V)- γ -Al₂O₃ sorption binding constants: monodentate, mononuclear compounds

Solid: γ -Al ₂ O ₃ A _{SP} : 130 m ² /g Data Source: Righetto et al. (1991) Concentration: [Pu(V)] = 2E-10 M			Rel Error (pH): (a) Abs Error (pH): (a) Rel Error (radionuclide): 0.10 Abs Error (radionuclide): 1.0E-13			Ionic Strength (electrolyte): 0.1 M NaClO ₄ N _S = 2.31 sites/nm ² M/V = 0.2 g/L			
No CO ₂	DLM			CCM			TLM		
	Log K ₊ = 6.85 Log K ₋ = -9.05			Log K ₊ = 6.92 Log K ₋ = -9.00			Log K ₊ = 6.40 Log K ₋ = -10.40 Log K _{Cat} = -7.95 Log K _{An} = 8.28		
	Log K	V _Y	$\sigma_{\text{Log K}}$	Log K	V _Y	$\sigma_{\text{Log K}}$	Log K	V _Y	$\sigma_{\text{Log K}}$
XO-PuO ₂ ⁰	-3.18	0.1	.0772	-3.17	0.1	.0773	-2.94	4.8	.1337
XOH-PuO ₂ ⁺	4.65	0.1	.0760	4.72	0.04	.0760	5.71	5.2	.2049
XO-PuO ₂ OH ⁻	-10.98	0.2	.0788	-11.04	0.2	.0790	-11.37	0.1	.0777
XOH-PuO ₂ OH ⁰	-3.18	0.1	.0772	-3.17	0.1	.0773	-3.15	0.1	.0772
XOH ₂ -PuO ₂ OH ⁺	4.65	0.1	.0760	4.72	0.04	.0760	5.08	0.03	.0768

(a) No error assigned to pH to allow convergence for extremely low radionuclide concentrations.

Table B-15. Thorium (IV)- γ -Al₂O₃ sorption binding constants: monodentate, mononuclear compounds

Solid: γ -Al ₂ O ₃ A _{sp} : 130 m ² /g Data Source: Righetto et al. (1988) Concentration: [Th(IV)] = 1E-11 M			Rel Error (pH): (a) Abs Error (pH): (a) Rel Error (radionuclide): 0.10 Abs Error (radionuclide): 8.0E-15			Ionic Strength (electrolyte): 0.1 M NaClO ₄ N _S = 2.31 sites/nm ² M/V = 0.01 g/L			
No CO ₂	DLM			CCM			TLM		
	Log K ₊ = 6.85 Log K ₋ = -9.05			Log K ₊ = 6.92 Log K ₋ = -9.00			Log K ₊ = 6.40 Log K ₋ = -10.40 Log K _{Cat} = -7.95 Log K _{An} = 8.28		
	Log K	V _Y	$\sigma_{\text{Log K}}$	Log K	V _Y	$\sigma_{\text{Log K}}$	Log K	V _Y	$\sigma_{\text{Log K}}$
XO-Th ³⁺	14.30	32.4	.0356	18.29	50.2	.0519	2.08	19.6	.0201
XO-ThOH ²⁺	9.51	46.1	.0470	11.62	52.3	.0550	-0.69	20.8	.0286
XO-Th(OH) ₂ ⁺	4.61	54.5	.0588	4.94	54.1	.0580	-3.57	37.6	.0395
XOH-Th(OH) ₂ ²⁺	9.51	46.1	.0470	11.62	52.3	.0550	4.13	35.5	.0379
XO-Th(OH) ₃ ⁰	-2.10	61.6	.0816	-1.74	55.7	.0610	-6.52	49.0	.0506
XOH-Th(OH) ₃ ⁺	4.61	54.5	.0588	4.94	54.1	.0580	1.19	47.7	.0490
XO-Th(OH) ₄ ⁻	-7.45	62.7	.0823	-8.42	57.1	.0641	-9.57	56.1	.0618
XOH-Th(OH) ₄ ⁰	-2.10	61.6	.0816	-1.74	55.7	.0610	-1.84	55.3	.0602
XOH ₂ -Th(OH) ₄ ⁺	4.61	54.5	.0588	4.94	54.1	.0580	5.88	54.5	.0586

Table B-16. Thorium (IV)-amorphous SiO₂ sorption binding constants: monodentate, mononuclear compounds

Solid: Amorphous SiO ₂ A _{SP} : 175 m ² /g Data Source: Righetto et al. (1991) Concentration:[Th(IV)] = 1E-11 M			Rel Error (pH): (a) Abs Error (pH): (a) Rel Error (radionuclide): 0.10 Abs Error (radionuclide): 1.0E-15			Ionic Strength (electrolyte): 0.1 M NaClO ₄ N _S = 2.31 sites/nm ² M/V = 0.06 g/L			
No CO ₂	DLM			CCM			TLM		
	Log K ₊ = (b) Log K ₋ = -7.20			Log K ₊ = (b) Log K ₋ = -7.04			Log K ₊ = 0.90 Log K ₋ = -4.90 Log K _{Cat} = -6.22 Log K _{An} = (b)		
	Log K	V _Y	σ _{Log K}	Log K	V _Y	σ _{Log K}	Log K	V _Y	σ _{Log K}
XO-Th ³⁺	3.43	61.1	.0329	3.43	61.1	.0329	8.15	34.8	.0418
XO-ThOH ²⁺	3.20	35.8	.0390	3.20	35.8	.0390	6.25	22.7	.0429
XO-Th(OH) ₂ ⁺	2.98	24.2	.0423	2.98	24.2	.0423	4.35	21.2	.0443
XOH-Th(OH) ₂ ²⁺	3.20	35.8	.0390	3.20	35.8	.0390	6.58	22.0	.0434
XO-Th(OH) ₃ ⁰	2.76	19.8	.0457	2.76	19.8	.0457	2.45	20.2	.0455
XOH-Th(OH) ₃ ⁺	2.98	24.2	.0423	2.98	24.2	.0423	4.68	20.7	.0448
XO-Th(OH) ₄ ⁻	2.54	18.0	.0479	2.54	18.0	.0479	0.56	19.4	.0458
XOH-Th(OH) ₄ ⁰	2.76	19.8	.0457	2.76	19.8	.0457	2.78	19.8	.0457
XOH ₂ -Th(OH) ₄ ⁺	2.98	24.2	.0423	2.98	24.2	.0423	5.01	20.3	.0453

(a) No error assigned to pH to allow convergence for extremely low radionuclide concentrations.
(b) Due to low zero-point of charge (pH_{ZPC}=2.1 for SiO₂), XOH₂⁺ (DLM, CCM) and XOH₂-An (TLM only) are assumed to be insignificant at slightly acid to basic pH [see discussion in Turner (1993)].

Table B-17. Uranium (VI)-magnetite sorption binding constants: monodentate, mononuclear compounds

Solid: Magnetite A _{sp} : 5 m ² /g Data Source: Venkataramani and Gupta (1991) Concentration: [U(VI)] = 1E-4 M			Rel Error (pH): 0.05 Abs Error (pH): 0.0 Rel Error (radionuclide): 0.10 Abs Error (radionuclide): 2.6E-9			Ionic Strength (electrolyte): 0.1 M NaCl N _S = 2.31 sites/nm ² M/V = 8 g/L			
No CO ₂	DLM			CCM			TLM		
	Log K ₊ = 6.72 Log K ₋ = -6.37			Log K ₊ = 6.26 Log K ₋ = -7.32			Log K ₊ = 4.70 Log K ₋ = -8.70 Log K _{Cat} = -5.47 Log K _{An} = 7.95		
	Log K	V _Y	σ _{Log K}	Log K	V _Y	σ _{Log K}	Log K	V _Y	σ _{Log K}
XO-UO ₂ ⁺	1.53	16.2	.0361	1.40	17.6	.0376	-4.11	98.8	.0526
XOH-UO ₂ ²⁺	7.46	59.0	.0377	7.76	51.7	.0423	2.67	98.9	.0687
XO-UO ₂ OH ⁰	-4.69	1.2	.0394	-5.12	2.8	.0375	-7.72	88.5	.0435
XOH-UO ₂ OH ⁺	1.53	16.2	.0361	1.40	17.6	.0376	1.11	93.3	.0527
XO-UO ₂ (OH) ₂ ⁻	-10.71	2.5	.0522	-11.44	10.1	.0464	-11.24	68.0	.0567
XOH-UO ₂ (OH) ₂ ⁰	-4.69	1.2	.0394	-5.12	2.8	.0375	-4.72	3.5	.0366
XOH ₂ -UO ₂ (OH) ₂ ⁺	1.53	16.2	.0361	1.40	17.6	.0376	1.98	71.6	.0560
XOH-UO ₂ (OH) ₃ ⁻	-10.71	2.5	.0522	-11.44	10.1	.0464	-8.14	19.6	.0629
XOH ₂ -UO ₂ (OH) ₃ ⁰	-4.69	1.2	.0394	-5.12	2.8	.0375	-2.32	13.1	.0633
XOH-UO ₂ (OH) ₄ ²⁻	-16.69	11.9	.0674	-17.78	16.3	.0547	-11.60	47.1	.0944
XOH ₂ -UO ₂ (OH) ₄ ⁻	-10.71	2.5	.0522	-11.44	10.1	.0464	-5.41	7.3	.0806

Table B-18. Uranium (VI)-ferrihydrite sorption binding constants: monodentate, mononuclear compounds

Solid: Ferrihydrite A _{sp} : 600 m ² /g Data Source: Hsi and Langmuir (1985) Concentration: [U(VI)] = 1E-5 M			Rel Error (pH): 0.05 Abs Error (pH): 0.0 Rel Error (radionuclide): 0.10 Abs Error (radionuclide): 1.0E-8			Ionic Strength (electrolyte): 0.1 M NaNO ₃ N _S = 2.31 sites/nm ² M/V = 1 g/L			
No CO ₂	DLM			CCM			TLM		
	Log K ₊ = 7.29 Log K ₋ = -8.93			Log K ₊ = 7.35 Log K ₋ = -8.45			Log K ₊ = 6.00 Log K ₋ = -10.00 Log K _{Cat} = -7.66 Log K _{An} = 8.43		
	Log K	V _Y	σ _{Log K}	Log K	V _Y	σ _{Log K}	Log K	V _Y	σ _{Log K}
XO-UO ₂ ⁺	2.51	13.8	.0314	2.86	13.8	.0314	-4.59	80.2	.0239
XOH-UO ₂ ²⁺	8.62	25.6	.0221	10.14	14.1	.0286	3.04	82.4	.0259
XO-UO ₂ OH ^o	-3.65	17.1	.0423	-4.40	14.3	.0337	-8.21	25.4	.0234
XOH-UO ₂ OH ⁺	2.51	13.8	.0314	2.86	13.8	.0314	-0.53	28.9	.0222
XO-UO ₂ (OH) ₂ ⁻	-9.67	21.4	.0521	-11.65	14.9	.0360	-12.14	14.2	.0345
XOH-UO ₂ (OH) ₂ ^o	-3.65	17.1	.0423	-4.40	14.3	.0337	-4.51	14.2	.0332
XOH ₂ -UO ₂ (OH) ₂ ⁺	2.51	13.8	.0314	2.86	13.8	.0314	3.17	13.7	.0322
XOH-UO ₂ (OH) ₃ ⁻	-9.67	21.4	.0521	-11.65	14.9	.0360	-8.43	17.8	.0448
XOH ₂ -UO ₂ (OH) ₃ ^o	-3.65	17.1	.0423	-4.40	14.3	.0337	-0.90	17.8	.0436
XOH-UO ₂ (OH) ₄ ²⁻	-15.56	23.5	.0575	-18.91	15.6	.0384	-12.21	21.0	.0555
XOH ₂ -UO ₂ (OH) ₄ ⁻	-9.67	21.4	.0521	-11.65	14.9	.0360	-4.52	21.9	.0525

Table B-19. Uranium (VI)-goethite sorption binding constants: monodentate; mononuclear compounds

Solid: Goethite A _{SP} : 50 m ² /g Data Source: Hsi and Langmuir (1985) Concentration: [U(VI)] = 1E-5 M			Rel Error (pH): 0.05 Abs Error (pH): 0.0 Rel Error (radionuclide): 0.10 Abs Error (radionuclide): 1.0E-8			Ionic Strength (electrolyte): 0.1 M NaNO ₃ N _S = 2.31 sites/nm ² M/V = 1 g/L			
No CO ₂	DLM			CCM			TLM		
	Log K ₊ = 7.35 Log K ₋ = -9.17			Log K ₊ = 6.47 Log K ₋ = -9.03			Log K ₊ = 6.00 Log K ₋ = -10.00 Log K _{Cat} = -7.64 Log K _{An} = 8.78		
	Log K	V _Y	σ _{Log K}	Log K	V _Y	σ _{Log K}	Log K	V _Y	σ _{Log K}
XO-UO ₂ ⁺	3.13	1.6	.0352	2.69	1.9	.0350	-3.17	45.0	.0400
XOH-UO ₂ ²⁺	9.86	10.8	.0278	9.56	8.3	.0338	6.57	43.3	.0638
XO-UO ₂ OH ⁰	-3.54	3.9	.0432	-4.08	2.0	.0377	-7.33	14.7	.0295
XOH-UO ₂ OH ⁺	3.13	1.6	.0352	2.69	1.9	.0350	0.97	18.3	.0385
XO-UO ₂ (OH) ₂ ⁻	-10.19	6.0	.0518	-10.77	2.4	.0411	-11.38	0.8	.0459
XOH-UO ₂ (OH) ₂ ⁰	-3.54	3.9	.0432	-4.08	2.0	.0377	-3.99	2.0	.0375
XOH ₂ -UO ₂ (OH) ₂ ⁺	3.13	1.6	.0352	2.69	1.9	.0350	4.29	0.7	.0458
XOH-UO ₂ (OH) ₃ ⁻	-10.19	6.0	.0518	-10.77	2.4	.0411	-7.96	2.5	.0530
XOH ₂ -UO ₂ (OH) ₃ ⁰	-3.54	3.9	.0432	-4.08	2.0	.0377	-0.55	4.9	.0461
XOH-UO ₂ (OH) ₄ ²⁻	-16.80	7.3	.0611	-17.39	2.2	.0457	-11.40	1.7	.0734
XOH ₂ -UO ₂ (OH) ₄ ⁻	-10.19	6.0	.0518	-10.77	2.4	.0411	-4.50	4.8	.0623

Table B-20. Uranium (VI)- α -Al₂O₃ sorption binding constants: monodentate, mononuclear compounds

Solid: α -Al ₂ O ₃ Asp: 0.229 m ² /g Data Source: Pabalan and Turner (1994) Concentration: [U(VI)] = 4.8E-7 M			Rel Error (pH): 0.05 Abs Error (pH): 0.0 Rel Error (radionuclide): 0.10 Abs Error (radionuclide): 1.0E-11			Ionic Strength (electrolyte): 0.1 M NaNO ₃ N _S = 2.31 sites/nm ² M/V = 2.5 g/L			
p(CO ₂) = 1E-3.5 atm	DLM			CCM			TLM (a)		
	Log K	V _Y	$\sigma_{\text{Log K}}$	Log K	V _Y	$\sigma_{\text{Log K}}$	Log K	V _Y	$\sigma_{\text{Log K}}$
	Log K ₊ = 8.33 Log K ₋ = -9.73			Log K ₊ = 8.12 Log K ₋ = -9.56			Log K ₊ = 6.90 Log K ₋ = -10.90 Log K _{Cat} = -7.73 Log K _{An} = 10.12		
XO-UO ₂ ⁺	3.39	166.3	.0092	3.36	177.3	.0073	-3.76	293.2	.0098
XOH-UO ₂ ²	11.39	214.3	.0085	12.03	140.5	.0081	4.94	286.7	.0112
XO-UO ₂ OH ^o	-5.64	282.4	.0091	-5.60	268.5	.0086	-7.63	255.4	.0110
XOH-UO ₂ OH ⁺	3.39	166.3	.00072	3.36	177.3	.0073	1.01	281.7	.0135
XO-UO ₂ (OH) ₂ ⁻	-14.84	333.1	.0119	-14.75	328.9	.0113	-12.58	140.6	.0140
XOH-UO ₂ (OH) ₂ ^o	-5.64	282.4	.0091	-5.60	268.5	.0086	-4.62	172.6	.0078
XOH ₂ -UO ₂ (OH) ₂ ⁺	3.39	166.3	.0072	3.36	177.3	.0073	4.91	133.7	.0142
XOH-UO ₂ (OH) ₃ ⁻	-14.84	333.1	.0119	-14.75	328.9	.0113	-11.08	254.6	.0194
XOH ₂ -UO ₂ (OH) ₃ ^o	-5.64	282.4	.0091	-5.60	268.5	.0086	-3.15	282.6	.0125
XOH-UO ₂ (OH) ₄ ²⁻	-23.93	349.6	.0135	-23.78	348.9	.0131	-16.72	262.6	.0338
XOH ₂ -UO ₂ (OH) ₄ ⁻	-14.84	333.1	.0119	-14.75	328.9	.0113	-9.59	287.5	.0262
XOH-UO ₂ CO ₃ ^o	16.77	174.6	.0055	16.75	154.2	.0083	17.17	156.5	.0056
XOH ₂ -UO ₂ (CO ₃) ₂ ⁻	30.05	120.2	.0081	30.09	102.0	.0077	33.95	174.5	.0204
XOH ₂ -UO ₂ (CO ₃) ₃ ³⁻	34.77	125.1	.0136	35.06	103.3	.0130	44.94	150.1	.0495
XOH ₂ -(UO ₂) ₂ CO ₃ (OH) ₃ ^o	12.68	309.1	.0051	12.64	303.0	.0050	14.52	472.2	.0061

(a) Convergence problems were encountered with FITEQL due to desorption edge. To obtain convergence, only data for ph < 7.5 were considered for the TLM.

Table B-21. Uranium (VI)-quartz sorption binding constants: monodentate, mononuclear compounds

Solid: Quartz A _{SP} : 0.03 m ² /g Data Source: Waite et al. (1993) Concentration: [U(VI)] = 1E-6 M			Rel Error (pH): 0.05 Abs Error (pH): 0.0 Rel Error (radionuclide): 0.10 Abs Error (radionuclide): 1.0E-9			Ionic Strength (electrolyte): 0.1 M KNO ₃ N _S = 2.31 sites/nm ² M/V = 100 g/L			
p(CO ₂) = 1E-3.5 atm	DLM			CCM			TLM		
	Log K ₊ = (a) Log K ₋ = -7.20			Log K ₊ = (a) Log K ₋ = -7.04			Log K ₊ = 0.90 Log K ₋ = -4.90 Log K _{Cat} = -6.22 Log K _{An} = (a)		
	Log K	V _Y	σ _{Log K}	Log K	V _Y	σ _{Log K}	Log K	V _Y	σ _{Log K}
XO-UO ₂ ⁺	-1.23	94.9	.0402	-1.23	95.0	.0402	-1.24	78.6	.0357
XOH-UO ₂ ²⁺	2.14	99.7	.0437	2.14	99.7	.0436	1.64	91.6	.0399
XO-UO ₂ OH ⁰	-4.34	8.5	.0292	-4.34	8.5	.0291	-4.04	15.6	.0291
XOH-UO ₂ OH ⁺	-1.23	94.9	.0402	-1.23	95.0	.0402	-0.89	43.2	.0296
XO-UO ₂ (OH) ₂ ⁻	-8.45	3.7	.0421	-8.50	4.9	.0422	-7.40	7.1	.0347
XOH-UO ₂ (OH) ₂ ⁰	-4.34	8.5	.0292	-4.34	8.5	.0291	-4.33	8.5	.0291
XOH ₂ -UO ₂ (OH) ₂ ⁺	-1.23	94.9	.0402	-1.23	95.0	.0402	-0.97	24.8	.0289
XOH-UO ₂ (OH) ₃ ⁻	-8.45	3.7	.0421	-8.50	4.9	.0422	-7.53	5.4	.0363
XOH ₂ -UO ₂ (OH) ₃ ⁰	-4.34	8.5	.0292	-4.34	8.5	.0291	-4.39	7.6	.0319
XOH-UO ₂ (OH) ₄ ²⁻	-12.29	4.7	.0595	-12.46	7.6	.0610	-10.55	18.4	.0485
XOH ₂ -UO ₂ (OH) ₄ ⁻	-8.45	3.7	.0421	-8.45	4.9	.0422	-7.52	8.9	.0403
XOH-UO ₂ CO ₃ ⁰	17.33	8.1	.0206	17.34	8.1	.0206	17.35	8.2	.0206
XOH ₂ -UO ₂ (CO ₃) ₂ ⁻	34.91	2.3	.0360	34.86	3.0	.0361	35.87	5.9	.0289
XOH ₂ -UO ₂ (CO ₃) ₃ ³⁻	49.10	2.5	.0725	48.81	4.0	.0759	46.77	5.9	.0263
XOH ₂ -(UO ₂) ₂ CO ₃ (OH) ₃ ⁰	14.82	36.1	.0364	14.82	36.1	.0364	14.83	35.9	.0364

(a) Due to low zero-point of charge (pH_{ZPC}=2.1 for SiO₂), XOH₂⁺ (DLM, CCM) and XOH₂-An (TLM only) are assumed to be insignificant at slightly acid to basic pH [see discussion in Turner (1993)].

Table B-22. Carbon-ferrihydrate sorption binding constants: monodentate, mononuclear compounds

Solid: Ferrihydrate A _{SP} : 600 m ² /g Data Source: Zachara et al. (1987) Concentration: [C _T] = 4.6E-6 M			Rel Error (pH): 0.05 Abs Error (pH): 0.0 Rel Error (radionuclide): 0.01 Abs Error (radionuclide): 4.6E-8			Ionic Strength (electrolyte): 0.1 M NaNO ₃ N _S = 2.31 sites/nm ² M/V = 0.773 g/L			
	DLM			CCM			TLM		
	Log K ₊ = 7.29 Log K ₋ = -8.93			Log K ₊ = 7.35 Log K ₋ = -8.45			Log K ₊ = 6.00 Log K ₋ = -10.00 Log K _{Cat} = -7.66 Log K _{An} = 8.43		
	Log K	V _Y	σ _{Log K}	Log K	V _Y	σ _{Log K}	Log K	V _Y	σ _{Log K}
XOH ₂ -CO ₃ ⁻	13.06	29.3	.0098	13.08	54.7	.0101	17.72	333.2	.0279
XOH ₂ -HCO ₃ ⁰	20.75	66.6	.0112	20.85	84.7	.0119	22.28	239.0	.0112
XOH-H ₂ CO ₃ ⁰	20.75	66.6	.0112	20.85	84.7	.0119	20.84	86.2	.0120

Table B-23. Neptunium (V)-biotite sorption binding constants: monodentate, mononuclear compounds

Solid: Natural Biotite $[K(Mg,Fe)_3AlSi_3O_{10}(OH)_2]$ A_{sp} : 8 m ² /g (Nakayama and Sakamoto, 1991) Data Source: Nakayama and Sakamoto (1991) Concentration: $[Np(V)] = 6E-6$ M		Rel Error (pH): 0.05 Abs Error (pH): 0.0 Rel Error (radionuclide): 0.10 Abs Error (radionuclide): 1.0E-9			Ionic Strength (electrolyte): 0.1 M NaNO ₃ $N_s = 2.31$ sites/nm ² $M/V = 1$ g/L					
Si:Al = 3:1 No CO ₂		DLM			CCM			TLM		
								(α -Al ₂ O ₃)	(SiO ₂)	
		Log K ₊ = 8.33 (α -Al ₂ O ₃) Log K ₋ = -9.73 (α -Al ₂ O ₃) Log K ₋ = -7.20 (SiO ₂)			Log K ₊ = 8.12 (α -Al ₂ O ₃) Log K ₋ = -9.56 (α -Al ₂ O ₃) Log K ₋ = -7.04 (SiO ₂)			Log K ₊ = 6.90 Log K ₋ = -10.90 Log K _{Cat} = -7.73 Log K _{An} = 10.12	Log K ₊ = 0.90 Log K ₋ = -4.90 Log K _{Cat} = -6.22	
Log K	V _Y	$\sigma_{Log K}$	Log K	V _Y	$\sigma_{Log K}$	Log K	V _Y	$\sigma_{Log K}$		
XO-NpO ₂ ⁰	SiOH	-3.99	51.0	.0171	-3.61	41.6	.0168	-2.83	44.9	.0141
	AlOH	-3.35	45.3	.0229	-4.00	40.2	.0182	0.02	41.7	.0188
XOH-NpO ₂ ⁺	SiOH	3.42	56.5	.0184	4.29	42.6	.0175	1.56	52.5	.0152
	AlOH	4.43	44.7	.0181	3.88	40.5	.0180	4.56	44.2	.0163
XO-NpO ₂ OH ⁻	SiOH	-11.64	42.8	.0179	-11.41	0.5	.0847	-8.78	0.6	.0907
	AlOH	-11.25	54.2	.0333	11.77	0.5	.1007	-6.26	0.5	.1818
XOH-NpO ₂ OH ⁰	SiOH	-3.99	51.0	.0171	-3.61	41.6	.0168	-4.03	43.2	.0171
	AlOH	-3.35	45.3	.0229	-4.00	40.2	.0182	-1.81	41.5	.0224
XOH ₂ -NpO ₂ OH ⁺	SiOH	3.42	56.5	.0184	4.29	42.6	.0175	0.93	45.3	.0199
	AlOH	4.43	44.7	.0181	3.88	40.5	.0180	2.99	40.8	.0189
OTHER SPECIES:										
(XO) ₂ -NpO ₂ ⁻	SiOH	-6.31	49.6	.0190	-5.82	41.4	.0193	-2.42	46.0	.0156
	AlOH	-4.61	50.3	.0536	-6.42	39.4	.0263	3.53	36.7	.0351

Table B-24. Neptunium (V)-kaolinite sorption binding constants: monodentate, mononuclear compounds

Solid: Kaolinite [Al ₂ Si ₂ O ₅ (OH) ₄] A _{Sp} : 11 m ² /g (Allard et al., 1983) Data Source: Kohler et al. (1992) Concentration: [Np(V)] = 1.25E-7 M		Rel Error (pH): 0.05 Abs Error (pH): 0.0 Rel Error (radionuclide): 0.10 Abs Error (radionuclide): 1.2E-11			Ionic Strength (electrolyte): 0.1 M NaClO ₄ N _S = 2.31 sites/nm ² M/V = 5 g/L					
Si:Al = 1:1 No CO ₂		DLM			CCM			TLM		
								(α-Al ₂ O ₃)	(SiO ₂)	
		Log K ₊ = 8.33 (α-Al ₂ O ₃) Log K ₋ = -9.73 (α-Al ₂ O ₃) Log K ₋ = -7.20 (SiO ₂)			Log K ₊ = 8.12 (α-Al ₂ O ₃) Log K ₋ = -9.56(α-Al ₂ O ₃) Log K ₋ = -7.04 (SiO ₂)			Log K ₊ = 6.90	Log K ₊ = 0.90	
								Log K ₋ = -10.90	Log K ₋ = -4.90	
								Log K _{Cat} = -7.73	Log K _{Cat} = -6.22	
								Log K _{An} = 10.12		
		Log K	V _Y	σ _{Log K}	Log K	V _Y	σ _{Log K}	Log K	V _Y	σ _{Log K}
XO-NpO ₂ ⁰	SiOH	-2.89	22.1	.0308	-2.92	23.0	.0311	-3.50	53.1	.0235
	AlOH	-2.67	29.3	.0383	-2.69	29.2	.0384	-2.20	21.2	.0307
XOH-NpO ₂ ⁺	SiOH	4.65	14.6	.0221	4.61	21.0	.0246	1.37	74.9	.0281
	AlOH	4.95	25.1	.0338	4.86	25.1	.0337	3.26	24.5	.0237
XO-NpO ₂ OH ⁻	SiOH	-10.52	27.6	.0360	-10.46	27.3	.0360	-8.12	26.4	.0351
	AlOH	-10.31	32.7	.0427	-10.26	33.2	.0434	-7.36	37.1	.0484
XOH-NpO ₂ OH ⁰	SiOH	-2.89	22.1	.0308	-2.92	23.0	.0311	-2.60	22.8	.0290
	AlOH	-2.67	29.3	.0383	-2.69	29.2	.0384	-1.78	31.5	.0413
XOH ₂ -NpO ₂ OH ⁺	SiOH	4.65	14.6	.0221	4.61	21.0	.0246	2.85	33.7	.0238
	AlOH	4.95	25.1	.0338	4.86	25.1	.0337	3.65	26.4	.0351
OTHER SPECIES:										
(XO) ₂ -NpO ₂ ⁻	SiOH	-5.99	25.4	.0329	-5.95	25.0	.0328	-4.10	49.7	.0234
	AlOH	-5.58	35.7	.0465	-5.55	36.6	.0477	2.12	34.8	.0459

B-25

Table B-25. Uranium (V)-kaolinite sorption binding constants: monodentate, mononuclear compounds

Solid: Kaolinite [Al ₂ Si ₂ O ₅ (OH) ₄] A _{sp} : 11 m ² /g (Allard et al., 1983) Data Source: Payne et al. (1992) Concentration: [U(VI)] = 1E-6 M		Rel Error (pH): 0.05 Abs Error (pH): 0.0 Rel Error (radionuclide): 0.10 Abs Error (radionuclide): 1.2E-11			Ionic Strength (electrolyte): 0.1 M NaNO ₃ N _s = 2.31 sites/nm ² M/V = 4 g/L					
Si:Al = 1:1 No CO ₂		DLM			CCM			TLM		
		Log K ₊ = 8.33 (α-Al ₂ O ₃) Log K ₋ = -9.73 (α-Al ₂ O ₃) Log K ₋ = -7.20 (SiO ₂)			Log K ₊ = 8.12 (α-Al ₂ O ₃) Log K ₋ = -9.56 (α-Al ₂ O ₃) Log K ₋ = -7.04 (SiO ₂)			Log K ₊ = 6.90 Log K ₋ = -10.90 Log K _{Cat} = -7.73 Log K _{An} = 10.12		
		Log K	V _Y	σ _{Log K}	Log K	V _Y	σ _{Log K}	Log K	V _Y	σ _{Log K}
XO-UO ₂ ⁺	SiOH	1.41	20.1	.0228	1.85	20.1	.0217	-4.46	60.1	.0239
	AlOH	3.02	30.1	.0453	2.93	30.1	.0453	-1.69	37.8	.0238
XOH-UO ₂ ²⁺	SiOH	6.82	76.9	.0276	8.49	24.2	.0223	0.02	70.9	.0261
	AlOH	9.68	12.2	.0238	9.90	20.0	.0326	2.93	47.0	.0231
XO-UO ₂ OH ⁰	SiOH	-5.16	28.8	.0409	-5.10	28.5	.0417	-6.72	30.1	.0263
	AlOH	-3.85	40.1	.0647	-4.03	36.2	.0562	-4.51	25.3	.0377
XOH-UO ₂ OH ⁺	SiOH	1.41	20.1	.0228	1.85	20.1	.0297	-2.00	35.2	.0240
	AlOH	3.02	30.1	.0453	2.93	30.1	.0453	0.40	25.0	.0306
XO-UO ₂ (OH) ₂ ⁻	SiOH	-12.05	38.9	.0608	-12.08	35.0	.0532	-9.89	32.3	.0488
	AlOH	-10.70	45.3	.0817	-10.96	40.1	.0659	-7.82	38.7	.0627
XOH-UO ₂ (OH) ₂ ⁰	SiOH	-5.16	28.8	.0409	-5.10	28.5	.0417	-4.92	28.4	.0404
	AlOH	-3.85	40.1	.0647	-4.03	36.2	.0562	-2.92	36.1	.0562
XOH ₂ -UO ₂ (OH) ₂ ⁺	SiOH	1.41	20.1	.0228	1.85	20.1	.0297	0.02	27.3	.0329
	AlOH	3.02	30.1	.0453	2.93	30.1	.0453	2.01	32.5	.0492
XOH-UO ₂ (OH) ₃ ⁻	SiOH	-12.05	38.9	.0608	-12.08	35.0	.0532	-8.24	40.3	.0657
	AlOH	-10.70	45.3	.0817	-10.96	40.1	.0659	-6.20	44.4	.0785
XOH ₂ -UO ₂ (OH) ₃ ⁰	SiOH	-5.16	28.8	.0409	-5.10	28.5	.0417	-3.31	37.4	.0594
	AlOH	-3.85	40.1	.0647	-4.03	36.2	.0562	-1.28	42.7	.0723
XOH-UO ₂ (OH) ₄ ²⁻	SiOH	-18.90	44.5	.0782	-19.01	39.2	.0632	-11.53	46.4	.0878
	AlOH	-17.54	47.9	.0970	-17.86	42.9	.0756	-9.50	48.2	.0988
XOH ₂ -UO ₂ (OH) ₄ ⁻	SiOH	-12.16	38.9	.0608	-12.08	35.0	.0532	-6.58	45.0	.0820
	AlOH	-10.81	45.3	.0817	-10.96	40.1	.0659	-4.58	47.5	.0931